UNIVERSIDAD AUTÓNOMA DE MADRID
Facultad de Ciencias
Departamento de Biología Molecular

Doctoral Thesis

Nonreplicative genomic HSV-1 derived vectors for dorsal root ganglion gene therapy of Friedreich's ataxia

María Ventosa Rosales

Madrid, 2016

UNIVERSIDAD AUTÓNOMA DE MADRID
Facultad de Ciencias
Departamento de Biología Molecular

Nonreplicative genomic HSV-1 derived vectors for dorsal root ganglion gene therapy of Friedreich's ataxia

---

Vectores genómicos no replicativos derivados del VHS-1 para el desarrollo de una terapia génica en los ganglios de la raíz dorsal para el tratamiento de la ataxia de Friedreich

Memoria presentada por la licenciada en Biotecnología
María Ventosa Rosales

Director de Tesis:
Dr. Filip Lim, PhD

Lugar de realización:
Universidad Autónoma de Madrid
University of Michigan

Madrid, 2016

UNIVERSIDAD AUTÓNOMA DE MADRID

Facultad de Ciencias

Departamento de Biología Molecular

Filip Lim, **PhD**, Associate Professor at the Department of Molecular Biology of the Autonomous University of Madrid,

DECLARES,

that **María Ventosa Rosales, MSc**, has carried out at the Department of Molecular Biology of the Autonomous University of Madrid and under his supervision, the original research entitled: "**Nonreplicative genomic HSV-1 derived vectors for dorsal root ganglion gene therapy of Friedreich's ataxia**", to obtain the Degree of Doctor of Philosophy (PhD).

Having reviewed the present work, I agree to its dissertation and defence.

Madrid, September 26, 2016

Filip Lim

UNIVERSIDAD AUTÓNOMA DE MADRID

Facultad de Ciencias

Departamento de Biología Molecular

Filip Lim, **PhD**, profesor titular del Departamento de Biología Molecular de la Facultad de Ciencias de la Universidad Autónoma de Madrid,

HACE CONSTAR,

Que **María Ventosa Rosales** ha realizado bajo su dirección y con el máximo aprovechamiento, el trabajo titulado: "**Vectores genómicos no replicativos derivados del VHS-1 para el desarrollo de una terapia génica en los ganglios de la raíz dorsal para el tratamiento de la ataxia de Friedreich**", para optar al Grado de Doctor.

Revisado el presente trabajo de investigación, quedo conforme con su presentación para ser juzgado.

Y para que así conste y surta los efectos oportunos, lo firmo en Madrid, a 26 de Septiembre de dos mil dieciséis.

Filip Lim

A mi madre

AGRADECIMIENTOS

Son muchas las personas que, de una forma u otra, han contribuido a esta tesis, y no hay palabras suficientes para agradecer a todos su aportación a mi formación científica y personal durante estos años.

En primer lugar, quería expresar mi más profundo agradecimiento a Filip por haberme dado la oportunidad de formar parte de su grupo cuando tan solo era una estudiante de licenciatura. De no ser por él, nada de esto habría sido posible. Agradezco la confianza que ha depositado siempre en mí, su cercanía, su infinita paciencia y todo el esfuerzo y tiempo dedicados a enseñarme y guiarme. Su continua motivación, inconformismo, interés por la ciencia y capacidad de encontrar siempre una solución a todo han sido el motor de esta investigación. Tengo que agradecerle conseguir sacar siempre lo mejor de cada uno de nosotros y luchar por nuestro trabajo. Por ello y por mucho más, ha sido un auténtico honor poder haber aprendido de él no sólo como científico sino también como persona.

Quiero agradecer de manera especial la oportunidad que he tenido de trabajar y aprender de Vega. Confió en mí desde el primer momento y me dio el impulso necesario para seguir por este camino, convirtiéndose en un apoyo fundamental a lo largo de estos años. Gracias por haberme transmitido su espíritu de trabajo y superación y brindarme una ayuda incondicional. Para mí es un ejemplo tanto fuera como dentro del laboratorio.

Es necesario mencionar en especial también a Predes y agradecerle su eterna predisposición a ayudarme y enseñarme todos estos años. Gracias por la alegría que aporta al departamento. También he tenido la suerte de tener cerca de alguien como Antonio Rodríguez, gracias por su ayuda y consejo siempre que lo he necesitado.

No tengo palabras para agradecer a Hena todos los momentos que hemos vivido juntas en el laboratorio. Gracias por ser mi profesora, mi compañera y ante todo mi amiga. Ha sido un apoyo fundamental para mi trabajo y mi vida. Gracias por hacerme más fácil cada día de laboratorio, por nuestras aventuras en los congresos, por las eternas charlas sobre nuestros trabajos y por todo lo que nos hemos reído juntas.

Del mismo modo quiero acordarme de los compañeros de laboratorio Alicia,

Alba, Hernán, Guille, Zulma, María José y Jorge, y agradecerles el tiempo juntos y todo lo que he aprendido de ellos.

Mi agradecimiento más sincero también a Marina Mata, David Fink y todo su grupo (Zetang, Jen, Howard, Kiu, Kawata). Gracias por abrirme las puertas de su laboratorio y hacerme sentir parte de él. Su ayuda desinteresada ha sido un pilar fundamental en este trabajo. Ha sido un honor conocer a personas tan maravillosas.

Por último un agradecimiento muy especial a mi familia y mis amigos. A mi madre por ser siempre mi principal apoyo, a mis hermanos, a mi abuela, a mi tio José Luis, a mi cuñado, a Rafa y a todos mis amigos. Gracias por el constante apoyo que me han brindado todos estos años.

SUMMARY

SUMMARY

Friedreich's ataxia (FRDA) is an autosomal recessive neurodegenerative disease caused by mutations in the frataxin gene (*FXN*), which lead to reduced levels of the essential mitochondrial protein frataxin (FXN). Currently there is no effective treatment or cure.

Recently, a clinical trial for intractable pain (Dr Fink, Michigan 2011) demonstrated that delivery of a therapeutic transgene by non-replicative genomic herpes simplex virus type-1 (HSV-1) vectors to the dorsal root ganglia (DRG), principal target of gene therapy for Friedreich's ataxia, did not produce any vector-related adverse effects. Following on from these encouraging results and considering previous observations of our laboratory demonstrating sustained expression driven by the *FXN* genomic locus, we aim to develop a gene therapy for FRDA neuropathology.

Our approach has consisted on the construction and preliminary characterization of a high capacity nonreplicative genomic HSV-1 vector (27_4_Or2_β22 FXNinlZ vector) carrying a reduced version of the human *FXN* genomic locus, comprising the 5 kb promoter and the *FXN* cDNA with the inclusion of intron 1. We show that the nonreplicative HSV-1 genomic vector deleted for 23 kb maintains its growth capacity and the *FXN* transgene cassette contains the elements necessary to preserve physiological neuronal regulation of human *FXN* expression. Transduction of cultured fetal rat DRG neurons with the 27_4_Or2_β22 FXNinlZ vector results in sustained expression of human *FXN* transcripts and FXN protein. Rat footpad inoculation with the 27_4_Or2_β22 FXNinlZ vector results in human *FXN* transgene delivery to the DRG, with expression persisting for at least 1 month.

Our results support the feasibility of using this vector for sustained neuronal expression of human FXN for future FRDA gene therapy.

RESUMEN

La ataxia de Friedreich (AF) es una enfermedad neurodegenerativa causada por una mutación en el gen de la frataxina (*FXN*), que genera una deficiencia de la proteína mitocondrial esencial frataxina (FXN). Esta enfermedad presenta un patrón de herencia autosómica recesiva y en la actualidad no se dispone de ninguna terapia efectiva para su tratamiento o cura.

Recientemente, un ensayo clínico para terapia del dolor (Dr Fink, Michigan 2011) demuestra que la administración de vectores genómicos no replicativos derivados del virus del herpes simple tipo 1 (VHS-1) en los ganglios de las raíces dorsales, principal diana para terapia génica de AF, no desencadena ningún efecto adverso. Basándonos en estos resultados y en experimentos previos de nuestro laboratorio que demuestran que mediante el uso del locus genómico de *FXN* se consigue una expresión sostenida de FXN, nuestro objetivo es el desarrollo de una terapia génica para el tratamiento de la neuropatología de AF.

El abordaje de este trabajo ha consistido en la generación y caracterización preliminar de un vector genómico no replicativo y de gran capacidad derivado del VHS-1 (vector 27_4_Or2_β22 FXNinlZ) que contiene una versión reducida del locus genómico humano de *FXN*: el promotor de 5 kb seguido de la secuencia del ADN complementario manteniendo el intrón 1. En este estudio se observa que: i) tras eliminar 23 kb del vector genómico no replicativo derivado del VHS-1 se mantiene su capacidad de crecimiento; ii) la versión reducida del locus *FXN* contiene los elementos necesarios para preservar la regulación fisiológica de la expresión de FXN humana en neuronas; iii) tras la transducción *in vitro* de neuronas de los ganglios de las raíces dorsales de fetos de ratas con el vector 27_4_Or2_β22 FXNinlZ, hay tanto una transcripción como una traducción sostenida de FXN. Finalmente, los experimentos *in vivo* demuestran que la inoculación intraplantar de nuestro vector en ratas permite la detección de la expresión de *FXN* humana en los ganglios de la raíces dorsales, la cual se mantiene al menos 1 mes tras la inoculación.

Nuestros resultados apoyan la idea del uso de nuestro vector 27_4_Or2_β22 FXNinlZ para la expresión a largo plazo de FXN humana en el desarrollo de una futura terapia génica para el tratamiento de AF.

INDEX

ABBREVIATIONS

1. ABBREVIATIONS

AAV	Adeno-associated virus
ATP	Adenosine triphosphate
BAC	Bacterial artificial chromosome
BDNF	Brain-derived neurotropic factor
cDNA	Complementary DNA
CMV	Cytomegalovirus
CPE	Cytopathic effects
DAB	3, 3'-Diaminobenzidine
DMSO	Dimethyl sulfoxide
DNA	Deoxyribonucleic acid
DRG	Dorsal root ganglia
dNTPs	Deoxyribonucleotide triphosphates
Dox	Doxycycline
dsDNA	Double stranded DNA
DTT	Dithiothreitol
E	Early
E. coli	*Escherichia coli*
EDTA	Ethylenediaminetetraacetic acid
FBS	Fetal bovine serum
FDU	fluoro-2deoxy-uridine
Fe–S	Iron–sulfur
FRDA	Friedreich's ataxia
FXN	Frataxin
GAA	Guanine-adenine-adenine
GFP	Green fluorescent protein
HCF	Host cell factor
HDAC	Histone deacetylase
HEPES	4-(2-hydroxyethyl)-1-piperazineethanesulfonic acid
hFXN	Human frataxin
HRP	Horseradish peroxidase
HSV	Herpes simplex virus
ICP	Infected cell polypeptide
IE	Immediate early

IPTG	Isopropyl β-D-l- thiogalactopyranoside
IR	Internal repeat
kb	Kilobase
kDa	Kilodalton
L	Late
L4-6	Lumbar levels 4-6
lacZ	β-galactosidase
LAP	Latency associated promoters
LAT	Latency associated transcript
LB	Lysogeny Broth
LV	Lentivirus
miRNA	microRNA
MOI	Multiplicity of infection
MPP	Mitochondrial processing peptidase
mRNA	Messenger RNA
NGF	Nerve growth factor
N-terminal	Amino-terminal
Oct-1	Octamer binding protein-1
OD	Optical density
PAGE	Polyacrylamide gel electrophoresis
PBS	Phosphate buffered saline
PBST	Phosphate buffered saline with Tween 20
PCR	Polymerase chain reaction
PDL	poly-D-lysine
PFA	Paraformaldehyde
Pfu	Plaque forming units
PTV1	Porcine teschovirus-1
qRT-PCR	Real time RT-PCR
RNA	Ribonucleic acid
RNA Pol	RNA polymerase
RT-PCR	Reverse transcription PCR
SDS	Sodium dodecyl sulfate
SDS-PAGE	SDS-Polyacrylamide gel electrophoresis
SOC	Super optimal broth with catabolite repression
SV40	Simian vacuolating virus 40
TAE	Tris-acetate EDTA

TALE	Transcription activator-like effector protein
TSS	Transcription start site
TR	Terminal repeat
UV	Ultraviolet
VP	Virion protein
WT	Wild-type
X-gal	5-bromo-4-chloro-3-indolyl-β-D-galactopyranoside

INTRODUCTION

2. INTRODUCTION

2.1. Herpes Simplex Virus-1 (HSV-1)

HSV-1 is a common human pathogen that belongs to the *Herpesviridae* family, a group of enveloped, double-stranded (ds) DNA viruses.[1] Based on genome size and content, speed of replication, host range and cell types where latency is established, herpesviruses are classified into three subfamilies: *Alpha-, Beta-* and *Gamma- herpesvirinae,* of which HSV-1 belongs to the fast-growing, neurotropic *Alphaherpesvirinae*. Mainly transmitted by oral contact; HSV-1 lifelong infection is usually benign, and commonly associated with oral, perioral, genital, skin and mucous membrane lesions. In rare cases, HSV-1 is known to migrate to the brain and provoke viral encephalitis.[2] On average, 90% of the adult population is seropositive for anti-HSV-1 antibodies.

2.1.1. Structure of the virion

The spherical HSV-1 virion has an approximate diameter of 180 nm and is formed by four main structural components: the external envelope, a cell membrane-derived bilayer which includes several virus-encoded glycoproteins involved in attachment and entry of the virion into the host cell; the tegument, an amorphous layer containing virus-encoded proteins with structural and regulatory roles very important for efficient infection; an icosahedral nucleocapsid, composed of 162 capsomers which are required for the packaging of the genome; and the dsDNA genome wound in an electron-dense core.[3]

2.1.2. Life cycle

HSV-1 exhibits two modes of life cycle: lytic, in highly replicative cells, and latent, in neuronal cell bodies (**Figure 1**). In epithelial cells of the skin or mucosa, following attachment to the target cell surface, the virion enters generally either by fusion of the virion envelope with the plasma membrane or through endosomes. The content of the tegument and the nucleocapsid is then released into the cytoplasm and transported via the host's cytoskeleton elements to the nuclear pores. There, lytic growth is characterized by viral DNA replication and assembly of the viral DNA core and nucleocapsid, followed by envelopment of new virions at the nuclear membrane.

Finally mature virions are transported to the outer cell membrane through cellular vesicles. Lysis of the host cell releases the viral progeny.

Virions, which during the course of infection gain access to sensory nerve terminals, undergo axonal retrograde transport from the nerve endings in peripheral tissue to neuronal cell bodies buried deep in the spinal cord where HSV-1 establishes life-long latency.[4] Periodic reactivation of the latent genome can occur spontaneously or in response to stimuli like ultraviolet (UV) light exposure, high temperature, fever, mental or physical trauma to the host[5,6], bringing infectious viral progeny back to the nerve endings through anterograde transport and provoking skin lesions or mucosal ulcers.[7]

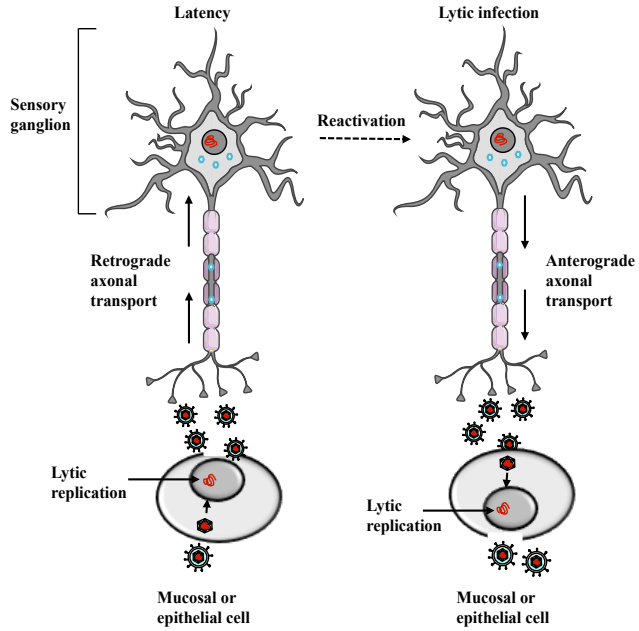

Figure 1. HSV-1 life cycle

Through fusion of the viral envelope with the plasma membrane of an epithelial cell of the skin or mucosa, HSV-1 enters and releases the nucleocapsid and tegument into the cytoplasm. Transport of the nucleocapsid to the nucleus is mediated by the host cytoskeleton and the genome is injected into the nucleus through nuclear pores. Following lytic replication in the infected epithelia, progeny virions which contact nerve endings are carried by retrograde transport to the cell bodies of sensory neurons innervating the infection site. Upon arrival in the cell body, the virus either initiates lytic expression or enters latency. Periodic reactivation from latency can occur spontaneously or in response to a variety of stimuli, resulting in the production of progeny virions that are moved by anterograde transport back to the nerve terminal to re-infect new epithelial cells, which leads to asymptomatic shedding or recurrent lesions.

2.1.3. Genome

The HSV-1 genome is a linear, large and structurally complex dsDNA of around 152 kilobases (kb) (**Figure 2**). It is partitioned into two segments of unique sequences, the unique long (U_L) and unique short (U_S), flanked by inverted repeat sequences (R_L and R_S with prefixes I or T denoting internal or terminal), which themselves are bounded by shorter repeated segments known as "a" sequences. The presence of the "a" sequences at the IR_L/IR_S junction and the termini of the linear genome, TR_L and TR_S, enables inversion of the orientation of U_L and U_S regions relative to each other, producing four possible genomic isoforms at approximately equimolar levels.[8] Moreover, the "a" sequences contain sites necessary for the packaging of viral DNA into the virion and in the TR region these sequences are asymmetrically partitioned and contain single base 3' extensions which serve as cohesive ends to circularize the genome prior to initiation of DNA synthesis.[9,10] DNA replication generally begins at specific sites on viral genomes known as origins of replication; three origins of replication have been identified within the HSV-1 genome: one within the U_L region (ori_L) and two copies flanking the U_S region within the repeat sequences (ori_S). The significance of the presence of three origins of replication in the HSV-1 genome still not well understood. Among the 80 virus-encoded genes, approximately half of them have been described as dispensable for *in vitro* viral replication, but play significant roles *in vivo* in virus-host interactions.[11,12]

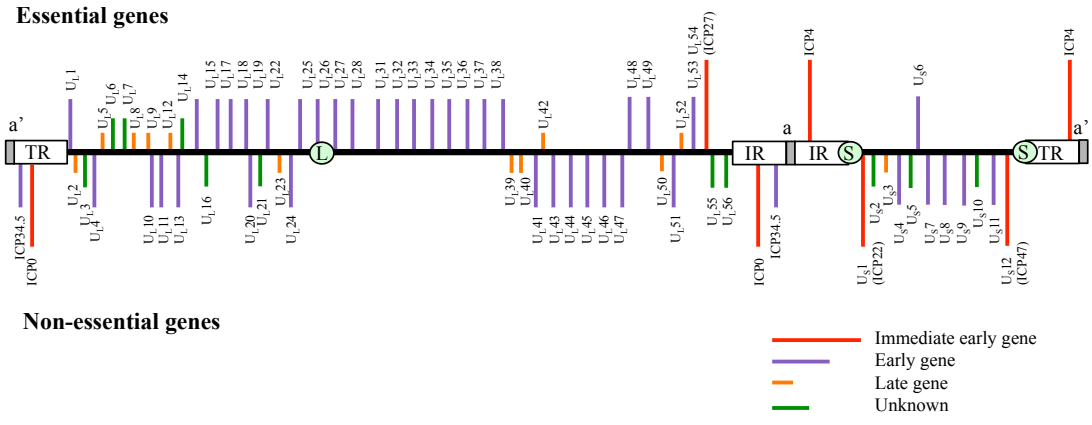

Figure 2. Schematic representation of HSV-1 genome

Schematic representation of the 152 kb double-stranded DNA genome of wild type HSV-1. The unique long (U_L) and the unique short (U_S) segments are shown flanked by the internal repeat (IR) and the terminal repeat (TR) which themselves are bounded by the packaging signals (a and a'). The unique origin of replication ori_L is present in the U_L segment (L

enclosed by circle) and two copies of ori_S (S enclosed by circle) are present flanking the U_S segment. The 80 genes expressed in lytic infection are indicated as essential or nonessential based on their requirement for viral replication in culture. Transcription of the viral genes occurs in three temporal phases after infection; immediate early (red lines), early (purple lines) and late (orange lines). The transcription stage of a few HSV-1 genes is not known (green lines).

2.1.3.1. Genome expression

Although HSV-1 depends on the transcriptional machinery of the host cell, the viral genome also encodes several proteins that modulate viral gene expression. HSV-1 gene products are synthesized in a coordinatedand sequentially ordered process. Based on the kinetics of their synthesis, three temporal groups of genes have been identified: immediate early (IE) or α genes, early (E) or β genes and late (L) or γ genes (**Figure 3**).[13]

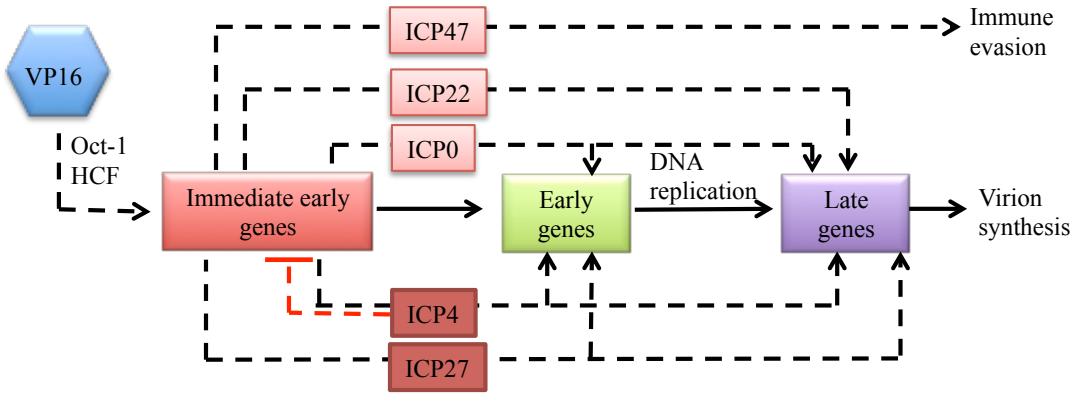

Figure 3. Expression and regulation of HSV-1 genes

Schematic diagram of the HSV-1 gene expression cascades during productive infection. VP16 interacts with Oct-1 and HCF to transactivate immediate early gene transcription. With the exception of ICP47, which is mainly involved in host immune evasion, the immediate-early gene products stimulate expression of early genes, which encode functions necessary for replication of the viral genome. Late genes are expressed after the initiation of DNA replication. Immediate early gene products thus regulate the coordinated expression of the HSV-1 genome. ICP4 and ICP27 are necessary for viral replication and transactivate the expression of early and late genes. ICP0 is a promiscuous transactivator of viral genes and in synergy with ICP4, transactivates early and late genes. ICP0 has nonetheless been described to be non essential for *in vitro* viral replication. ICP4 is also a repressor of *ICP0* and its own transcription. Although ICP22 is dispensable for viral replication in some cell types, it is important for the optimal expression of late genes.

The IE genes are the first to be transcribed in the absence of *de novo* viral protein synthesis, reaching a peak of expression between 2 to 4 hours post infection.[13]

The E genes, which encode products including enzymes and viral DNA-binding proteins necessary for replication, are transcribed only once IE genes have been expressed, and reach a peak of expression between 5 to 7 hours post infection.[13] The L genes, which mainly encode the structural polypeptides of the virion, are finally transcribed after both IE gene expression and completion of DNA replication, and reach a peak of expression between 12 to 15 hours post infection.[13]

The three groups of genes are also characterized by the structure of their promoter regions. Although IE promoters contain common eukaryotic *cis*-acting regulatory elements such as a TATA element and Sp1 response elements, the most remarkable feature of this type of promoters is the presence of *cis*-acting regulatory sequence motifs (consensus TAATGARAT, where R is a purine), responsible for the transactivation effect of virion protein 16 (VP16), a component of the viral tegument. Upon permissive infection of the host cell, VP16 is transported to the nucleus and activates transcription by binding, along with the cellular factor Oct1 and host cell factor (HCF), to the TAATGARAT element [14,15], followed by recruitment of the host RNA polymerase II transcription machinery to close proximity of IE promoters.[16,17] In contrast to IE promoters, early promoters contain a TATA box and transcription factor binding sites without the presence of virus-specific *cis*-acting regulatory elements[18], while late promoters include only the TATA element and initiator elements.[19,20]

2.1.3.2. Immediate early proteins

Among the five IE proteins (**Figure 3**), also termed infected cell proteins (ICP)- 4, 27, 0, 22 and 47, ICP4 and ICP27 have been described as essential for viral productive infection due to their crucial requirement for progression from the transcription of IE genes to the transcription of the rest of the viral genome. [21,22] ICP4 (encoded by a diploid gene) acts both as a transactivator at low-affinity sites and as a repressor at high-affinity sites at the transcription initiation signals of its own promoter and those of several other genes.[23,24,25] ICP27 acts mainly at the post-translational level by regulating the processing of viral and cellular mRNAs. [26,27,28]

Although ICP0 and ICP22 are considered as non-essential for viral growth, they enhance the transactivation of viral genes and are required for efficient lytic replication. In addition to the major role of ICP0 (encoded by a diploid gene) in viral gene transactivation and genome reactivation from latency, an important contribution

of this protein in productive infection is the suppression of host intrinsic and innate defence machinery to prevent silencing of the viral genome.[29,30,31] ICP22, on the other hand, is involved in regulation of transcription of the viral genome through phosphorylation of cellular RNA polymerase II and reorganization of host cell molecular chaperones into nuclear inclusion bodies.[32] The fifth IE protein, ICP47, also considered as non-essential for viral productive cycle, has been described as the only IE protein not involved in regulation of the viral genome expression. Instead, ICP47 interferes with host cell adaptive immunity by preventing major histocompatibility class I antigen presentation.[33]

2.2. HSV-1 derived vectors

Effective gene delivery is crucial for the success of gene therapy. The natural biology of HSV-1 makes it a promising tool for this purpose in the nervous system. In particular, this virus is capable of infecting both non-dividing and dividing cells from a wide range of hosts with high efficiency. It has evolved to be neurotropic; its survival strategy enables it to persist in neurons of immune-competent hosts in a lifelong, non-integrated latent state without causing insertional mutagenesis or disease. Notably, HSV-1 also has a large genome-packaging capacity (up to 152 kb), which widely exceeds that of most other viral vectors in current use.

Two types of HSV-1 derived vectors for gene therapy can be distinguished depending on the target tissue and purpose of the gene delivery[34,35,36,37]: 1) replication-competent vectors, which are constructed to provoke toxicity (eg. for brain tumor treatment) using viruses carrying different attenuating mutations to restrict the spread and lytic replication of the virus only to actively dividing cells without harming normal tissues; 2) replicative-incompetent vectors, constructed for therapeutic gene transfer using viruses deleted or mutated for one or more essential viral genes, thus rendering them devoid of the capacity for lytic replication (**Figure 4**).

2.2.1. Replication incompetent vectors

Replication-incompetent HSV-1 vectors, also known as recombinant replication-defective vectors, are disabled, nonpathogenic mutants unable to disseminate out of inoculated cells, but which like the wild type (WT) virus, are able to establish an intra-nuclear quiescent state in neurons. Two classes of these vectors

have been developed following different strategies: amplicon and genomic vectors.[38,39,40]

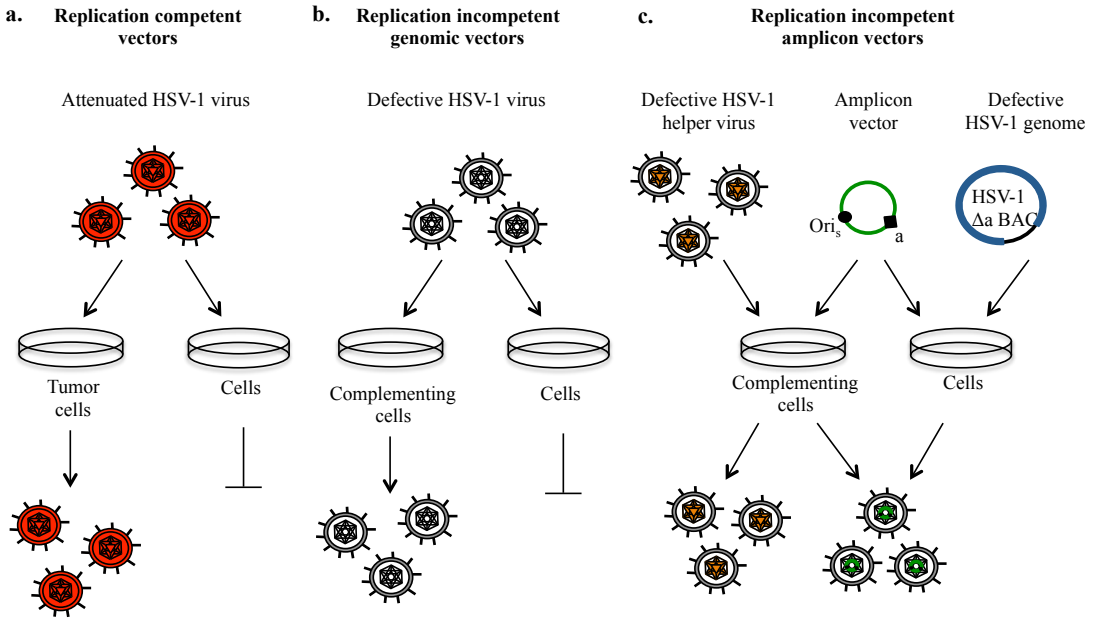

Figure 4. Production of HSV-1 derived vectors

Schematic diagram of the three different classes of HSV-1 vectors and their respective production strategies.

a. Replication-competent vectors are attenuated by removal of neuropathogenic accessory genes for targeting of brain tumors without harming normal brain tissue. These vectors are propagated by infection of tumor cells.

b. Replication-incompetent genomic vectors are deleted for one or more essential viral genes and must be grown in cell lines that complement these deleted functions *in trans*. Infection of non-complementing cells will not allow viral replication.

c. Replication-incompetent amplicon vectors are plasmids that contain the HSV-1 origin of replication (ori_S) and packaging (a) sequences. Two main strategies can be performed to produce amplicon vectors: transfection of the amplicon DNA and infection with a defective helper virus, which supplies viral functions needed to replicate the amplicon DNA in complementing cells, thus generating helper and amplicon viruses; or co-transfection of the amplicon DNA and a bacterial artificial chromosome (BAC) DNA carrying the HSV-1 genome without the packaging (Δa) sequences, thus generating helper-free amplicon viruses.
Two main helper systems have been developed: using replication-defective helper viruses, which are deleted for an essential gene; or using the HSV-1 LaLdeltaJ helper viruses which in addition to be deleted for the essential *ICP4* gene and the *ICP34.5* gene, carry a unique and ectopic packaging signal flanked by two *loxP* sites. The LaLdeltaJ helper viruses supply viral functions needed to replicate the amplicon DNA in complementing cells expressing Cre and to generate amplicon viruses less contaminated with helper viruses.

2.2.1.1. Amplicon vectors

Consecutive high-dose passages of HSV-1 result in generation of defective viral particles which interfere with viral stocks and carry only a minimal subset of DNA sequences from the WT genome. Genomes from these defective particles include the HSV-1 origin of DNA replication and cleavage/packaging site but have lost the complete set of lytic functions needed to support productive virus replication.[41] These observations led to the creation of amplicon vectors, plasmids carrying these minimal HSV-1 sequences that allow them to be packaged into virus particles with the aid of replication-defective HSV-1 mutants (helper viruses) or packaging-defective HSV-1 genomes cloned as plasmids.[38,42] The absence of almost the entire viral genome, and therefore the lack of expression of any viral proteins, has conferred upon these vectors ideal features for gene transfer: transgene capacity up to around 150 kb of foreign DNA; absence of cytotoxicity and pathogenesis; and as simple plasmids, easy handling and construction. However, complexity of their production remains a major obstacle to overcome for large-scale production of high titer amplicon vectors.

2.2.1.2. Genomic vectors

A second strategy for the generation of nonreplicative HSV-1 derived vectors takes advantage of the hierarchical cascade organization of gene expression from the viral genome. Two major approaches have been followed to inactivate the virus for the generation of so-called genomic vectors by disabling components which initiate the lytic cycle: the VP16 protein and IE gene expression.

In the first case, mutations have been introduced to abolish the capacity of the VP16 protein to transactivate IE gene expression while maintaining its essential structural function required for virion assembly.[43,44] Although propagation of such vectors was initially achieved by growth in cells supplemented with a compound with stimulatory activity of IE gene expression (Hydroxymethyl bisacetamide (HMBA))[45], a more efficient system has been developed using cell lines expressing the equine herpes virus homolog of VP16, following the discovery that this protein can transactivate the HSV-1 IE genes without being packaged into HSV-1 virions.[46]

The second approach for generating nonreplicative genomic vectors is based on the fact that deletion of the IE gene *ICP4* results in an impaired expression of early and late gene products and does not produce infectious viral progeny.[23] Nonetheless,

this mutant is highly cytotoxic.[47] Deletion of the other essential IE gene *ICP27* has been shown to drastically further reduce levels of early and late gene expression.[48] However infection with such modified HSV-1 viruses remains toxic to cells in culture, which was hypothesized a consequence of the expression of the other IE gene products ICP0 and ICP22.

After additional inactivation of either *ICP22*[49] or *ICP0*[50] decreased levels of cytotoxicity were observed, thus forming the basis for the generation of multiply deleted HSV-1 genomic vectors[51] including a mutant which was simultaneously deleted for the five IE genes.[52] This mutant was shown by several criteria to be non-toxic in all infected cell types and silent for transcription of nearly all the viral genes.

Almost 30 years of development culminated in the first use of a nonreplicative genomic HSV-1 vector inactivated for ICP4, ICP27, ICP22, and ICP47, in human clinical trials for treatment of cancer-related pain.[53] This study demonstrated that the vector, which has now been administered to more than 30 patients, did not produce any vector-related adverse effects when delivered to the dorsal root ganglia (DRG) by skin inoculation.

2.2.1.2.1. Production of genomic vectors: complementing cell lines

Since nonreplicative genomic vectors are deleted for genes essential for viral growth in culture, the generation of complementing cell lines, which provide the missing gene products *in trans*, is clearly a critical step to produce and amplify these vectors. However, constitutive cellular expression of many of these essential functions is cytotoxic, thus posing an obstacle for generating stable cell lines modified with these genes. Nonetheless, this problem has been overcome by using inducible promoters that are responsive to viral infection, such as some of the HSV-1 IE promoters. In uninfected cells stably transfected by these promoters, the expression of the complementing protein is shut off, and only activated by the virion protein VP16 upon infection. However, engineering of such complementing cell lines remains a challenge due to the lack of control over the copy number of complementing genes that will integrate, or their position in the cellular genome; both of these variables affect the final expression level and kinetics of these genes.

Vero, BHK and U2OS have been some of the cell lines engineered to complement ICP4, ICP27 and ICP0 alone or in combination[46,48,50,51,52,54,55,56] although no cell line complementing the absence of all the IE genes have been

generated to date.

2.2.1.2.2. Transgene expression in neurons from genomic vectors

Identifying promoter elements capable of directing sustained, long-lasting gene expression in neurons from non-replicative genomic HSV-1 vectors has proved challenging. Viral promoters such as the cytomegalovirus (CMV) IE promoter or HSV-1 IE and E promoters, have been shown to direct strong, but transient gene expression, being subject to silencing upon establishment of latency in infected neurons.[57,58,59]

In neurons the viral genome is silenced with the exception of the latent associated transcripts (LAT).[60,61] Thus, the LAT locus region escapes the general cellular suppression of the activity of HSV-1 promoters during latency, becoming an ideal candidate for transgene expression in the context of HSV-1 genomic vectors. The most abundant 2-kb LAT is a stable intron [62,63] with one promoter element (latency associated promoter 1, LAP1) located 700 bp upstream of the intron[64] and a second (LAP2) located downstream of LAP1 and just proximal to the LAT intron.[65] Elements of the region active in latency including both LAP1 and LAP2 have been confirmed capable of sustaining functional transgene expression even at genomic locations outside of the latency locus and for extended times in the central and peripheral nervous system.[58,65,66,67,68,69,70]

Non-viral promoters have been less well studied in the context of nonreplicative genomic vectors although recently, a cellular injury-specific promoter (galanin promoter)[71] was shown to drive functional transgene expression in the spinal cord of mice after viral vector administration by injection into the plantar hind paw. Also of interest, the use of inducible promoters such as the Tet-inducible system has been studied to control transgene expression in HSV-1 genomic vectors[72,73,74] although their leakiness remains an obstacle.[75,76,77]

2.3. Friedreich's ataxia (FRDA)

2.3.1. Introduction

Friedreich's ataxia [FRDA; OMIM229300] is a predominantly neurodegenerative disorder named after German physician Nikolaus Friedreich, who

first reported the condition and its clinical and pathologic features during the 1860s and 1870s.[78,79,80,81,82] This autosomal and recessive disease is the most common form of hereditary ataxia [83] and is caused by mutations in the frataxin gene (*FXN*), which lead to a partial deficiency of the encoded mitochondrial frataxin protein (FXN).[84] FRDA primarily affects Caucasians and disease incidence is estimated at 2-3:100.000 in the Western European population with 1 carrier per 100 people.[85] Symptoms usually appear late in the first decade of life and mainly include progressive gait and limb ataxia, sensory loss, dysarthria, dysmetria, dysphagia, muscular weakness, visual loss, and hearing deficit.[86,87] In addition, patients develop non-neurological manifestations such as risk of hyperglycemia, diabetes mellitus and development of hypertrophic cardiomyopathy. [83,88] Within 20 years after the first appearance of symptoms, affected individuals are confined to a wheelchair and most commonly die in early adulthood from the associated heart diseases.[89] There is currently no treatment for FRDA.

2.3.2. FRDA pathophysiology

FRDA is a severe disease affecting peripheral and central nervous systems, heart, endocrine pancreas and skeleton.

2.3.3. Neuropathological features

Clinical symptoms and neurological examinations [86,87,90,91] indicate that FRDA corresponds to a mixed sensory and cerebellar ataxia, which affects the proprioceptive pathways in the peripheral nervous system, spinal cord, and nuclei of the cerebellum.

2.3.3.1.1. Peripheral lesions

Atrophy of the dorsal root ganglia (DRG) is a major hallmark of FRDA with a reduction in the overall size of nerve cells and loss of large neurons. As the disease progresses, neuronal destruction becomes manifest by satellite cell proliferation coupled with the formation of residual nodules, clusters of nuclei from residual neurons and a thickened rim of ferritin-positive cells. Both DRG neurons and satellite cells exhibit iron dysmetabolism.[92,93,94] Where the primary pathological process occurs is still uncertain. Neuropathy of peripheral sensory nerves also contributes to the disability of FRDA patients. Observations on the sural nerves of FRDA patients showed loss of large myelinated fibers and degeneration of large axons in the

DRG[95,96]; this axonopathy has been associated with a dying back mechanism.[97,98] Further studies have recently suggested a critical role of Schwann cells in this afferent neuropathy although no clear evidence on the primary involvement of these cells exists. [99]

2.3.3.1.2. Spinal cord and brainstem lesions

An anterograde effect of axonal neuropathy provokes degeneration of the posterior column; atrophy is observed in the dorsal spinocerebellar fibers and nerve cells of Clarke's column, where the spinocerebellar tracts originate. In the dorsal column, medial, gracile and cuneate nuclei show trans-synaptic degeneration with intense gliosis. Although peripheral motor neurons are not affected, atrophy of pyramidal Betz cells and corticospinal tracts constitute secondary intrinsic lesions.[91,98,100]

2.3.3.1.3. Cerebellar lesion

The main lesions in the brain of FRDA patients are found in the dentate nucleus of the deep cerebellar nuclei with progressive and selective atrophy of large glutamatergic neurons and proliferation of corticonuclear synaptic terminals, termed grumose degeneration.[101] Moreover, the dentate nucleus is small and has a high concentration of iron that is not properly removed from the affected brain tissue. In contrast, Purkinje cell somata and dendrites in the cerebellar cortex remain intact.[102]

2.3.3.2. Non-neuropathological features

Heart disease in FRDA evolves independently of the neurological manifestations of FRDA and sometimes may precede it.[90,103,104] Cardiac dysfunction, which develops during the fourth decade of patient lifetime, is present in more than 90% of the patients and is the most frequent cause of death, most commonly from congestive heart failure or arrhythmia.[83,89,103] Pathological changes are observed in the left ventricle mainly including cellular hypertrophy, diffuse fibrosis, and focal myocardial necrosis.[102,105,106] Intra-cytoplasmic granular deposits of iron were observed in histological studies of necropsic hearts.[107]

In FRDA patients, the incidence of diabetes mellitus and glucose intolerance is estimated to be around 10% and 30% respectively.[86,90] Furthermore, skeletal deformities are very common in FRDA patients including pes cavus (hammer toes) and kyphoscoliosis (abnormal lateral and posterior curvature of the vertebral

column).[86,90]

2.3.4. The frataxin gene (*FXN*)

The *FXN*, located at chromosome 9q21.11 [OMIM 606829], is transcribed in the centromere-to-telomere direction and has 7 exons spread over 80 kb of genomic DNA: the coding exons 1, 2, 3, 4, together with the alternate exons 5a and 5b, and a sixth non-coding exon.[108]

Factors controlling *FXN* transcription are not completely understood. Two transcription start sites (TSS), designated TSS1 and TSS2, have been identified at 221 base pairs (bp) and 62 bp upstream of the TSS, respectively.[84] Moreover, two transcription factors, the serum response factor (SRF) and transcription factor activator protein 2 (TFAP2), have been reported to bind directly to the region between TSS1 and TSS2 and regulate *FXN* expression.[109] An early study with reporter luciferase constructs in mouse skeletal muscle cells suggested that FXN promoter activity is contained within the first 1,255 bp immediately upstream of exon 1[110] although later findings showed that an extended region, comprising 5,577 bp upstream of exon 1, indeed contains important regulatory elements essential for maximal *FXN* gene expression.[111] This region includes a highly conserved non-coding region, which allocates a 17 bp sequence (between 4,944 bp and 4,961 bp) containing an Oct-1 binding site, and was shown to be sufficient and necessary for fully *FXN* expression.

The implication of the sequences within intron 1 in regulation of the *FXN* expression has been also reported and mapping of the region immediately upstream of GAA repeats (724 bp) identified sequences that enhance *FXN* promoter activity (**Figure 5**).[109,112,113]

2.3.4.1. *FXN* expression

Three different *FXN* transcripts were primarily described. Among them, the most abundant (*FXN* isoform I; FXN-I) is composed by exons 1-4 and 5a (NM_000144) and encodes for a 210-amino acids protein (NP_000135) (**Figure 5**).[84] A second minor alternative transcript was described to contain exon 5b in place of exon 5a (NM_001161706), sometimes followed by the noncoding exon 6, and to encode a shorter protein of 171 amino acids (NP_001155178). A third splice variant of *FXN* was identified to be composed of exons 1–4 and 5a (NM_181425) but differs from isoform I by an insertion of 8 bp due to an alternative splice site at the 5′ end of

intron 4. The 8 bp insertion generates a frame shift that introduces a stop codon, so that this transcript encodes a shorter protein of 196 amino acids (NP_852090).[114,115] These second and third transcripts have not been studied in detail and no functional data about these protein isoforms have been reported. The functional significance of these three transcripts is still uncertain.

Recently, two novel *FXN* transcript variants have been identified encoding isoform II (FXN-II) and isoform III (FXN-III) (**Figure 5**).[116] These transcripts differ from isoform I in the amino terminal (N-terminal) region encoded by the first exon while exons 2-5a are present in all three *FXN* isoforms. Alternate splicing was shown to generate either an intact exon 1, contained in *FXN* isoform I; exon 1 lacking 141 nucleotides, contained in a *FXN* transcript encoding a 164 amino acid protein (isoform III); or an exon 1B lacking 18 nucleotides and contained in a *FXN* transcript encoding a protein of 135 amino acids (isoform II). Furthermore, contrary to the mitochondrial localization of the canonical isoform I, isoform II exhibits cytoplasmic expression in the central nervous system and isoform III, nuclear localization in the heart. Further functional analyses have pointed to their implication in the metabolism of iron-sulfur (Fe-S) clusters, suggesting a complementary role with isoform I and a direct mechanism by which FXN deficiency could cause tissue-specific pathology in Friedreich's ataxia.[116]

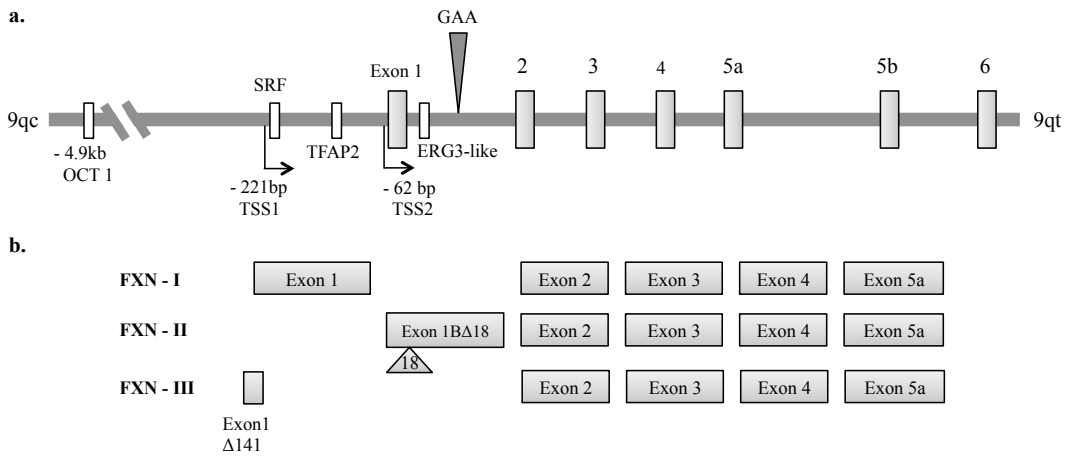

Figure 5. Schematic representation of the human *FXN* genomic locus and *FXN* isoforms I, II and III

a. Schematic (not to scale) representation of the genomic structure of the human *FXN* locus on the long arm of chromosome 9 with centromeric (9qc) to telomeric (9qt) orientation

indicated. *FXN* contains seven exons: exons 1, 2, 3, 4, alternate exons 5a/5b, and a sixth non-coding exon (gray vertical boxes). Localization of the trinucleotide guanine-adenine-adenine repeats (GAA) is shown in intron 1, the expansion of these triplet repeats being identified as the major cause of FXN depletion in FRDA. Two transcription start sites TSS1 and TSS2 (black arrows with arrow heads representing the direction of the transcription) are shown located at 221 base pairs (bp) and 62 bp upstream of the translational start site (ATG), respectively. Several protein-binding sites (white vertical boxes) known to be important for *FXN* regulation include sites for the octamer binding transcription factor 1 (OCT1), the serum response factor (SRF), the transcription factor activator protein 2 (TFAP2) and the early growth response protein 3-like factor (EGR3-like).
b. Schematic representation of three of the *FXN* transcript variants described. Exons 1-5a encode the canonical *FXN* isoform (FXN-I). Exons 1B**Δ**18-5a encode the predominantly nervous system-expressed *FXN* isoform (FXN-II). Exons 1**Δ**141-5a encode the predominantly heart-expressed *FXN* isoform (FXN-III).

The *FXN* gene is considered ubiquitously expressed at a relatively low level even in healthy individuals.[117,118] Transcript variants and levels of *FXN* mRNA as well as FXN protein show specificity to tissues with high mitochondrial content such as the brain, heart, pancreas, skeletal muscle, liver and brown adipose tissue[119] a distribution which partially correlates with the sites of the disease. The basis of the differential sensitivity of tissues to FXN deficiency is not clear but it has been suggested that it depends on cell type-specific metabolic pathways, the somatic instability of expanded GAA triplet repeats and tissue-specific *FXN* isoforms.[116,120,121,122,123,124] Highlighting the importance of FXN in development, mice lacking FXN display embryonic lethality early in gestation.[125] On the other hand, over-expression of *FXN* was shown to be toxic in cultured fibroblasts and in a Drosophila model, thus suggesting the importance of a fine balance in *FXN* regulation.[126,127]

2.3.5. FRDA mutations: GAA Repeat Expansions

The *FXN* gene is unique in the human genome in that normal alleles contain up to 66 uninterrupted guanine-adenine-adenine (GAA) trinucleotide repeats within intron 1. Approximately 98% of individuals suffering from FRDA have between 67 to over 1300 GAA repeats in both *FXN* alleles, with a minority of 2% of the patients having expansions in only one allele and a point mutation in the coding region of the other.[84] This repetitive sequence in intron 1 plays an important regulatory role in *FXN*, with the number of GAA repeats higher than the pathological threshold

resulting in impaired *FXN* transcription.[84] Relative to healthy individuals, *FXN* is expressed in FRDA patients at 5-30% of normal levels.[115,120] Furthermore, an inverse correlation has been described between the size of the expanded GAA sequence and *FXN* transcript levels, the amount of residual FXN produced and the age of onset of FRDA symptoms.[128]

2.3.5.1. Effect of the GAA repeat expansion on *FXN* expression

Although there is still some debate about the exact cause of FXN depletion in FRDA, some mechanisms have been proposed to contribute. These include GAA repeat-dependent structural changes in the DNA, which physically block the transcriptional machinery[129,130,131]; and epigenetic modifications, such as higher levels of DNA methylation[132,133], heterochoromatinization and altered histone modifications in the intronic region surrounding the expanded repeats. [112,134,135,136]

Since the size of the triplet expansion accounts only for 50% of the variability in the age of onset for FRDA [128] other factors have been proposed to impact on the disease including toxic RNAs, repeat-associated proteins, aberrant splicing, and altered expression of *FXN* isoforms.

2.3.6. Frataxin protein (FXN)

FXN is a predominantly mitochondrial and highly conserved protein with homologs present in gram-negative bacteria, yeast, *Caenorhabditis elegans* and mammals.[137,138,139,140]

2.3.6.1. FXN structure and processing

The human *FXN* gene encodes a 210 amino acids poly-peptide (23 kDa), the precursor form of FXN. After translation of this nuclear gene product in cytoplasmic ribosomes, an N-terminal targeting signal encoded by the first 20 amino acids [120] directs transport of the precursor protein into the mitochondria [139,141] to undergo two-step proteolytic processing, mediated by the mitochondrial processing peptidase (MPP).[142,143] MPP first cleaves the precursor form to remove the 20 N-terminal residues, containing the mitochondrial signal peptide. This is followed by the generation of an intermediate form of 19 kDa cleaved between G41 and L42 (residues 42–210), which is then converted into a mature soluble form found within the mitochondrial matrix.[143]

Identification of the site involved in the second step of processing to generate

the mature form remains a controversy. *In vivo* experiments have established that a FXN form termed m81-FXN (14.3 kDa) is the normal mitochondrial mature form in living cells and the most abundant species both in normal individuals and in FRDA patients. However, two other mature forms termed m56-FXN (17.2 kDa) and m78-FXN (14.7 kDa) can be produced *in vivo* when normal processing is impaired or when processing is carried out *in vitro* although the physiological relevance is not clear.[143,144,145]

2.3.6.2. FXN function

A clear essential cellular function of the FXN protein is still not fully established but it has been generally accepted to be a multi-functional protein with a major role in the regulation of cellular iron homeostasis. FXN has been described as a metallochaperone that can bind iron to supply iron-dependent metalloenzymes such as the Fe-S cluster protein aconitase [146]; the penultimate protein in heme biosynthesis, ferrochelatase[147], and complex II of the respiratory chain, succinate dehydrogenase.[148] FXN also binds the cysteine desulfurase Nfs1 and scaffold protein Isu, which are components of the Fe-S cluster assembly complex.[149]

Mitochondria are present in every cell type, but are especially important in the nervous system. This organelle is essential for cellular biochemistry and ATP generation as well as being a well-known location for dynamic electron transport and redox chemistry. Furthermore heme and Fe-S cluster biosynthesis are the two major iron-related metabolic processes in the mitochondrion for delivery, storage and usage of iron. Therefore, FXN has a direct impact on mitochondrial function and the respiratory chain.[119,148]

2.3.7. FRDA molecular pathology

The clinical and pathological phenotype of FRDA has been widely accepted to be caused by decreased levels of FXN which leads to several biochemical imbalances such as impaired Fe–S cluster synthesis, resulting in the dysfunction of respiratory chain complexes and aconitase, mitochondrial iron overload coupled to cellular iron deregulation and oxidative stress hypersensitivity.[121,150,151,152,153,154] However, the primary dysfunction in FRDA pathogenesis is still uncertain and affected pathways and functions show a distinct pattern in different organs and tissues.

2.3.8. Therapeutic approaches

Currently, no therapy has proven effective in treating FRDA or slowing its progression; however, numerous approaches have been trialed and others are in various phases of development and testing.[155] These approaches can be classified based on two criteria, the nature of the treatment, divided into drug-based therapies and gene therapies; and the therapeutic target, divided into therapies against pathogenic cascades downstream of FXN deficiency and therapies to increase *FXN* expression.

2.3.8.1. Pharmacological therapies

Pharmacological compounds include: 1) antioxidant compounds such ascoenzyme Q, its synthetic analog idebenone, deuterated polyunsaturated fatty acids (D-PUFAs), and resveratrol; 2) iron-chelating compounds like deferiprone; 3) epigenetic modifying compounds like benzamide histone deacetylase inhibitors orinterferon gamma; 4) FXN stabilizers and enhancers including erythropoietin and ubiquitin; and 5) neurotrophic factors such as insulin-like growth factor-1.[156] Several pharmacological agents have shown promising results in animal and cellular models but to date none have revealed conclusive and definitive therapeutic benefits in clinical trials.

2.3.8.2. Gene Therapy

Gene therapy of monogenic diseases resulting from a loss of function of an essential protein such as FRDA, can be approached directly by the introduction of a transgene into target cells to induce or express viable levels of the missing protein.

2.3.8.2.1. Non-viral delivery systems

Several technologies for activation of the inhibited *FXN* gene are currently emerging and mainly include: transcription activator-like effector protein (TALE) engineered to bind to the *FXN* promoter [157] and fused to a transcription activation domain (VP64); zinc finger nuclease-mediated approaches to excise the expanded GAA repeat region from the *FXN* gene[158]; and anti-GAA duplex RNAs or single-stranded locked nucleic acids which interfere with R-loop formed between the expanded repeat RNA and complementary genomic DNA.[159] Finally, *in vivo* intrathecal delivery into the DRG of *FXN* mRNA encapsulated in lipid particles was recently demonstrated.

2.3.8.2.2. Viral delivery systems

In early studies, expression of human *FXN* (h*FXN*) complementing DNA (cDNA) coupled to the cytomegalovirus promoter (CMV) and cloned into both a lentiviral vector (LV) and an adeno-associated viral vector type-2 (AAV2), was able to partially reverse the increased sensitivity to oxidative stress of fibroblasts derived from FRDA patients.[126] However, total rescue to the normal phenotype was not achieved and it was postulated by the authors that this may be because overexpression of *FXN* in cultured primary fibroblasts is toxic.

More recent studies with AAV vectors have reported encouraging results for the cardiac symptoms of FRDA.[160] In these studies, intravenous injection of AAV vectors of serotype sh10 (cardiotropic serotype) expressing the h*FXN* cDNA driven by the CAG promoter was shown to prevent and reverse severe cardiomyopathy in a mouse model with complete FXN deletion in cardiac and skeletal muscle (The CAG promoter consists of the enhancer from the cytomegalovirus immediate-early gene, the promoter, splice donor and intron from the chicken β-actin gene, and the splice acceptor from the rabbit β-globin gene). Treated asymptomatic mice remained indistinguishable from WT mice at 35 weeks of age. Moreover, recovery of 7 week untreated mice with advanced cardiac insufficiency showed a cardiac phenotype that correlated with strong expression and normal mitochondrial localization of hFXN in the heart at 1 week to 22 weeks after treatment. However, the development of severe peripheral striated muscle atrophy and kyphosis, attributed to a low level of *hFXN* transgene expression in skeletal muscle of the mouse model, led to the death of several of these mice. Notably, transgene expression was robust not only in heart, but also in the liver of treated mice, although no adverse effects were reported from this FXN overexpression.

In agreement with these results, another group has also demonstrated that intraperitoneal injection in a FRDA mouse model of an AAV vector of serotype 9 (also cardiotropic serotype) expressing the *hFXN* cDNA, increased life expectancy up to threefold.[161] In this mouse model with complete ablation of the mouse *FXN* gene in the heart and a partial ablation in the muscle, liver, kidney, and brain, robust expression of hFXN was detected in the heart, liver and skeletal muscle. In the brain however, hFXN was detected at much lower levels and only with the highest viral dose assayed. Injected mice developed nervous pathological symptoms, which were attributed to insufficient expression of FXN in the brain of the mice during early

embryogenesis.

A proof-of-concept study using helper-dependent HSV-1 amplicon vectors showed that *FXN* cDNA expression driven by the HSV-1 IE4/5 promoter was able to reverse neurological defects to restore motor coordination in a localized FRDA mouse model generated and treated by stereotaxic injection in the brainstem.[162] Despite these encouraging results the duration of the effect was transient. As this transience of transgene expression was mainly attributed to the fact that viral immediate-early promoters were used, subsequent studies took advantage of the large packaging capacity of amplicon vectors to deliver the entire human FRDA genomic locus, thus maintaining the native promoter, enhancer, and silencer elements, similar to that of the native chromosomal gene. [163] FRDA patient fibroblasts transduced with this FXN vector showed a physiological level of FXN expression and functional restoration of the WT cellular phenotype in response to oxidative stress.

In a second study with these viral vectors encoding the entire FXN locus, long-term persistence of hFXN expression in the brain was observed after stereotaxic injection into the adult mouse cerebellum.[164] Interestingly, transgene expression driven by the *FXN* locus was shown to persist for at least 75 days at approximately the same levels, while injection of a control amplicon vector carrying a *GFP* reporter gene driven by the HSV-1 IE4/5 promoter showed transient transgene expression which decreased down to 20–50% during the same period. Moreover, delivery of the 135 kb *hFXN* genomic DNA locus by amplicon vectors was recently shown to give rise to the different frataxin isoforms both *in vitro* and *in vivo*[165], supporting the potential use of HSV-1 vectors containing the human *FXN* genomic locus for FRDA therapeutic applications.

Results from these studies indicate that increasing FXN levels can improve phenotype and ultimately clinical outcome, encouraging further studies testing the corrective potential of these gene therapies for FRDA. Finally, promising data in FRDA animal models has also been obtained using a number of FRDA gene therapy strategies to deliver other transgenes, such as HSV-1 amplicon vector delivery of the gene encoding brain-derived neurotropic factor (BDNF)[166] or AAV9 vector delivery of the TALEs proteins.[167]

OBJECTIVES

3. OBJECTIVES

The overall aim of this dissertation was to test the hypothesis that a novel nonreplicative genomic HSV-1 vector is able to deliver and maintain the expression of a human frataxin (*FXN*) transgene in the dorsal root ganglia to develop a gene therapy for the neurological symptoms of Friedreich's ataxia (FRDA).

A recombinant nonreplicative genomic HSV-1 vector used in a recent clinical trial demonstrated an excellent safety profile even at high doses.[53] However, the transgene capacity of this vector is limited to approximately 10 kb which restricts its use for delivery of large sequences such as the *FXN* genomic locus previously used by our group in preclinical experiments. To test if an increased transgene capacity can be achieved without compromising scalable high-titer vector production, we deleted further HSV-1 genome sequences and analysed the *in vitro* effects of these deletions on the growth capacity of the resulting vectors.

Since the human *FXN* genomic locus fragment we previously used may be larger than necessary for gene therapy, we generated a construct comprising the 5 kb promoter and the *FXN* cDNA with the inclusion of intron 1. To test *in vitro* if this reduced genomic *FXN* transgene retains the regulatory elements necessary to preserve the physiological neuronal regulation, we analysed the *FXN* alternative splicing as well as the FXN protein expression in a neuronal cell line.

The trimmed human *FXN* transgene was coupled to the new high capacity non-replicative genomic HSV-1 vector. To test if the resulting recombinant mutant preserves the main characteristics of both the transgene and the vector, we first analysed *in vitro* the transgene expression in the context of the genomic vector in fetal rat dorsal root ganglion neurons. Finally, we examined the transgene delivery and expression in the dorsal root ganglia following inoculation of rat footpads.

My approach consisted of the following specific aims:

I. To generate a nonreplicative genomic HSV-1 vector with a 23 kb genome deletion while retaining its growth capacity.

II. To generate a reduced version of the human *FXN* genomic locus while maintaining the elements necessary to undergo physiological neuronal regulation.

III. To determine if the generated nonreplicative genomic HSV-1 vector carrying the reduced version of the human *FXN* genomic locus is able to deliver and sustain the human *FXN* transgene expression in dorsal root ganglia after rat footpad inoculation.

MATERIALS AND METHODS

4. MATERIALS

4.1. Reagents

Dulbecco's Modified Eagle Medium (DMEM), Neurobasal Medium, Leibovitz's L-15 Medium, Opti-MEM, TrypLE and Trypsin-EDTA were purchased from Gibco/Life Technologies, Paisley, UK. Antibiotics used in cell cultures and bacterial cultures (penicillin G, streptomycin sulfate, zeocin, ampicillin, kanamycin, tetracycline, chloramphenicol, G418), L-arabinose, doxycycline hyclate (Dox), nerve growth factor (NGF), fluoro-2deoxy-uridine (FDU), uridine, poly-D-lysine, Ketamine and Xylazine were purchased from Sigma-Aldrich (St. Louis, MO). B-27, Glutamax I, Albumax I supplements and laminin were obtained from Gibco/Life Technologies (Grand Island, NY). Fetal bovine serum (FBS, product number F7524) and Isopropylβ-D-1-thiogalactopyranoside (IPTG) and 5-bromo-4-chloro-3-indolyl-β-D-galactopyranoside (X-Gal) were from Sigma-Aldrich (St. Louis, MO) whereas TRIzol, Lipofectamine-LTX and Plus reagents were purchased from Life Technologies (Carlsbad, CA).

4.2. Bacterial strains

Strain	**Genotype**	**Source/ Ref**
DH10B	F– mcrA Δ(*mrr-hsd*RMS-*mcr*BC) Φ80dlacZΔM15 ΔlacX74 *end*A1 *rec*A1 *deo*R Δ(*ara,leu*)7697 *ara*D139 *gal*U *gal*K *nup*G *rpsL* λ-	(Durfee et al, 2008; Grant et al, 1990)[168,169]
DH5α	F– Φ80*lac*ZΔM15 Δ(*lac*ZYA-*arg*F) U169 *rec*A1 *end*A1 *hsd*R17 (rK–, mK+) *pho*A *sup*E44 λ–*thi*-1 *gyr*A96 *rel*A1	(Taylor et al, 1993)[170]
PIR1	F– *Δlac169 rpoS(Am)*	Life Technologies

	robA1 creC510 hsdR514 endA recA1 uidA(ΔMluI)::pir-116	(Carlsbad, CA), catalogue number-C1010-10

4.3. Cell lines

Cell line	Origin	Culture Media	Source/Ref of the plasmid used for construction of stable cell lines
Vero	African green monkey kidney epithelial cell line	F10 medium consisting of DMEM supplemented with 10% FBS, 100U/ml penicillin G and 100 µg/ml of streptomycin sulfate	ATCC* CRL 1586 (Earley EM et al, 1988)[171]
2-2	Vero cell line expressing the *ICP27* gene	F10 medium supplemented with G418 (500µg/ml)	(Smith et al, 1991)[172]
E5	Vero cell line expressing the *ICP4* gene	F10 medium supplemented with G418 (500µg/ml)	(DeLucca & Shaffer 1987)[54]
7b	Vero cell line expressing both the *ICP27* and the *ICP4* gene	F10 medium supplemented with G418 (500µg/ml)	(Krisky et al, 1998)[51]
Neuro-2a	Mouse neuroblastoma cell line	F10 medium	ATCC* CCL 131 (Klebe and Ruddle, 1969)[173]
HEK-293	Human embryonic kidney cell line	F10 medium	ATCC* CRL 1573 (Graham et al, 1977)[174]

SH-SY5Y	Human bone marrow neuroblastoma cell line	F10 medium	ATCC* CRL 2266 (Biedler et al, 1978)[175]

*ATCC is the registered trademark of the American Type Culture Collection.

4.4. Plasmids

Plasmid	**Selection marker**	**Source / Ref**
FXN-WT BAC	Choramphenicol	(Gomez-Sebastian 2007)[163]
pBluescriptKSII(+)	Ampicillin	(Alting-Mees & Short, 1989)[176]
pCTP-T	Tetracycline	(Saeki et al, 2001)[177]
pDRIVE-CAG	Zeocin	Invivogen, San Diego, CA
pGEMT Easy	Ampicillin	Promega, A1360
pGZI27Spe	Ampicillin Zeocin	Polymerase chain reaction (PCR) amplified *Sh ble* gene using primers PACSPE and I27DZ cloned into pGEMT Easy vector
pHG	Ampicillin	(Saeki et al, 2001)[177]
pLCG	Ampicillin	*EcoRI/BgIII* pUcCombi_CMV blunted with Klenow and religated into *Bam*HI/*Nru*I pLOsG
pLCG-ZEO	Zeocin	PCR amplified *Sh ble* gene

		using primers PACSPE and R7 cloned into pLCG
pLOsG	Ampicillin	*Sal*I/*Spe*I pHG blunted with Klenow and religated in presence of dNTPs
pLVfrat	Ampicillin	(Fleming et al, 2005)[126]
pSK+Kana-RPSL	Ampicillin, Kanamycin	Addgene, Cambridge MA, (Wang et al, 2009)[178]
pSKC481.9	Ampicillin	*Xho*I/*Eco*RI Cos48 ligated into pBluescriptSK
pSKOrisZ	Zeocin	*Not*I/*Spe*I pGZI27Spe cloned into *Not*I/*Spe*I pSKC481.9
pUcCombi_CMV	Kanamycin	(Schultze N et al, 1996)[179]

4.5. Virus

The parental virus strain used in this study was strain F of HSV-1.[180] The viral genome of strain F cloned in a bacterial artificial chromosome (BAC) plasmid[181] was used for the construction of all the mutants.

4.6. Oligonucleotides

PCR: Red/ET recombination		
Primer	**Sense**	**Sequence (5'-3')**
FL5111K	Backward	TGGAATGCAATTTGATACATCACCTTAAT ATTAATATAGATTAAATTCAT**ATAACTTC GTATAATGTATACTATACGAAGTTAT**CAG

		AAGAACTCGTCAAGAAGGC ***loxP511***
I43P	Backward	GCCACAGGTGAAACCAACAGAGCACGGCGC ACTCCGCACGTCACACGTCATTAATTAATCA GAAGAACTCGTCAAGAAGGCGAT
I45P	Forward	TCTAGAAAGCATCGACCGGTCCGCGCTAGT TCCGCGTCGACGGCGGGGGTCGTCGGTTAA TTAAGTTTTATGGACAGCAAGCGAACCGG
I4OS5	Forward	TCTAGAGTCTGCGGGCGTCGGTCGCGCCGG GCCTTTATGTGCGCCGGAGAGACCCGTTAA TTAAGTTTTATGGACAGCAAGCGAACCGG
I27DZ	Forward	CTCGAGACGCGTCATATGCAAATGAAAATC GGTCCCCCGAGGCCACGTGTAGCCTGAATT AAATTTTTCAAAAGTAGTTGAC
I27DA	Forward	ACGCGTCATATGCAAATGAAAATCGGTCCC CCGAGGCCACGTGTAGCCTGGCACTTTTCG GGGAAATGTG
IRTGA	Backward	CGGCGGGCGGGACCGGGGGCCCGGGGACG GCCAACGGGCGCGCGGGGCTCCAGTTACCA ATGCTTAATCAG
IRTGZ	Backward	CGGCGGGCGGGACCGGGGGCCCGGGGACG GCCAACGGGCGCGCGGGGCTCCCTTTTCTG AAACTCAATTCTTATC
PACSPE	Backward	GACTAGTTAATTAAGTTGAAAAAAGGGGCC
T7TN5	Forward	ATATTGCTCTAATAAATTTGCGGCCGCTAAT ACGACTCACTATAGGGAGAGTTTTATGGACA GCAAGCGAACCGG
US3Z	Backward	CTCGAGAAATGTCGGCCATCCAGAAAACGT CCCGGAGGACCACAGTGGCTTCCCCCCGGA TCCTATCGGTACCTTTTCTGAAACTCAATTC TTATC
Z143P	Backward	CGTCAAATTAAATTTTTCAAAAGTAGTTGAC

PCR: Red/ET recombination		
Primer	**Sense**	**Sequence (5'-3')**
FL5111K	Backward	TGGAATGCAATTTGATACATCACCTTAAT ATTAATATAGATTAAATTCAT**ATAACTTC GTATAATGTATACTATACGAAGTTAT**CAG AAGAACTCGTCAAGAAGGC ***loxP511***
I43P	Backward	GCCACAGGTGAAACCAACAGAGCACGGCGC ACTCCGCACGTCACACGTCATTAATTAATCA GAAGAACTCGTCAAGAAGGCGAT
I45P	Forward	TCTAGAAAGCATCGACCGGTCCGCG CTAGTTCCGCGTCGACGGCGGGGGT CGTCGGTTAATTAAGTTTTATGGACA GCAAGCGAACCGG
I27DZ	Forward	CTCGAGACGCGTCATATGCAAATGAAAATC GGTCCCCCGAGGCCACGTGTAGCCTGAATT AAATTTTTCAAAAGTAGTTGAC
I27DA	Forward	ACGCGTCATATGCAAATGAAAATCGG TCCCCCGAGGCCACGTGTAGCCTGGC ACTTTTCGGGGAAATGTG
IRTGA	Backward	CGGCGGGCGGGACCGGGGGCCCGGGGAC GGCCAACGGGCGCGCGGGGCTCCAGTTAC CAATGCTTAATCAG
IRTGZ	Backward	CGGCGGGCGGGACCGGGGGCCCGGGGAC GGCCAACGGGCGCGCGGGGCTCCCTTTTC TGAAACTCAATTCTTATC
PACSPE	Backward	GACTAGTTAATTAAGTTGAAAAAAGGGGCC
T7TN5	Forward	ATATTGCTCTAATAAATTTGCGGCCGCTA ATACGACTCACTATAGGGAGAGTTTTATG GACAGCAAGCGAACCGG
US3Z	Backward	CTCGAGAAATGTCGGCCATCCAGAAAACGT CCCGGAGGACCACAGTGGCTTCCCCCCGGA

		TCCTATCGGTACCTTTTCTGAAACTCAATTC TTATC
Z143P	Backward	CGTCAAATTAAATTTTTCAAAAGTAGTTGAC

PCR: plasmid construction			
Target	**Primer**	**Sequence (5'-3')**	**Plasmid generated**
FXN cDNA ex2-5a	R3	GTACTGCAGTTCGAACCAACGTGGCC TC	pF2A
	R4	GGCCTATTCCGGAAAAGATGCT**GGA AGCGGAGCTACTAACTTCAGCCTG CTGAAGCAGGCTGGAGACGTGGAG GAGAACCCTGGACC**CATGGACGTTA A **PTV1 2A**	
Kan^R	R5	ACGTTAATTAATAACTTCGTATAATG TATGCTATACGAAGTTATGTTTTATG GACAGCAAGCGAACCGG	pF2ALRK
	R6	GCCTTCTTGACGAGTTCTTCTGACATC AAAAAAATTGTAAAACAAGCCACAG TTCTGACTTTTACGACTGCACGTCGA CTCA	
Zeo^R	R7	GCGGCCGCGGGAATTCGATTCTCGAG TTATAACCCCGGGGGTCATTCCCAAC GATCACATGCAATCTAACTGGCTCAA TTAAATTTTTCAAAAGTAGTTGAC	pLCG_Zeo
	PACSPE	GACTAGTTAATTAAGTTGAAAAAAGG GGCC	
Zeo^R	I27DZ	CTCGAGACGCGTCATATGCAAATGAA AATCGGTCCCCCGAGGCCACGTGTAG CCTGAATTAAATTTTTCAAAAGTAGT TGAC	pGEMTeasyZ

	PACSPE	GACTAGTTAATTAAGTTGAAAAAAGG GGCC	
PCR: neuro-2a cells			
Target	**Primer**	**Sequence (5'-3')**	**Annealing temperature**
hFXN isoform I	P1 P2	CGGAGCAGCATGTGGACTCT TGGTTGAGGCCACGTTGGTTC	57ºC
hFXN isoform II	P3 P4	GACATTTTGTCCTGCGGTGCGACT GGCTTGTCTGCAAGGTCTTC	60ºC
GFP	P5 P6	TTTGCACGGGAGGAACGTCC AAGTCGTGCTGCTTCATGTG	57ºC
β-Actin	P7 P8	CCTGAACCCTAAGGCCAACCGTGAA AAGATGAC GGCATAGAGGTCTTTACGGATGTCA ACGTC	60ºC
PCR: cultured DRG neurons			
Target	**Primer**	**Sequence (5'-3')**	**Annealing temperature**
LacZ	P9 P10	TACCTGTTCCGTCATAGCGATAACG AGCGTCACACTGAGGTTTTCC	57ºC
GFP	P5 P6	TTTGCACGGGAGGAACGTCC AAGTCGTGCTGCTTCATGTG	57ºC
GAPDH	P11 P12	CGGCCGAGGGCCCACTAAAG GAGCAATGCCAGCCCCAGCA	60ºC
PCR: L4-6 rat DRG			
Target	**Primer**	**Sequence (5'-3')**	**Annealing temperature**
hFXN	P13 P14	CCGCCGCGCAAGTTCGAACC CCACTGGATGGAGAAGATAG	57ºC

GAPDH	P15	GCCAAGGCTGTGGGCAAGGT	60ºC
	P16	GGCAGGTTTCTCCAGGCGGC	
qRT-PCR: cultured DRG neurons			
Target	**Primer**	**Sequence (5'-3')**	**Annealing temperature**
LacZ	P17	ATCTCTATCGTGCGGTGGTT	60ºC
	P18	GATGATGCTCGTGACGGTTA	
GFP	P19	AAGAAGATGGTGCGCTCCTG	60ºC
	P20	GCTACCCCGACCACATGAAG	
GAPDH	P15	GCCAAGGCTGTGGGCAAGGT	60ºC
	P16	GGCAGGTTTCTCCAGGCGGC	

Secuencing		
Primer	**Sense**	**Sequence (5'-3')**
3'TN5pr	Backward	TTCCCAACCTTACCAGAGGGCG
AMP3'OUT	Forward	CCCGTATCGTAGTTATCTAC
GK3P	Forward	CTGTTCCATCATCCTCTCGGGCATC
ICP225'OUT	Backward	CGCTTTTACACAAGGCGCAA
LACZ3OUT	Forward	TCGCTACCATTACCAGTTGG
MARIZEO	Forward	CACTTTGTGGCAGAGGAGCAGGA
prG	Backward	GGCTTGTCTGCAAGGTCTTC
RPrev	Backward	GGAGTGGTAGTATATACACGAG
SEQK5	Forward	CGTGCTTTACGGTATCGCCG
SU1LOXHSV	Forward	TGCAGGAATTCGATATCAAG
SU2LOXHSVUL4	Backward	CGCCCTGGAATACGCAGACA
Z5PRV	Backward	TGTGAGCACTGGGACAGCAC

4.7. Antibodies

Primary	Secondary	Dilution/ Assay
Anti-Frataxin mouse monoclonal (Abcam, Cambridge, UK)	anti-mouse IgG peroxidase conjugate (1:2000) (Sigma-Aldrich, St. Louis, MO).	1:1000 Western
Anti-β-Galactosidase mouse monoclonal (Promega, Madison, WI)	anti-mouse IgG peroxidase conjugate (1:2000) (Sigma-Aldrich, St. Louis, MO)	1:2000 Western
Anti-GFP rabbit polyclonal (Chemicon, Temecula, CA)	anti-rabbit IgG peroxidase conjugate (1:2000) (Sigma-Aldrich, St. Louis, MO)	1:1000 Western
Anti-β-Actin mouse monoclonal (Sigma-Aldrich, St. Louis, MO)	anti-mouse IgG peroxidase conjugate (1:2000) (Sigma-Aldrich, St. Louis, MO)	1:2000 Western
Anti-HSV-1 rabbit polyclonal (Dako Cytomation, Glostrup, Denmark)	anti-rabbit IgG peroxidase conjugate (1:2000) (Sigma-Aldrich, St. Louis, MO)	1:1000 Immunosubstrate staining

4.8. Buffers and solutions

1X Tris-acetate (TAE)	40mM Tris, 20mM acetic acid, and 1mM EDTA
1X Phosphate buffered saline (PBS)	137mM NaCl, 2.7mM KCl, 10mM Na_2HPO_4 and 1.8mM KH_2PO_4
1X Electrophoresis buffer	25 mM Tris, 192 mM glycine, 0.1% SDS

1X Transfer buffer	25 mM Tris, 192 mM glycine, 20% methanol, 0.1% SDS
1X Phosphate Buffered Saline with Tween 20 (PBST)	1XPBS, 0.05% Tween 20

5. METHODS

5.1. MOLECULAR BIOLOGY TECHNIQUES

5.1.1. Agarose gel electrophoresis

1% (percent weight/volume (w/v)) gels were prepared using 1X Tris acetate EDTA (TAE) buffer (**see section 4.8**) and adding ethidium bromide staining solution to a final concentration of 0.5 µg/ml (Sigma-Aldrich, St. Louis, MO). Blue/Orange 6X loading dye (Promega, Madison, WI) was added to a final concentration of 1X to each DNA sample prior to loading. For DNA size markers a 100 bp DNA ladder (NEB) was used in all gels. The bands were visualized using a PC-based image analysis system (ChemiDoc XRS System; Bio-Rad, Hercules, CA).

5.1.2. Restriction enzyme digestions

Restriction enzyme digests were performed on plasmid DNA in a total volume of 30 µl containing 0.5 µg (plasmid) - 2µg (BAC) DNA, 0.5 – 1µl restriction enzyme (10 U/µl), 3µl of the corresponding restriction buffer (10X) and double-distilled water. The digests were incubated at 37°C from 1 hour to overnight followed by electrophoresis on a 1% agarose gel as described in the previous **section 5.1.1**.

5.1.3. DNA extraction and purification from gel bands – Phenol/Ethanol method

To perform standard DNA extraction and purification from gel bands, a small hole was made in the bottom of a 0.5 ml microcentrifuge tube and covered with glass wool. The agarose slice containing the DNA band of interest was excised using a clean scalpel and placed in the microcentrifuge tube on top of the glass wool. The tube containing the gel slice was then placed inside a larger (1.5 ml) microcentrifuge tube and centrifuged at 11,000 x*g* for 1 minute. The liquid obtained in the 1.5 ml microcentrifuge tube was collected and added to buffered phenol (Phenol solution equilibrated with 10mM Tris HCl, pH 8.0 and 1mM EDTA; Sigma-Aldrich, St. Louis, MO) at a ratio of 1:1. The liquids were mixed by vortexing and then centrifuged at 11,000 x*g* for 5 minutes to separate the aqueous and organic phases. The upper aqueous phase was collected with a pipette, transferred to a new 1.5 ml microcentrifuge tube and DNA precipitated by the addition of 0.1 volumes 3M sodium acetate (pH 5.4), 3 volumes ethanol and 10 ng/µl of glycogen carrier. The

tube was incubated at -20ºC for 1 hour and then centrifuged at 11,000 x*g* for 30 minutes at 4°C. The DNA pellet obtained was washed once with 1 ml of 70% ethanol, air dried and dissolved in double-distilled water. The concentration of purified DNA was measured at 260 nm using a nanodrop spectrophotometer (ND-1000) and the relationship that an absorbance reading at 260 nm of 1.0 for a 1 cm path length of a solution of double-stranded DNA corresponds to a concentration of 50 µg/ml.

5.1.4. DNA extraction and purification from gel bands – Gel extraction kit

In order to sequence DNA PCR products, the DNA band of interest was excised and purified from agarose gel using a gel extraction kit according to the guidelines provided by the manufacturer (Quiagen, Valencia, CA). The concentration of purified DNA was measured using a nanodrop spectrophotometer (ND-1000).

5.1.5. DNA ligation reactions

For each ligation reaction, 50 ng of vector DNA was mixed at a 1:3 molar ratio with the insert DNA along with 0.2 µl (5 U/µl) of T4 DNA ligase (Thermo Scientific, Carlsbad, CA) in ligase buffer (Thermo Scientific, Carlsbad, CA) in a final volume of 10 µl. A control sample with no insert DNA was always included to reveal uncut or religated vector. Reaction mixtures were incubated overnight at 16°C or 1 hour at room temperature.

5.1.6. Total RNA extraction - TRIzol method

Total RNA was extracted from isolated rat dorsal root ganglia (DRG) of lumbar levels 4-6 (L4-6) 7 days or 30 days after viral injection using TRIzol following supplier guidelines (Invitrogen, Carlsbad, CA). DRG were resuspended and disrupted in 1 ml of TRIzol with a homogenizer (Micro homogenizer, OMNI-Inc, Kennesaw, GA). Homogenized samples were then incubated for 10 minutes at room temperature and 0.2 ml of chloroform per 1ml of TRIzol added, followed by shaking of samples for 15 seconds. The mixture was incubated for a further 3 minutes at room temperature and then centrifuged at 12,000 x*g* for 15 minutes at 4°C to separate the 3 layers: a lower red phenol-chloroform phase, an interphase, and a colorless upper aqueous phase. The upper aqueous phase was collected carefully in a new microcentrifuge tube and 0.5 ml isopropanol was added. The mixture was incubated at room temperature for 10 minutes and then centrifuged at 12,000 x*g* for 10 minutes

at 4°C to yield an RNA pellet. The pellet was washed with 75% ethanol and then dried at room temperature to ensure that no contaminating ethanol remained. Ribonuclease-free water was added (10-20 µl, depending on the size of the RNA pellet).

5.1.7. Total RNA extraction - RNeasy Plus kit (Qiagen)

Total RNA from cultured cells was extracted 48 hours after transfection or infection using RNeasy plus kit (Qiagen, Valencia, CA) according to the manufacturer´s instructions.

5.1.8. Complementary DNA (cDNA) synthesis

First strand complementing DNA (cDNA) was synthesized from extracted total RNA by reverse transcription polymerase chain reaction (RT-PCR) using the Superscript III first-strand synthesis system following the supplier's instructions (Invitrogen, Carlsbarg, CA) and then used as template for a second amplification step by PCR or real-time PCR (qPCR)

5.1.9. Polymerase chain reaction (PCR)

All primers used for PCR are listed in **section 4.6**. PCR amplification of plasmid DNA or cDNA derived from total RNA extracted from Neuro-2a cells was performed using 1 µl (0.1 ng) or 2 µl of template DNA respectively, added to a PCR mix containing 5 µl 5X GoTaq flexi buffer, 2.4 µl 25 mM magnesium chloride ($MgCl_2$), 0.5 µl 10 mM dNTPs mixture, 0.5 µl of each 5 mM primer and 0.2 µl GoTaq DNA polymerase (1 U) (Promega, Madison, WI). The volume was made up to 25 µl using double-distilled water. The PCR mixture was incubated in an automated thermocycler running a three step amplification protocol: an initial denaturing step at 95°C for 5 min followed by 30 cycles (of 95°C for 30 seconds, 55-65°C for 30 seconds, 72°C for 0.5-1 minutes) and a final extension cycle at 72ºC for 5 minutes. PCR amplification of *FXN* isoform II in transfected Neuro-2a cells was performed using 40 cycles for increased sensitivity.

PCR amplification of cDNA derived from total RNA extracted from cultured DRG neurons or from L4-6 rat DRG was carried out using 1.5 µl or 0.6 µl of cDNA respectively, in 25 µl PCR reactions. Template DNA was added to 2.5 µl 10X buffer, 0.75 µl 50 mM $MgCl_2$, 0.5 µl 10 mM dNTPs mixture, 0.5 µl of each 10 mM primer and 0.1 µl Platinium Taq DNA polymerase (1 U) (Invitrogen, Carlsbarg, CA). The

volume was made up to 25 µl using double-distilled water. The PCR mixture was incubated in an automated thermocycler running a three step amplification protocol: an initial denaturing step at 94°C for 2 minutes followed by 30 cycles (of 94°C for 30 seconds, 55-60°C for 30 seconds, 72°C for 0.5-1 minutes) and a final extension cycle of 72°C for 2 minutes. Following the first PCR amplification of cDNA derived from L4-6 rat DRG, a second identical amplification for increased sensitivity was carried out using 0.1 µl of the first PCR product as template.

PCR products were resolved on a 1% agarose gel and bands were visualized using a PC-based image analysis system (ChemiDoc XRS System; Bio-Rad, Hercules, CA).

5.1.10. Real-time PCR (qPCR)

Following cDNA synthesis, real-time PCR (qPCR) was performed using the iQ5 SybrGreen Supermix (Bio-Rad Laboratories, Hercules, CA, USA) in an iQ5 Real-Time PCR detection system (iQ™ optical system software). qPCR reactions were performed in 96-well plates (Microamp, Applied Biosystems) in triplicates. A final volume of 20 µl mastermix was prepared containing 10 µl of 2X SYBR green mastermix, 1 µl each of 5 µM forward and reverse primers and 1.5 µl of cDNA. The volume was made up to 20 µl using double-distilled water. Plates were centrifuged for 1 minute at 1000 x*g* and amplification was carried out using a two-step qPCR protocol with the initial denaturing step at 95°C for 3 minutes followed by 40 cycles (95°C for 10 seconds, 60°C for 30 seconds). Relative quantification values were identified by the $2^{-\Delta\Delta Ct}$ method[182] using levels of GAPDH mRNA as an internal control for normalization.

5.1.11. Western blotting

Cultured cells were collected 48 hours after transfection or infection and resuspended in lysis buffer consisting of 62.5 mM Tris–HCl, pH 6.8, 2% sodium dodecyl sulfate (SDS), 10% glycerol, 1X protease inhibitor cocktail (Roche, Mannheim, Germany), 1X phosphatase inhibitor (ThermoFisher Scientific, Carlsbad, CA). Samples were heated at 95°C for 5 minutes and sonicated for 4 seconds (Ultrasonicator Amplichron®, LKB instruments). The cell debris was removed by centrifugation (13,000 x*g* for 10 minutes) and supernatant was collected. Protein concentration was determined by using the Bio-Rad Dc protein assay (Bio-Rad, Hercules, CA) and 200 mM of dithiothreitol (DTT; Sigma-Aldrich, St. Louis, MO)

and 0.002% Bromophenol Blue (Sigma-Aldrich, St. Louis, MO) were added to each measured sample.

Total cell extract was separated by SDS–polyacrylamide gel electrophoresis (Invitrogen, Carlsbarg, CA) (protein per lane: 80 μg of Neuro-2a cells, and 20 μg of DRG cells and HEK-293 cells), transferred overnight to an Immobilon-P membrane (0.45 μm; Millipore, Bedford, MA, USA) and blocked for 1 hour at room temperature with blocking buffer (5% non-fat milk in PBST). Blots were first incubated overnight at 4ºC with primary antibody diluted in incubation buffer (2% non-fat milk in PBST) followed by incubation with horseradish peroxidase (HRP)-conjugated secondary antibody diluted in incubation buffer (1:2000, Sigma-Aldrich, St. Louis, MO)for 1 hour at room temperature.

Membranes were stripped 30 minutes with western stripping buffer (Thermo Scientific, Carlsbarg, CA) and re-incubated overnight with alternative primary antibodies and their corresponding secondary antibodies coupled to HRP (1:2000, Sigma-Aldrich, St. Louis, MO). Finally membranes were treated with SuperSignal Western Dura Extended Duration Substrate (Thermo Scientific) according to manufacturer's protocol and the relative intensity of each band was quantified using a PC-based image analysis system (ChemiDoc XRS System; Bio-Rad, Hercules, CA).

5.1.12. Detection of β-galactosidase expression

The culture medium was removed from the plates 48 hours after transfection and cells were washed twice with PBS and fixed with 4% paraformaldehyde (PFA; Sigma-Aldrich, St. Louis, MO) for 15 minutes at room temperature. The cells were washed three times with PBS and incubated at 37°C with X-gal stock solution (1 mg/ml X-Gal [5-bromo-4-chloro-3-indolyl-β-D-galactopyranoside dissolved in Dimethylformamide]) diluted 1:40 in warmed X-Gal dilution buffer (PBS supplemented with 2 mM $MgCl_2$, 5 mM potassium ferrocyanide $[K_4Fe(CN)_6].3H_2O$, 5 mM potassium ferricyanide $K_3Fe(CN)_6$, 0.02% NP-40 and 0.01% sodium deoxycholate) until stained. The X-Gal stain was then removed and the cells were washed with PBS.

5.1.13. Bacterial cell culture

All bacterial cultures were grown in LB (lysogeny broth)[183] or semi-solid agar plates containing LB and bacterial agar (1.5% w/v) (Nzytech, Lisbon, Portugal). LB was autoclaved at 121°C for 20 minutes at 15lb/inch^2. Antibiotics were added as

required just before use.

5.1.14. Chemically competent cells

Competent cells used for transformation of plasmid DNA were prepared using $CaCl_2$. A single bacterial colony was grown overnight in 3 ml of LB containing no antibiotics at 37°C. The saturated overnight culture was diluted 500-fold in 100 ml of LB containing no antibiotics. The cells were allowed to grow at 37°C until the optical density (OD) derived from absorbance measured at 600 nm reached between 0.3-0.4. Cells were pelleted by centrifugation at 10,000 x*g* for 10 minutes at 4°C. The supernatant was discarded and the pellet resuspended gently in 25 ml of ice-cold 100 mM $MgCl_2$. Cells were pelleted as before, resuspended in 4 ml of ice-cold 100 mM $CaCl_2$ and kept on ice for 10 minutes. Glycerol was added to the bacterial suspension to a final concentration of 10% (v/v). Competent cells were aliquoted and stored at -80°C.

5.1.15. Bacterial transformation

A volume of 50 µl of bacterial chemically competent cells was thawed on ice and cells were pipetted into 1.5 ml microcentrifuge tubes for each transformation. 1-5 µl of ligation mix or 50 ng of plasmid DNA was added to the cells, mixed gently, and incubated on ice for 30 minutes. The cells were subjected to heat shock for 30 seconds in a 42°C water bath and tubes were placed on ice for 10 minutes. 950 µl of pre-warmed SOC (super optimal broth[184] with 20 mM added glucose) was added to each tube and incubated at 37°C for 1 hour with agitation. The transformed cells were plated in two different volumes on LB agar plates containing the appropriate antibiotic and incubated overnight at 37°C in a standard bacterial incubator. Two different volumes were plated to ensure well-spaced colonies in at least one sample.

5.1.16. Plasmid amplification

Positive clones were inoculated into and grown overnight with agitation at 37°C and plasmid DNA was extracted using a Qiagen Plasmid Mini/ Maxi preparation kit (Valencia, CA) following the guidelines provided.

5.1.17. DNA sequencing

Plasmid (100 ng/µl) and BAC (200 ng/µl) DNA was sequenced by the Sanger dideoxy method in the Secugen S.L sequencing service (Madrid, Spain). Primers

were synthesized by Isogen Life Science (Veldzigt, the Netherlands) and were used at a final concentration of 5 μM.

PCR products (3 ng/μl) amplified from cDNA derived from total RNA extracted from L4-6 rat DRG as described above, were sequenced by the Sanger dideoxy method at the University of Michigan DNA sequencing core (Ann Arbor, MI). Primers were synthesized by Invitrogen (Ann Arbor, MI) and were used at a concentration of 10 μM. All primers used for DNA sequencing are listed in **Table 3** and **section 4.6.**

5.2. CELL CULTURE TECHNIQUES

All cell culture manipulations were carried out under sterile conditions using standard aseptic techniques.

5.2.1. Vero, Vero-derived, Neuro-2a, HEK-293 and SH-SY5Y cells

5.2.1.1. Regeneration of cell lines

Frozen cells were removed from the liquid nitrogen tank and quickly thawed by immersing the vial in a water bath at 37°C. Cells were rapidly transferred into a 15 ml conical tube containing 3 ml of pre-warmed DMEM medium supplemented with 10% FBS, 100U/ml penicillin and 100 μg/ml of streptomycin (F10 medium) to minimise the risk of cell damage by ice crystal formation and centrifuged. Cell pellets were resuspended in pre-warmed F10 medium and transferred to 100 mm cell culture dishes.

5.2.1.2. Cryopreservation of cell lines

Cells from one 100 mm cell culture dish were trypsinized until brought into suspension, centrifuged, resuspended in 1.8 ml freezing mixture (10% (v/v) dimethyl sulfoxide (DMSO) and 90% (v/v) FBS) and aliquoted in 2 cryovials, which were slowly cooled to -80°C by maintaining in a cryobox (Nalgene Mr Frosty, Sigma-Aldrich, St. Louis, MO) containing 2-propanol and then stored in a liquid nitrogen tank.

5.2.1.3. Culture and passage procedure

Cells were grown in 100 mm cell culture dishes or in 175 cm^2 flasks in F10 medium with the appropriate antibiotics if necessary **(Table 2**). They were incubated at 37°C in a humidified cell incubator with 5% CO_2 and passaged when 75-80% confluent. The growth medium was removed by vacuum suction and cells were gently washed with PBS. Cells were incubated with 1 ml or 12.5 ml of the recombinant enzyme TrypLE (Substitute for Trypsin; Life Technologies, Paisley, UK) (for 100 mm cell dish or 175 cm^2 flask respectively) until detached from the plate surface. An equal volume of F10 medium was added to the plate to neutralize the effect of the TrypLE and suspension was centrifuged in a 15 ml conical centrifuge tube at 200 x*g* for 5 minutes. The resultant cell pellet was resuspended in a small volume of fresh medium and seeded at a ratio of 1:10 in F10 medium with the appropriate antibiotics where necessary **(Table 2).**

5.2.1.4. Transfection

Cells were transfected using the Lipofectamine-LTX and Plus reagent (ThermoFisher Scientific, Carlsbad, CA) according to the manufacturer's instructions. One day prior to transfection, cells were seeded in a 35 mm cell culture dish to achieve 70-80% cell confluency on the day of transfection. In a sterile 1.5 ml microcentrifuge tube, 1 μg (plasmid) – 2 μg (BAC) DNA was diluted into 100 μl of Opti-MEM medium and mixed with Plus reagent in a ratio of 1:2 (plasmid DNA) or 1:3 (BAC DNA). The mixture was incubated for 15 minutes at room temperature. In another microcentrifuge tube, 12 μl of Lipofectamine-LTX reagent was diluted in 100 μl of Opti-MEM and added to the DNA-Plus mixture tube. The Lipofectamine, DNA and Plus mixture was allowed to form complexes over 30 minutes at room temperature. The cell culture medium was replaced with 0.8 ml Opti-MEM and the Lipofectamine-DNA-Plus mixture (200 μl) was gently added to the cells in drops. After 4 hours, the medium with transfection mixture was replaced with pre-warmed cell culture medium and cells were grown under normal conditions.

5.2.2. Rat fetal dorsal root ganglion (DRG) neuronal cells

5.2.2.1. Coating plates

Prior to DRG cell culture, plates were coated adding 1 ml poly-D-lysine solution (PDL, 100 μg/ml) to each well of 12 well plate, then covered and incubated

with agitation overnight at 4°C. The next day the PDL solution was removed and 0.5 ml laminin solution was added to each well (10 μg/ml) (Sigma-Aldrich, St. Louis, MO). Plates were covered and incubated with agitation overnight at 4°C. Laminin was then removed, wells were rinsed with sterile water and plates were used or stored at 4°C.

5.2.2.2. DRG cell extraction and culture procedure

Dissection media containing dorsal root ganglia isolated from rat fetuses (as described in **see section 5.5.1)** were transferred into sterile 50 ml conic tube and centrifuge 1200 x*g* for 5 minutes at 4°C. Resulting pellets were dissociated in 6 ml of 2.5 g/l Trypsin-1 mmol/l EDTA for 25 min at 37°C followed by centrifugation 1200 x*g* for 10 minutes at 4°C. The pellets (containing DRG cells) were resuspended and washed with 10 ml of Neurobasal medium to break remaining tissue fragments. The cell suspension was filtered through a cell strainer (70 μm pore size; BD biosciences, San Jose, CA) to remove excessive debris followed by centrifugation at 2600 x*g* for 1 minutes at 4°C. Cells were resuspended and plated in Neurobasal medium supplemented with 1X B27, 2mM Glutamax I, 0.5 μg/ml Albumax I, 50 U/ml penicillin G, 50 μg/ml streptomycin sulfate, and 0.1 μg/ml 7.0S nerve growth factor, at a density of $3X10^5$ cells per well of PDL/laminin coated 12 well plate.

One day after plating, expansion of non-neuronal dividing cells in the DRG culture was inhibited by addition of 5′-fluoro-2′-deoxy-uridine/uridine mixture (Sigma-Aldrich, St. Louis, MO) with a working concentration of 0.125 mg/ml for each. Half of the medium was changed three times per week.

5.2.3. DRG infection

DRG neurons were infected seven days after seeding at a multiplicity of infection (MOI) of 1 (plaque forming units per cell) during 90 minutes followed by change of half of the medium.

5.3. BAC RECOMBINEERING TECHNIQUES

5.3.1. Generation of mutants by homologous recombination

The construction of mutants by lambda Red-mediated homologous recombination[185,186] was carried out following the guidelines provided with a

commercial kit (Gene bridges, K001, version 2.7). Briefly, it involved the following steps:

5.3.1.1. Generation of the linear targeting fragment flanked by homology arms

A targeting fragment including an antibiotic selection marker gene flanked by homologous sequence arms of DNA shared by the two molecules that recombine, was generated by PCR using customized oligonucleotides. The 5' oligonucleotide consisted of a 50 nucleotides homology arm (which allows recombination with the homologous sequence 5' of the intended insertion site), followed by a 20-nucleotide stretch, which primes the 5' end of the PCR amplification of the targeting fragment. The 3' oligonucleotide was similarly designed, with a stretch of 50 nucleotides that is homologous to the region 3' of the intended insertion site, followed by a 20-nucleotide stretch that primes the 3' end of the PCR amplification of the targeting fragment. Linear targeting fragments of the constructed mutants were generated as follows:

5.3.1.1.1. 27_22_Or

For construction of the 27_22_Or vector, the targeting fragment was generated by PCR amplification of the *Sh ble* gene (conferring zeocin resistance, Zeo^R) using oligonucleotides I27DZ and US3Z (**see Table 2**) and plasmid pDRIVE-CAG as template DNA. The resulting targeting fragment was recombined into the ΔIR vector backbone (Khalique et al, submitted to J Gene Med).

5.3.1.1.2. 22_4 and 22_4_Or

For construction of the 22_4 and 22_4_Or vectors, the targeting fragment was generated by PCR amplification of the RP-Kan^R cassette composed by the *Escherichia coli* (*E. coli*) ribosomal *S12* (*rpsL*) gene (RP) which results in streptomycin sensitivity and the aminoglycoside phosphotransferase (*aph*) gene which confers kanamycin resistance (Kan^R) using oligonucleotides I4OS5 and I43P for 22_4 construction and oligonucleotides I45P and I43P for 22_4_Or construction (**see Table 2**). Plasmid pSK+KanaRpsL was used as template DNA. Both targeting fragments were recombined into the ΔIR backbone.

5.3.1.1.3. 27_22_4_Or

For 27_22_4_Or construction, the targeting fragment was generated by PCR amplification of the *Sh ble* gene using oligonucleotides I27DZ and US3Z (**see Table**

2) and plasmid pDRIVE-CAG as template DNA. The resulting targeting fragment was recombined into the 22_4_Or backbone.

5.3.1.1.4. 27_4_Or2

The targeting fragment used for construction of mutant 27_4_Or2 was generated by digestion of plasmid pSKOrisZ with *Xho*I and *Spe*I restriction enzymes and the resulting fragment was recombined into the 22_4_Or backbone.

For the construction of pSKOrisZ, the *Sh ble* gene was amplified by PCR using primers I27DZ and PACSPE (**see Table 2**) and plasmid pDRIVE-CAG as template DNA. The resulting fragment was ligated into the pGEM-T Easy vector generating the pGEM-T EasyZ vector. This was then digested with *NotI/SpeI* to obtain the Zeo^R cassette which was then religated into the pSKC481.9 plasmid to generate pSKOrisZ.

5.3.1.1.5. 27_4_Or2_β22

For 27_4_Or2_β22 construction, the targeting fragment was generated by PCR amplification of the beta lactamase (*bla*) gene (conferring ampicillin resistance, Amp^R) using oligonucleotides I27DA and IRTGA (**see Table 2**) and plasmid pSK+KanaRpsL as template DNA. The resulting targeting fragment was recombined into the 27_4_Or2 backbone.

5.3.1.1.6. 27_4_Or2_β22_β47

For 27_4_Or2_β22_β47 construction, the targeting fragment was generated by PCR amplification of the *Sh ble* gene using oligonucleotides IRTGZ and Z143P (**see Table 2**) and plasmid pDRIVE-CAG as template DNA. The resulting targeting fragment was recombined into the 27_4_Or2_β22 backbone.

The position and length of the deletions of each of these HSV-1 vectors are listed in **Table 1.**

5.3.1.1.7. FXN-p

For FXN-p construction, the targeting fragment was generated by PCR amplification of the RP-Kan^R cassette using oligonucleotides T7TN5 and FL511K (**see Table 2**) and plasmid pSK+KanaRpsL as template DNA. The resulting targeting fragment was recombined into the FXN-WT backbone (**see Supplementary figure 2)**.

5.3.1.1.8. FXNinlZ

For FXNinlZ construction, we first deleted all of the genomic insert sequences 3' to *FXN* exon 2 up to the *sacB* gene located within the BAC vector, replacing this region by a Zeo^R cassette. In a second round of recombination we next replaced the Zeo^R cassette with the F2ALRK cassette which encodes the *FXN* cDNA from exon 2 to 5a, the Porcine teschovirus-1 (PTV1) 2A sequence[187] including a 5' linker sequence encoding glycine-serine-glycine, the *E. coli lacZ* gene, the polyadenylation (polyA) signal derived from the simian virus 40 (SV40), a *loxP* site and a RP-Kan^R cassette (**see Supplementary figure 2)**.

For construction of the F2ALRK targeting plasmid, a *FXN* cDNA fragment comprising exons 2, 3, 4 and 5a, was amplified and fused at the 3' end to the PTV1 2A sequence by PCR using the plasmid pLVfrat [126] as template DNA and the primers R2 and R3 (**Table 2).** This PCR product was digested by *Pst*I/*Nco*I restriction enzymes and cloned into Bluescript KSII+ digested with *Pst*I/*Nco*I to generate the pF2A plasmid. An *Nco*I/*Pac*I fragment containing the *lacZ* gene and the SV40 polyA signal from the pDRIVE-CAG plasmid was then ligated into the pF2A plasmid digested with *Nco*I/*Pac*I to generate the pF2AL plasmid. The Kan^R gene was next amplified by PCR from the template plasmid pSK+KanaRpsL using the primers R5 and R6 (**Table 2)**. The PCR product was digested with *Pac*I/*Sal*I and ligated into pF2AL digested with *Pac*I/*Sal*I to generate the pF2ALRK targeting plasmid. The final F2ALRK cassette was then generated by digestion of the pF2ALRK plasmid with *Pst*I/*Sal*I restriction enzyme.

Table 1. Deletions in wild type HSV-1 F strain

Mutant	Nucleotide positions	Total kb
27_22_Or	113217-132468	19.2
22_4	146029-151773	5.7
22_4_Or	146874-151773	4.8
27_22_4_Or	113217-132468 146874-151773	24
27_4_Or2	113217-131408 146874-151773	23
27_4_Or2_β22	113217-131672	23.3

	146874-151773	
27_4_Or2_β22_β47	113217-131672 146312 -151773	23.8

5.3.1.2. Transformation with Red/ET expression plasmid

A sample of glycerol stock of *E. coli* strain DH10B[168,169] containing the target BAC was streaked on a LB agar plate containing the appropriate antibiotics. The plate was incubated overnight at 37°C in a bacterial incubator. Next day one colony from the streaked plate was inoculated in a 1.5 ml microcentrifuge tube containing 1 ml of LB containing the appropriate antibiotics and incubated on shaker at 37°C overnight.

The second day, two microcentrifuge tubes containing 1.4 ml of LB conditioned with the appropriate antibiotics were inoculated with 30 µl of the overnight culture and incubated at 37°C for 2 hours with agitation. After incubation, electrocompetent bacterial cells were prepared by three consecutive washes with ice-cold water, centrifugation at 11,000 x*g* for 1 minute at 2°C between each, followed by a final resuspension in 50 µl ice-cold double-distilled water.

For transformation, 1 µl of the pRed/ET plasmid (100 ng) was added to the electrocompetent cells of one of the microcentrifuge tubes and mixed gently. The other tube was used as an electroporation control (without pRed/ET). Electroporation was performed in ice-cold cuvettes (Bio-Rad Laboratories, Inc., 1 mm electrode gap) using a Bio-Rad MicroPulser at 1.8 kV, untruncated time setting. After electroporation, 1 ml of pre-warmed SOC medium was added to the cuvettes to facilitate recovery of the cells which were then incubated at 30°C for 1 hour with shaking. Cells were spread onto LB agar plates containing the appropriated antibiotics (see **Table 2**) and tetracycline (3 µg/ml) and incubated overnight in a bacterial incubator at 30°C.

5.3.1.3. Insertion in the genome of linear fragments with desired mutations using selection markers and reporter genes

A single colony was picked from the LB plate containing Red/ET plasmid and target BAC and inoculated into a 1.5 ml microcentrifuge tube containing 1 ml LB broth with the appropriate antibiotics (see **Table 2**) and tetracycline (3 µg/ml). The tubes were incubated overnight at 30°C with agitation.

On the next day four microcentrifuge tubes (2 for experiment and 2 for control) containing 1.4 ml fresh LB supplemented with the appropriate antibiotics (see **Table 2**) and 3 μg/ml tetracycline were inoculated with 30 μl of the saturated overnight culture. All the four tubes were incubated at 30°C until the OD derived from absorbance measured at 600 nm reached between 0.3-0.4. Expression from the pRed/ET plasmid was induced in two tubes (1 from the experiment and 1 from the control) by addition of 50 μl of 10% L-arabinose and incubation for 45 minutes at 37°C before chilling on ice for 15 minutes. The electrocompetent cells were prepared as described above (see **section 5.3.1.2**). For transformation, 100 ng (1-2 μl) of the linear targeting fragment was added to the electrocompetent cells on ice (both L-arabinose-induced and uninduced experimental tubes). Electroporation was performed on all the four cultures (induced and uninduced experimental tubes, induced and un-induced control tubes) in ice-cold cuvettes (1 mm electrode gap) using a Bio-Rad MicroPulser at 1.8 kV, untruncated time setting. After electroporation, 1 ml of pre-warmed SOC medium was added to the cuvettes to facilitate recovery of the cells which were then incubated at 37°C for 1 hour with shaking and inoculated onto LB agar plates containing the appropriate antibiotics (see **Table 2**). The next day, several independent colonies were picked and tested for correct recombination by colony PCR or restriction digest analysis of purified BAC DNA.

5.3.2. Generation of mutants by Cre recombinase-mediated site-specific DNA insertion or deletion

Construction of mutants by Cre recombinase-mediated site-specific DNA insertion into the *loxP* site of the BAC plasmid or deletion of selection marker cassettes was carried out following the protocol previously described by Saeki and co-workers.[177]

5.3.2.1. Plasmid insertion

This strategy was used for construction of vectors 27_22_4_Or2, 27_4_Or3, 27_22_4_OrG, 27_4_Or2G, 27_4_Or2_β22 GFP (see **Supplementary figure 1)** and insertion of the green fluorescent protein (GFP) reporter cassette into each of the three FXN BAC DNAs.

Electrocompetent bacterial cells containing the BAC DNA (27_22_4_Or, 27_4_Or2, FXN-WT, FXN-p or FXNinlZ) were prepared as described above in

section 5.3.1.2. The cells were electroporated with a mixture containing 10 ng each of the temperature sensitive (ts) helper plasmid pCTP-T (which expresses Cre recombinase *in trans*) and the insertional shuttle plasmid.

Insertional shuttle plasmids used were: 1) the plasmid pHG (which contains a *loxP* site, the IE4/5 promoter, the *GFP* reporter gene (*gfp),* the HSV-1 packaging signal and the Amp^R gene) for the generation of 27_22_4_Or2, 27_4_Or3 and labelling of the three FXN BAC DNAs; 2) the plasmid pLCG (which contains a *loxP* site, the citomegalovirus (CMV) promoter, the *GFP* reporter gene and Amp^R gene) for the generation of 27_22_4_OrG and 27_4_Or2G; or 3) the plasmid pLCG-ZEO (which contains a *loxP* site, the CMV promoter, the GFP reporter gene and the Zeo^R gene) for the generation of 27_4_Or2_β22 GFP.

After electroporation, cells were resuspended into 1 ml SOC medium containing heat-inactivated tetracycline (20 μg/ml) to induce Cre expression in two tubes and incubated for 4 hours at 30°C (permissive temperature for the helper plasmid pCTP-T) with shaking. The integrated recombinants were selected at 43°C (restrictive temperature for the pCTP-T) on LB agar plates supplemented with the appropriated antibiotics (see **Table 2**). The next day, several independent colonies were picked and tested for correct recombination by colony PCR or restriction digest analysis of purified BAC DNA.

5.3.2.2. BAC insertion

This strategy was used for construction of the 27_4_Or2_β22 FXNInLZ vector. Electrocompetent bacterial cells containing the 27_4_Or2_β22 BAC DNA were prepared as described above in **section 5.3.1.2.** The cells were first electroporated with 10 ng of helper plasmid pCTP-T. The resulting culture was plated onto LB plates containing the appropriate antibiotics (see **Table 2**) and plates were incubated overnight at 30°C. On the next day, a single colony was picked and inoculated in 1ml LB broth with the appropriated antibiotics overnight at 30°C with agitation. On the third day, electrocompetent bacteria containing the 27_4_Or2_β22 BAC and the pCTP-T plasmid were electroporated with 100ng of the FXNinlZ BAC (FXNinlZ BAC without the GFP cassette). Cells were then transferred into 1 ml SOC medium containing heat-inactivated cTc (20 mg/ml) to induce Cre expression and incubated for 4 hours at 30°C with shaking. The resulting culture was then plated onto LB plates containing appropriate antibiotics (see **Table 2**), 100mM isopropyl β-

D-1-thiogalactopyranoside (IPTG) and Xgal reagents, which induce expression of the *lac* operon in *E. coli* to detect β-galactosidase activity thus allowing blue/white screening of the colonies. Plates were incubated overnight at 43°C. The next day, several independent colonies were picked and tested for correct recombination by colony PCR or restriction digest analysis of purified BAC DNA.

5.3.2.3. Selection marker cassette deletion

Deletion of the RP-Kan^R cassette from the FXN-p and FXNinlZ mutants was performed as follows. Electrocompetent bacterial cells containing FXN-p or FXNinlZ BAC DNA were prepared as described above in the **section 5.3.1.2.** The cells were electroporated with 10 ng of the plasmid pCTP-T. After electroporation, cells were resuspended into 1 ml SOC medium containing heat-inactivated tetracycline (20 μg/ml) to induce Cre expression and incubated for 4 hours at 30°C with shaking. The integrated recombinants were grown at 43°C (restrictive temperature for the pCTP-T) on LB agar plates supplemented with the appropriated antibiotics (see **Table 2**). Next day, screening of positive recombinants was achieved by negative selection on LB agar plates supplemented with the appropriated antibiotics in presence and absence of Kanamycin. The next day, several independent colonies were picked and tested for correct recombination by colony PCR or restriction digest analysis of purified BAC DNA.

Table 2. Selection markers expressed by HSV-1 and FXN mutants.

Mutant	**Selection markers***
ΔIR	Chloramphenicol, Ampicillin
27_22_Or	Chloramphenicol, Ampicillin, Zeocin
22_4	Chloramphenicol, Ampicillin, Kanamycin
22_4_Or	Chloramphenicol, Ampicillin, Kanamycin
27_22_4_Or	Chloramphenicol, Kanamycin, Zeocin
27_22_4_Or GFP	Chloramphenicol, Ampicillin, Kanamycin, Zeocin
27_22_4_Or2	Chloramphenicol, Ampicillin, Kanamycin, Zeocin
27_4_Or2	Chloramphenicol, Kanamycin, Zeocin

27_4_Or2 GFP	Chloramphenicol, Kanamycin, Zeocin Ampicillin
27_4_Or3	Chloramphenicol, Ampicillin, Kanamycin, Zeocin
27_4_Or2_β22	Chloramphenicol, Ampicillin, Kanamycin
27_4_Or2_β22_β47	Chloramphenicol, Ampicillin, Zeocin
27_4_Or2_β22 GFP	Chloramphenicol, Ampicillin, Kanamycin, Zeocin
27_4_Or2_β22 FXNinlZ	Chloramphenicol, Ampicillin, Kanamycin
FXN-p	Chloramphenicol, Ampicillin
FXNinlZ	Chloramphenicol

*Antibiotic final concentration: chloramphenicol 15 μg/ml, ampicillin 50μg/ml, zeocin 25 μg/ml, kanamycin 15 μg/ml.

5.3.3. Verification of modified BAC by DNA sequencing

Positive recombinant BAC clones were purified by a second round of electroporation (as described above, **section 5.3.1.2)** and DNA samples were sent to the sequencing service for final confirmation (**see section 5.1.17**) using oligonucleotides designed for sequencing across the recombination junctions. The oligonucleotides used for sequencing of mutants and their sequences are listed in **Table 3** and **section 4.6**.

Table 3. Oligonucleotides used for sequencing of HSV-1 and FXN mutants.

Mutant	**Oligonucleotides**
27_22_Or	GK3P, ICP225'OUT
22_4	RPREV, SEQK5
22_4_Or	RPREV, SEQK5
27_22_4_Or	GK3P, ICP225'OUT
27_22_4_Or GFP	S1LOXHSV, SU2LOXHSVUL4
27_22_4_Or2	S1LOXHSV, SU2LOXHSVUL4
27_4_Or2	GK3P, ICP225'OUT

27_4_Or2 GFP	S1LOXHSV, SU2LOXHSVUL4
27_4_Or3	S1LOXHSV, SU2LOXHSVUL4
27_4_Or2_β22	GK3P, AMP3'OUT
27_4_Or2_β22_β47	MARIZEO, Z5PRV
27_4_Or2_β22 GFP	S1LOXHSV, SU2LOXHSVUL4
27_4_Or2_β22 FXNinlZ	S1LOXHSV, SU2LOXHSVUL4 RPrev (RP-Kan^R deletion)
FXN-p	SEQK5, 3'TN5pr (RP-Kan^R insertion) RPrev (RP-Kan^R deletion)
FXNinlZ	prG, LACZ3OUT

5.4. VIRAL AMPLIFICATION TECHNIQUES

5.4.1. Viral stock preparation

Table 4. Cell lines used for propagation and titering of viral stocks.

HSV-1 BAC	**Cell line**
WT, IR	Vero
27_22_Or	2-2
22_4, 22_4_Or	E5
27_22_4_Or (GFP) 27_22_4_Or2, 27_4_Or2 (GFP) 27_4_Or3 27_4_Or2_β22 (GFP/FXNInLZ) 27_4_Or2_β22_β47	7b

5.4.1.1. Seed stock

According to the mutations present in the viral mutant, appropriate permissive cells (see **Table 4**) were seeded in a 35 mm cell culture dish to obtain 70% confluence on the day of transfection. Cells were transfected with 2 μg of BAC DNA encoding viral genome as described above in **section 5.2.1.4** and 4 hours after transfection the cells were overlaid with 0.7% sterile agarose dissolved in F2 medium (DMEM supplemented with 2% FBS, 100U/ml penicillin G and 100 μg/ml of

streptomycin sulfate) and incubated at 37°C. Viral viability and propagation were evident by visible cytopathic effects (CPE) in cells and the formation of plaques. The times for these visible changes to appear varied dramatically depending on the vector backbone and the cell line. If the virus was able to replicate, a single plaque was picked using a P 20 Gilson pipette stabbing through the agarose into the cells. The agarose plug with the cells were transferred into a 0.5 ml microcentrifuge tube containing 40 µl of FBS and stored at -80°C until further use. Such a single plaque sample was used to infect fresh Vero cells seeded in a 35 mm culture dish for WT and ΔIR viral stocks or the appropriate complementing Vero-derived cells seeded in a 3.8 cm^2 well from a 12 well plate for the rest of the viral stocks. When the majority of the cells had rounded up but were not detached from the well surface, they were harvested by lifting the cells with a plastic scraper into the medium which was then subjected to three freeze-thaw cycles followed by sonication to release intracellular viral particles. Cell debris was removed by centrifugation (2060 x*g* for 10 minutes) and the clarified supernatant was collected and stored at -80°C.

5.4.1.2. Working stock

To prepare a regular WT or IR master stock, Vero cells were seeded in a 100mm cell culture dish and infected with 50 µl of the seed stock in 8 ml of F2 medium. After 1-2 days when CPE were obvious, cells were harvested and the supernatant containing the virus collected and stored as described for seed stock preparation.

To prepare a regular master stock from the seed stock of the rest of the mutants, two rounds of amplification were performed. For the first one (termed second amplification), appropriated complementing cells for each mutant (**see Table 4)** were seeded in a 35 mm cell culture dish and infected with 1/70 (for 27_22_Or and 22_4_Or) or 1/30 of the seed stock (for 27_22_4_Or2, 27_4_Or2, 27_4_Or3, 27_4_Or2_β22 and 27_4_Or2_β22_β47) in 1 ml of F2 medium. When CPE were obvious (depending on the virus to be grown), cells were harvested and the supernatant containing the virus collected and stored as described for seed stock preparation. To perform the second round of amplification (termed third amplification), the same process was repeated in a 100 mm cell culture dish. Viral preparations were collected and stored in aliquots at -80°C.

5.4.1.3. Large-scale stock: 27_4_Or2_β22 GFP and 27_4_Or2_β22FXNlnZ mutants

For large-scale propagation, eight 850 cm^2-roller bottles were seeded with $1x10^7$ 7b cells in F10 media supplemented with 0.025M HEPES per bottle to buffer the medium if the roller bottles were not incubated in a CO_2 incubator. When the monolayer reached approximately 75% of confluence (2-3 days post seeding), cells from each roller bottle were infected with 1/8 of the total volume of the second amplification regular stock in fresh 30 ml of F2 medium and incubated at 37°C for 90 minutes. At the end of this adsorption period, 50 ml of F2 media supplemented with 0.025M HEPES was added to each bottle which was incubated at 37°C until CPE became visible (3-4 days). Cells were then detached into the media by swirling the media around the inside of the roller bottle and the cell suspension was centrifuged at 2060 x*g* for 10 min at 4°C. The supernatant was decanted into a 500 ml polypropylene centrifuge bottle and stored on ice. The pellet was resuspended in cold PBS and centrifuged again at 2060 x*g* for 10 min at 4°C. The resulting supernatant was added to the previous stored supernatant and the pellet was stored in PBS at 4°C.

To harvest the viruses from the supernatant, combined supernatants were centrifuged for 1 hour at 18,600 x*g* in a Beckmann preparative centrifuge JLA10.5 rotor. Meanwhile the stored pellet suspension was subjected to manual homogenization and used to resuspend the resulting second pellet. The final suspension was stored 90 minutes at 4°C and transferred to two Beckman ultra-clear centrifuge tubes. A volume of 3ml of 50% Iodixanol (OptiPrep, Axis-shield density gradient media, Alere Technologies AS, Oslo, Norway) was added to each tube and the tubes were topped with PBS, followed by centrifugation for 35 minutes at 131,500 x*g* in a SW32 rotor in a Beckmann XL-90 ultracentrifuge. Finally, the bottom 7.5 ml (3 ml 50% opti-prep, 4.5 ml PBS and virus) were collected, gently mixed and stored at -80°C.

5.4.1.4. Viral stock Purification: iodixanol gradient

For large-scale viral stock purification, the concentrated solution was transferred to a 13 ml Beckman pollyallomer quick-seal tube adding 15 ml 20% Iodixanol (OptiPrep, Axis-shield density gradient media, Alere Technologies AS, Oslo, Norway) followed by centrifugation for 4.5 hours at 342,000 x*g* in a NVT65 rotor in a Beckmann XL-90 ultracentrifuge. Viral particles were banded by the self-

generated gradient towards the bottom of gradient while any contaminating cellular material was banded at lower densities. To harvest the virus, a needle was inserted to vent the top of the tube, and using another needle with a 5 ml syringe, 5 ml of the viral band from the bottom of the gradient was aspirated. This extracted viral solution was centrifuged (19500 x*g* for 35 minutes at 4ºC), resuspended in 0.5 ml of cold PBS and stored in aliquots at -80°C.

5.4.1.5. Viral stock titration

5.4.1.5.1. Assay for infectious particles

Titration assays to detect infectious virions were performed by infecting monolayers of the appropriate complementing cells (**see Table 4**) with serial dilutions of the viral preparation in F2 medium. After absorption for 90 minutes, the medium was replaced with 0.7% sterile agarose dissolved in F2 medium to prevent secondary spread of virus. Following overnight incubation, cells were fixed with 4% paraformaldehyde (PFA; Sigma-Aldrich, St. Louis, MO) and the agarose was removed. Cells were incubated in blocking buffer (PBS containing 1% FBS and 0.2% Triton X-100) for 30 minutes at room temperature and incubated with a polyclonal anti-HSV-1 antibody (1:1000) for 2 hours at room temperature. After incubation, cells were washed 3 times in PBS and then incubated with anti-rabbit secondary antibody/peroxidase conjugate (1:2000, Sigma-Aldrich, St. Louis, MO) for 1 hour at room temperature. Peroxidase-labelled cells were visualized by incubation with a mixture of 0.05% 3, 3'-Diaminobenzidine (DAB; Acros Organics, Geel, Belgium) and 0.015% hydrogen peroxide (H_2O_2; Panreac, Barcelona, Spain) for 5 minutes. The DAB mixture was removed and cells were washed once with PBS to stop the staining process. HSV-1 positive cells (stained brown) were counted by microscopy to calculate infectious HSV-1 particles per millilitre (IP/ml).

5.4.1.5.2. Assay for plaque forming units

Titration assays for plaque-forming units were performed by infecting in suspension $7X10^5$ appropriated complementing cells **(see Table 4)** with serial dilutions of the viral preparation in F2 medium. Infected cells were rotated in a rotisserie manner on a LabQuake rotary shaker at 37°C for 90 minutes and then plated in 6 well plates. Next day, the medium was removed and replaced with DMEM containing 1.25% methylcellulose to prevent secondary spread of virus. Plaque

formation (usually 4-5 days after infection) was verified by confocal microscopy and quantified by counting plaque forming units (PFU) by removing medium and staining with crystal violet (2 mg/ml) in a 50:50 mixture of methanol and deionized water. One hour after staining, the wells were washed with water and plaques counted by microscopy.

5.4.1.6. Cell complementation analysis

Viral replication in non-complementing and complementing cell lines was determined following infection of the assayed cells at MOI 1 (infectious particle per cell) in F2 medium. Cells were incubated at 37°C for 90 minutes to allow the virus to be absorbed after which media was replaced with fresh F2 medium and the cultures incubated at 37°C for 6 days. Cells were harvested into the medium which was subjected to three freeze-thaw cycles followed by sonication. The cell lysate was centrifuged at 2060 x*g* for 10 minutes and titration by infected cells assay of the viral supernatant was performed as described above.

5.4.2. *In vitro* multi-cycle growth kinetics assay

Approximately $1.8X10^5$ appropriate permissive cells (**see Table 4**) were seeded in 35 mm cell culture dishes and infected at MOI of 0.05 (infectious particle per cell) in F2 medium. Cells were incubated at 37°C for 90 minutes to allow the virus to be absorbed after which the medium was replaced with fresh F2 medium and the cultures incubated at 37°C for stated time points. Progeny viruses were harvested into the medium which was then subjected to three freeze-thaw cycles followed by sonication. The cell lysate was centrifuged at 2060 x*g* for 10 minutes and titration for infectious particles in the viral supernatant was performed as described above.

5.5. ANIMAL TECHNIQUES

5.5.1. Isolation of rat fetal dorsal root ganglia

Sprague Dawley female rats (day 17 p.c. (post coitum)) (Charles River, Portage, MI) were sacrificed in a CO_2 chamber. The uterine horns were dissected out carefully, and place in ice-cold dissection Leibovitzs L-15 medium supplemented with 25 U/ml penicillin G and 25 μg/ml of streptomycin sulfate. Each embryo was separated from its placenta and surrounding membranes. The brain region, dark red organs and as much blood as possible were removed from the embryos in order to

isolate the spinal cords under the microscope and place them in a clean culture dish with dissecting medium. Dorsal root ganglia were separated from both sides of the spinal cord which was then discarded.

5.5.2. Viral inoculation of rat footpads

Under isoflurane anesthesia, male Sprague-Dawley rats (Charles River, Portage, MI) weighing 200 to 250g were inoculated in the plantar surface of both hind feet with 30µl of PBS containing 1.5 x 10^6 pfu of the 27_4_Or2_β22 FXNinlZ vector or 3 x 10^6 pfu of the control 27_4_Or2_β22 GFP vector. Three rats were inoculated with each vector.

5.5.3. Isolation of dorsal root ganglia from adult rats

Seven days or one month after inoculation, animals from each group were treated by intraperitoneal injection with 300 mg/kg Ketamine and 30 mg/kg Xylazine and sacrificed. L4-6 rat DRG were extracted and stored at -80ºC.

5.6. STATISTICAL ANALYSIS

Spreadsheet and graphical representations were performed using Microsoft Excel 2007 software.

Data are expressed as the mean ± standard deviation (SD) of three experiments. Statistical comparison of the data sets was performed by paired two-tailed Student's *t* test. The differences are given with their corresponding *P* value, which is the probability that the difference occurred merely by chance under the null hypothesis. *P* values below 0.05 are considered statistically significant.

RESULTS

6. RESULTS

6.1. HSV-1 deletion mutants defective for IE gene expression

For the generation of a recombinant vector for neurological gene therapy of Friedreich's ataxia (FRDA), our first goal was the construction of a nonreplicative herpes simplex virus type-1 (HSV-1)-derived genomic vector with a high cargo capacity while retaining its growth capacity for large scale production. To increase the transgene capacity of the HSV-1 viral genome as a vector and to facilitate further modifications, we previously deleted the entire internal repeat (IR; joint) region to remove all duplicated sequences in the genome, thus ensuring unambiguous targeting of the remaining gene copies in the terminal repeat (TR) region (Khalique et al, submitted to J Gene Med). In concordance with studies of similar mutants constructed previously[188,189,190], we observed that this ΔIR mutant undergoes efficient lytic replication in Vero cells, indicating that only a single copy of all the genetic elements in HSV-1 is sufficient for efficient viral growth in culture (Khalique et al, submitted to J Gene Med).

Since other non-replicative genomic HSV-1 vectors based on the elimination of IE gene expression have already been used in human clinical trials [53], we next modified our ΔIR mutant by further deletion of the two essential IE genes encoding ICP27 and ICP4. Furthermore, of special relevance to this aim, it should be noted that the deletion of the entire IR region eliminates one copy of the IE gene *ICP0*, one copy of the IE gene *ICP4* and truncates the IE4/5 promoter of the IE gene *ICP22*. Although the U_S1 protein coding region for ICP22 is in the U_S component of the HSV-1 genome, the promoter and the 5' portion of the transcribed region reside in the flanking IR sequence.

The *U_L54* gene, which encodes ICP27, is separated from the IR region by the *U_L55* and *U_L56* genes, which have been described to be nonessential in the context of wild type (WT) HSV-1.[191] Therefore, to eliminate ICP27 expression and simultaneously increase transgene capacity we extended the ΔIR deletion by eliminating *U_L56, U_L55* and *U_L54*, to generate the mutant 27_22_Or (**Figure 6a**, our nomenclature includes "Or" to indicate the copy number of origins of replication, the relevance of which will become clear below). As expected, this 27_22_Or mutant was able to replicate in the ICP27-complementing 2-2 cell line [172], indicating that the

U_L55 and *U_L56* genes are also nonessential for lytic replication in the background of a HSV-1 genome deleted for IR and ICP27. Inability of this mutant to grow in Vero cells confirmed that the essential *ICP27* gene had indeed been deleted (**Figure 7a**).

In parallel to the deletion described above, to eliminate ICP4 expression, we generated the 22_4 mutant from the ΔIR backbone by deleting the remaining copy of the *ICP4* gene as well as the adjacent sequences in the TR region, which include the IE4/5 promoter region. The IE4/5 promoter is quite unusual in that it contains a viral origin of replication, ori_S, embedded within the transcriptional regulatory sequences between the TATA box and the TAATGARAT motifs that confer IE kinetics to ICP22 and ICP47 (**Figure 6b**). This viral replication origin was previously demonstrated to be nonessential since a fully replicative HSV-1 mutant lacking both copies of the ori_S region was isolated. [192] Surprisingly, however, our 22_4 mutant was unable to grow on the ICP4-complementing E5 cell line [54], which supports replication of other ICP4-defective mutants.

We hypothesized that the deletion of the remaining copy of ori_S in the multiply deleted ΔIR backbone could be responsible for the loss of replication competence. We thus generated the 22_4 _Or mutant by deleting only the *ICP4* gene and leaving intact the adjacent ori_S; this mutant was able to replicate in E5 cells, confirming that the absence of ori_S copies results in a major growth impairment in the 22_4 mutant. Inability of this mutant to grow in Vero cells confirmed that both copies of the essential *ICP4* gene had indeed been deleted (**Figure 7a**).

6.2. Growth deficiency of HSV-1 IE mutants can be compensated for by addition of the ori_S region

Since we had successfully generated viable mutants deleted for either ICP27 or ICP4 in the background of our ΔIR backbone, our next step was to combine the two deletions in ΔIR to eliminate both ICP27 and ICP4 expression to generate the 27_22_4_Or mutant genome (**Figure 6a**). Unexpectedly, we were unable to obtain viral plaques when this mutant was transfected into the ICP4/ICP27-complementing cell line 7b. [51] Since as described above, we had just observed that the growth defect of the 22_4 mutant could be rescued by addition of an ori_S copy, we tested whether the same strategy could be used to achieve replication competence of the 27_22_4_Or mutant, since the ΔIR deletion in this mutant removed the ori_S copy embedded in the ICP22 IE 4/5 promoter region. We thus generated the 27_22_4_Or2 mutant (**Figure**

6a) in which an ori_S copy embedded in the IE4/5 promoter region linked to the *GFP* reporter gene, was inserted ectopically into the 27_22_4_Or genome at the U_L3-U_L4 intergenic region (**Supplementary figure 1**), which has previously been described as a non-disruptive insertion site for transgene cassettes.

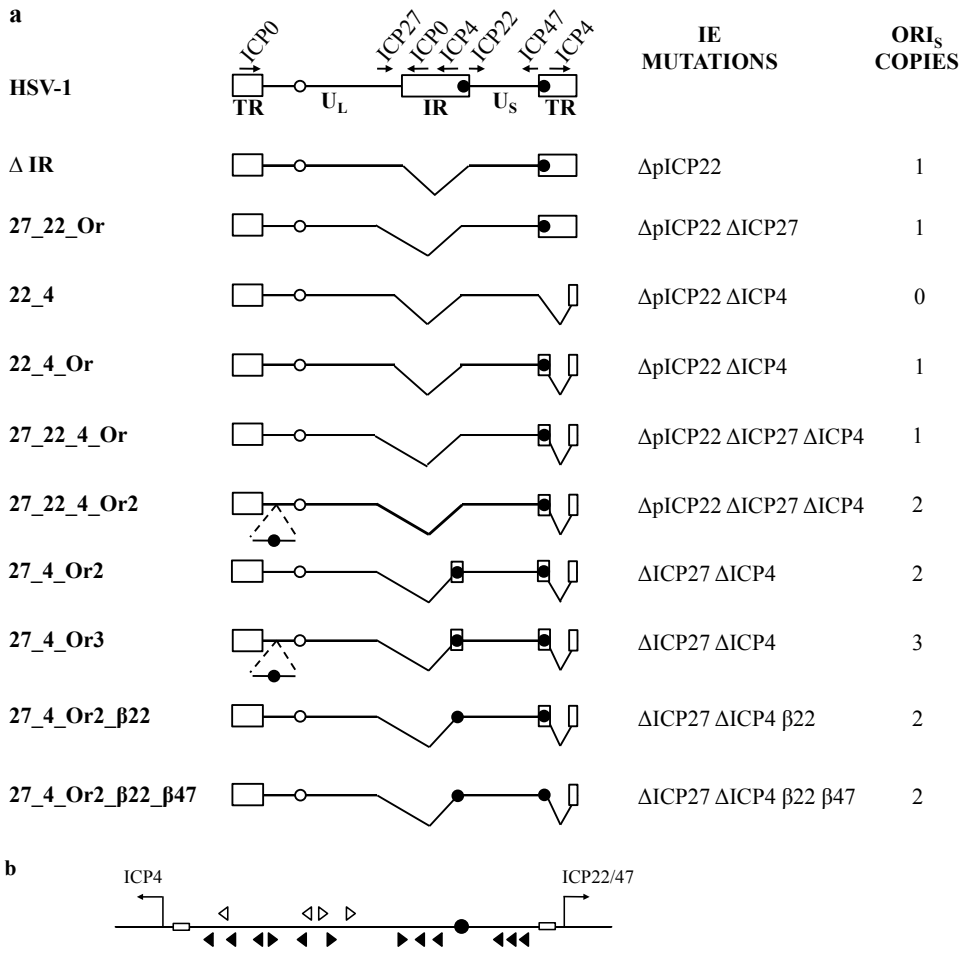

Figure 6. Structure of non-replicative genomic HSV-1 mutants.

a. Schematic representation of HSV-1 WT and HSV-1 mutant linear genomes. The unique long (U_L) and the unique short (U_S) segments (open boxes) are shown flanked by the internal repeat (IR) and the terminal repeat (TR). The unique origin of replication ori_L is present in the U_L segment (open circle), the two origins of replication ori_S are present in IR and TR (filled circle), and the ori_S (filled circle) inserted ectopically between the *U_L3* and *U_L4* genes by Cre/loxP recombination Inverted peaks represent HSV-1 sequence deletions. Deletions regarding immediate early genes (Δ, IE mutations) and number of ori_S copies are listed next to each mutant; "p" represents promoter sequence and "β" TAATGARAT sequence.

b. Schematic representation of the 822-bp intergenic HSV-1 region between the divergently transcribed genes encoding ICP4 and ICP22 or ICP47 (ICP22/47). The positions of the TAATGARAT elements (open arrowheads), binding sites for the transcription factor SP1 (filled arrowheads), TATA boxes (open boxes), and ori_S (filled circle) are shown relative to the transcription start sites of *ICP4* and *ICP22/47* (arrow heads indicate the direction of the

transcription).

Transfection of 7b cells with 27_22_4_Or2 DNA yielded micro-plaques, but successful amplification of 27_22_4_Or2 virus (**Figure 7a**) in the absence of complete cell lysis was possible since viral spread could be followed by visualization of GFP expression in infected cells (**Figure 7b**). To determine if this GFP labeling strategy could also enable amplification of the 27_22_4_Or mutant, we also introduced the *GFP* reporter gene into the U_L3-U_L4 intergenic region of this mutant (**Supplementary figure 1**) under the control of the CMV promoter (which does not contain an embedded ori_S copy). Transfection of 7b cells with DNA of this GFP-labelled version of 27_22_4_Or revealed that only transfected cells expressed the GFP reporter and infection foci were not observed at any time point. We thus concluded that the 27_22_4_Or mutant was indeed replication-incompetent, and that ectopic addition of a second ori_S element rescued this growth impairment, although a significant defect with reduced viral titers was still evident (**Figure 7a**).

In an attempt to increase the replication efficiency observed with the 27_22_4_Or2 genome, we next generated the 27_4_Or2 mutant, in which the extent of the IR deletion from the 27_22_4_Or mutant was reduced to maintain the ICP22 promoter-regulatory sequences intact, thus conserving the ori_S element in its natural location (**Figure 6a and Supplementary figure 1**). To facilitate the optimization of viral titers by monitoring of viral spread as described above, we also introduced the *GFP* reporter gene under the control of the CMV promoter, into the U_L3-U_L4 intergenic region of the 27_4_Or2 mutant. Compared to 27_22_4_Or2, this mutant could be grown in 7b cells up to significantly higher titers (**Figure 7a and 8a**). Interestingly, GFP expression driven by the CMV promoter was weaker compared to that driven by the IE4/5 promoter (**Figure 7b**), consistent with fact that the latter is more strongly activated than the former by HSV-1 proteins.

To test if additional ori_S copies could further increase viral titers, we inserted the IE 4/5 promoter region-GFP reporter transgene cassette ectopically in the U_L3-U_L4 intergenic region of the 27_4_Or2 genome, thus adding a third ori_S sequence, to generate the 27_4_Or3 mutant (**Figure 6a and Supplementary figure 1**). Compared to the 27_4_Or2 mutant, no significant increase in 27_4_Or3 titers could be detected (**Figure 7a and 7c**).

a

Virus	E5 cells (ICP4)	2-2 cells (ICP27)	7B cells (ICP4/ ICP27)	Vero cells	IP(10^6)/ ml	Transgene cassette
27_22_4_Or GFP	-	-	-	-	-	HCMV-GFP
27_22_4_Or2 GFP	-	-	+	-	0.35	IE4/5-GFP
27_4_Or2	-	-	+	-	1.89	HCMV-GFP
27_4_Or3	-	-	+	-	2.51	IE4/5-GFP

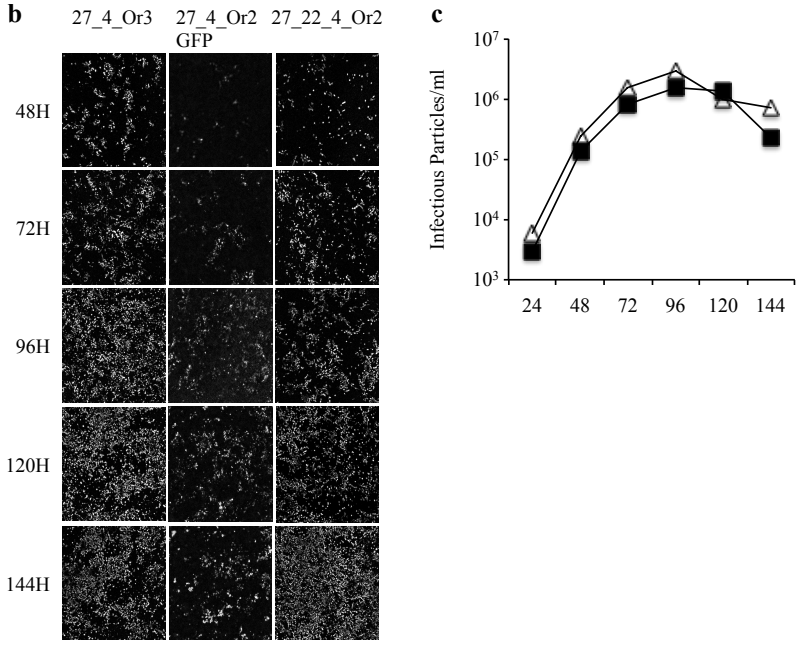

Figure 7. Growth characteristics of non-replicative genomic HSV-1 mutants

a. Viral replication in non-complementing and complementing cell lines was determined following infection with IE gene deletion mutants. In samples where replication was observed, the titer of infectious particles per milliliter (IP/ml) was measured 24 hours after infection.

b. Spread of infection of 27_22_4_Or, 27_4_Or2 GFP and 27_4_Or3 mutants revealed by autofluorescence of the *GFP* reporter gene encoded by each mutant. 7b cells were infected at a multiplicity of infection (MOI) of 0,05 and photographed by fluorescent microscopy at the indicated time points.

c. Replication kinetics of 27_4_Or2 (filled triangles), 27_4_Or3 (open circles) in 7b cells infected at a MOI of 0.05.

Taken together, these results indicate that synergistic interactions between deletions of the ori_S replication origins and deletions of the IR region, the genes encoding for ICP27, U_L55, U_L56, and the remaining ICP4 copy, provoke growth

impairments of HSV-1. On the other hand, adding extra ori_S copies does not confer additional replicative advantage.

6.3. Presence of the intact IE4/5 promoter affects the growth of HSV-1 IE mutants

Although the single deletion of IE protein ICP22 from the HSV-1 genome does not greatly affect viral growth and viability in culture [193,194], in the context of multiple IE deletion mutants, ICP22 has been shown to provide growth advantages. [51] To maintain these growth advantages while eliminating IE expression of ICP22 as previously described by Samaniego and coworkers [52], we deleted a 270-bp sequence containing the TAATGARAT elements from the ICP22 IE4/5 promoter in the 27_4_Or2 genome, thus generating the 27_4_Or2_β22 mutant (**Figure 6a and 6b**).

Viral stocks of 27_22_4_Or2, 27_4_Or2, and 27_4_Or2_β22 were then prepared to perform multi-cycle growth kinetics (**Figure 8a**) for a more detailed analysis of the effect of modulating *ICP22* expression via modifications of the IE4/5 promoter region in our multiply deleted genomes. As expected, elimination of the IE4/5 promoter region in 27_22_4_Or2 delayed peak virus yields by two days, and reduced titers almost 10-fold compared to those of 27_4_Or2. Modification of the IE4/5 promoter region to convert ICP22 expression from IE to E kinetics in 27_4_Or2_β22 resulted in peak virus yields one day before that of 27_22_4_Or2 and with more than a 3-fold increase. While cultures infected by either 27_4_Or2 or 27_4_Or2_β22 showed cytopathic effects in more than 95% of the cells by 4 and 5 days respectively, those infected by 27_22_4_Or2 did not show cytopathic effects at the same multiplicity of infection (0.05 infective particles/cell). In the permissive 7b cell line, all of the mutants exhibited slower growth kinetics and lower peak viral titers compared to HSV-1 WT, indicating incomplete complementation by this cell line.

Since the IE4/5 promoter is present in two inverted copies upstream of both the *ICP22* and the *ICP47* genes (**Figure 6b**), U_S-isomerization events during viral replication could revert the TAATGARAT-deleted ICP22 promoter in our 27_4_Or2_β22 mutant by recombination with the wild-type copy upstream of the *ICP47* gene. Since our mutant genomes are also deleted for the IR region, we predicted that U_S-isomerization is unlikely, but to rule out this possibility we next constructed a double deletion mutant in which we also eliminated the TAATGARAT

elements from the ICP47 IE4/5 promoter of 27_4_Or2_β22, thus generating the 27_4_Or2_β22_ β47 mutant (**Figure 6a**). Multi-cycle growth kinetics in 7b cells comparing 27_4_Or2_β22 and 27_4_Or2_β22_β47 (**Figure 8b**) revealed highly similar growth curves, indicating that isomerization-mediated restoration of the wild-type IE4/5 promoter at the *ICP22* locus in 27_4_Or2_β22 does not occur.

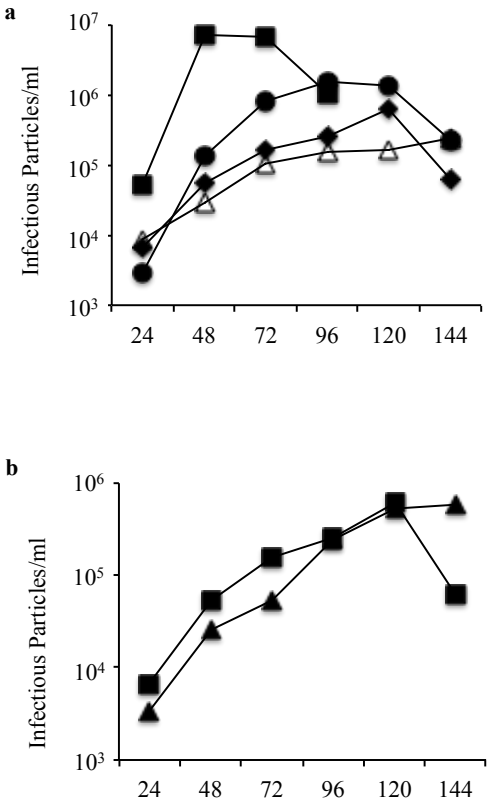

Figure 8. Comparison of growth kinetics of non-replicative genomic HSV-1 mutants

a. Replication kinetics of HSV-1 WT (solid squares) in Vero cells and 27_22_4_Or2 (open triangles), 27_4_Or2 (filled triangles) and 27_4_Or2_β22 (filled diamonds) in 7b cells infected at a MOI of 0.05.

b. Replication kinetics 27_4_Or2_β22 (filled diamonds) and 27_4_Or2_β22_ β47 (open diamonds) in 7b cells infected at a MOI of 0.05.

We have thus generated the 27_4_Or2_β22 vector; a high capacity nonreplicative genomic HSV-1 vector deleted for 23 kb of viral genome sequences in which transgenes can be inserted by Cre/loxP-mediated recombination into the vector-encoding BAC plasmid. Our results show that the genome deletions in this

27_4_Or2_β22 vector do not seriously impair vector production.

6.4. Human frataxin expression from a reduced genomic FXN-reporter construct

For the generation of a recombinant herpes virus vector for long-lasting neurological gene therapy of Friedreich's ataxia (FRDA), our second goal was to construct a human *FXN* transgene which fits within the cargo size limit of the 27_4_Or2_β22 vector while retaining all the regulatory elements necessary for physiological expression.

Starting from our BAC plasmid encoding the human *FXN* genomic locus (FXN-WT) [163], we generated two progressively deleted constructs, resulting in the decrease of the *FXN* transgene cassette from 135 kb down to 20 kb. We first eliminated 42.51 kb of the 5' upstream region to generate the FXN-p vector, which maintains 5 kb of the 5' upstream sequence described as containing the promoter regulatory elements necessary for physiological control of the *FXN* gene expression (**Figure 9a**). [111] Subsequent modifications were made as described in Methods to reduce the transgene down to 20 kb, resulting in the FXNinlZ construct which comprises the 5 kb promoter, *FXN* exon 1, intron 1 and a partial cDNA encoding exons 2 to 5a. To more easily monitor *FXN* transgene levels in expression studies we incorporated the *lacZ* reporter gene to be co-expressed via a 2A peptide cassette [195,196] located at the 3' end of the *FXN* open reading frame (**Figure 9a**). Correctly modified clones for the two generated constructs were confirmed by *Bam*HI digestion followed by electrophoresis. Deletion boundaries were further confirmed by DNA sequencing analysis.

Recently, Xia and co-workers identified two novel tissue-specific *FXN* isoforms (II and III), which may contribute to the pathological mechanism of Friedreich's ataxia.[116] These transcript variants have been described to arise from differential processing within the first intron, their remaining structure being identical from exons 2 to 5. Of particular relevance to our interest in gene therapy for the neurological aspects of FRDA, isoform II appears to be specifically expressed in nervous tissue. To evaluate if our reduced *FXN* transgene constructs maintain the regulatory elements necessary for alternative splicing of human *FXN*, we transfected mouse neuroblastoma cells (Neuro-2a) with each of the three FXN constructs and compared lysates of these samples to those from non transfected Neuro-2a cells and

the human neuroblastoma cell line SH-SY5Y as a positive control for human neuronal *FXN* isoforms. Using human isoform-specific primer pairs for reverse transcription polymerase chain reaction (RT-PCR) analysis, we were able to detect both the major *FXN* splice isoform (FXN-I) as well as the neuron-specific splice isoform (FXN-II) in Neuro-2a cells transfected by the three FXN constructs (**Figure 9b**), confirming that our reduced transgenes containing intron 1 maintain the desired splicing regulation for neuronal gene therapy.

We next analysed human FXN protein expression in mouse Neuro-2a cells transfected with our *FXN* transgenes (**Figure 9c**). Western blots of lysates from cells transfected with FXN-WT and FXNinlZ revealed three forms of FXN not present in non-transfected Neuro-2a cells (mock) corresponding to the precursor, intermediate and mature forms; as expected, migration of the bands in lysates from FXNinlZ-transfected cells was retarded with respect to those in the FXN-WT samples due to the 22 amino acid C-terminal fusion to the 2A peptide sequence. In FXNinlZ samples a full-length translation product (hFxn-2A-βgal) can be detected, indicating that 2A peptide cleavage is incomplete. We confirmed that the β-Galactosidase reporter was functional by X-Gal staining of FXNinlZ-transfected Neuro-2a cells (**Figure 9d**).

These results indicate that a reduced version of the *FXN* genomic locus, comprising the 5 kb promoter, FXN cDNA and the complete sequence of intron 1, maintains the regulatory elements necessary to express the frataxin isoforms normally found in neurons. Co-expression of the FXN-β-Galactosidase reporter in this transgene using the 2A peptide system offers an alternative means to monitor vector transduction.

6.5. Human frataxin expression in cultured dorsal root ganglion neurons transduced by the FXNinlZ non-replicative genomic HSV-1 derived vector

The third goal for the generation of a gene therapy vector targeting dorsal root ganglia (DRG) for FRDA was the construction of the 27_4_Or2_β22 vector carrying the FXNinlZ transgene. With this aim, as described in Methods, we used Cre/loxP-mediated recombination to introduce the FXNinlZ construct or a reporter gene expression cassette consisting of the CMV promoter and the *GFP* gene into the U_L3-U_L4 intergenic region of the 27_4_Or2_β22 vector thus generating the 27_4_Or2_β22 FXNinlZ vector and the 27_4_Or2_β22 GFP control vector respectively (**Figure 10a**).

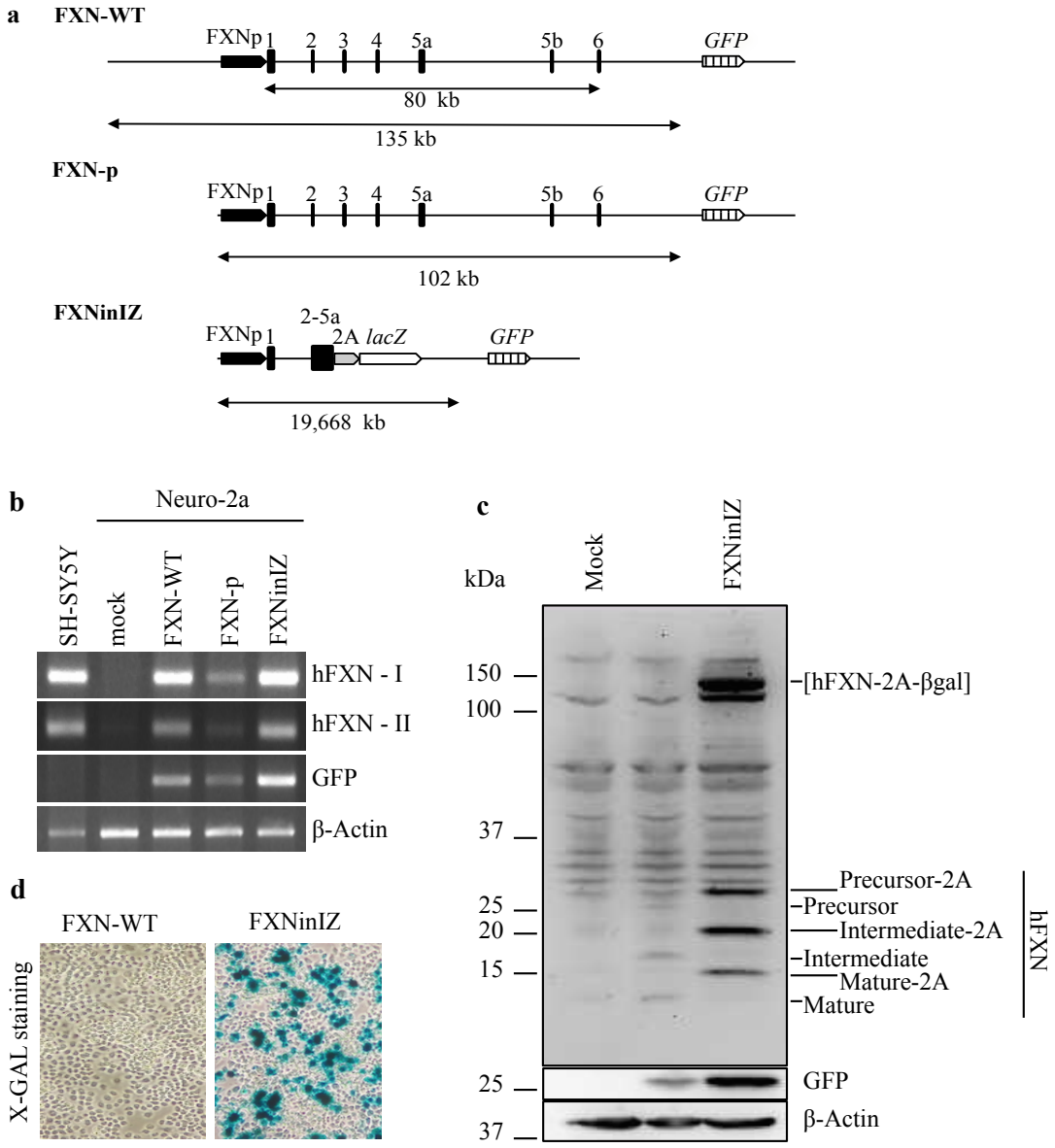

Figure 9. Human FXN expression from a size-reduced *FXN* genomic transgene.

a. Schematic (not to scale) of the transgenic cassettes encoding: the 80kb human *FXN* locus within a 135-kb genomic DNA fragment (top, FXN-WT), showing the FXN promoter (FXNp, black arrowed box) and exons 1 to 6 (black vertical boxes); a reduced transgene (middle, FXN-p) with all 5' upstream sequences deleted except for the 5kb promoter (black arrowed box, FXNp); a reduced transgene (bottom, FXNinlZ) with the 5kb promoter, exon 1, intron 1 and a partial cDNA encoding exons 2-5a fused in-frame to the *E.coli lacZ* reporter gene (open arrowed box) via the 2A linker peptide (grey arrowed box). All FXN constructs described in this study also contain the green fluorescent protein reporter gene (hatched arrowed box, GFP).

b. RT-PCR detection of human *FXN* isoforms I and II in total mRNA prepared 48 hours after transfection of Neuro-2a cells with FXN-WT, FXN-mp and FXNinlZ DNA. The human neuroblastoma cell line (SH-SY5Y) was used as a positive control for human FXN and non

transduced Neuro-2a as negative control. Transduction efficiency and sample loading were monitored by detection of *GFP* and *β-Actin* respectively.
c. Western blot of extracts derived from Neuro-2a cells 48h after transfection with FXN-WT and FXNinlZ DNA. Incubation of the blot with human FXN-specific antibody revealed the three human FXN forms fused to the 2A peptide (precursor-2A, intermediate-2A and mature-2A) expressed by FXNinlZ with a lower mobility compared to those expressed by FXN-WT. Non transfected Neuro-2a (Mock) were used as negative controls for human FXN expression. Uncleaved FXNinlZ protein (hFXN-2A-βGAL) expressed by FXNinlZ can be also detected. As controls for transfection efficiency and loading, blots were also incubated with antibodies specific for GFP and β-Actin respectively. Numbers to the right indicate the molecular weight (kDa) of protein marker standards.
d. Histochemical staining of Neuro-2a cells with X-Gal (5-bromo-4-chloro-3-indolyl-β-D-galactopyranoside) following transfection with FXN-WT and FXNinlZ DNA. Enzymatic β-Galactosidase activity is clearly evident in cells transduced by FXNinlZ (right) but not by FXN-WT (left).

PCR analysis and DNA sequencing confirmed correct recombinant junctions for the two generated vectors (**Supplementary figure 2**) which were then propagated and titered in the ICP4/ICP27-complementing 7b cell line. Large laboratory-scale cultures were concentrated and purified to yield 0.5 ml of each vector (**Figure 10a**), with titers of 10^8 plaque-forming units (pfu) per millilitre (27_4_Or2_β22 GFP) and $5x10^7$ pfu/ml (27_4_Or2_β22 FXNinlZ).

Following transport of wild-type HSV-1 into sensory neurons, the virus enters a latent state in which nearly all of the viral genome is silenced, and expression is restricted to a single locus which produces the latency-associated transcripts. Many nonreplicative genomic HSV-1 vectors currently employ transgene cassettes with viral immediate-early promoters which direct strong expression, but which is transient and can be subject to silencing in spinal ganglia.[37,66] We previously demonstrated that while such silencing of the IE4/5 promoter occurs in HSV-1 amplicon vectors injected into the adult mouse cerebellum, transgene expression driven from the *FXN* genomic locus was persistent.[164]

To investigate whether *FXN* genomic sequences can also provide sustained transgene expression from nonreplicative genomic HSV-1 vectors in DRG, we compared the expression of the *FXNinlZ* transgene (driven by the FXN promoter) to the expression of a *GFP* reporter gene driven by the CMV promoter after transduction of primary rat DRG neurons with our two vectors (27_4_Or2_β22 FXNinlZ or the 27_4_Or2_β22 GFP control vector) using a multiplicity of infection (MOI) of 1. RT-PCR analysis showed expression of FXNinlZ mRNA at 2 days post

infection (dpi) which increased at 6 dpi (**Figure 10b**, first 2 lanes). In contrast, *GFP* gene expression of the control vector was high at 2 dpi but decreased to almost undetectable levels at 7 dpi (**Figure 10b**, lanes 3 and 4). The opposing expression patterns of the two vectors were confirmed by real-time RT-PCR (qRT-PCR) measurements at the same time points (**Figure 10c and 10d**).

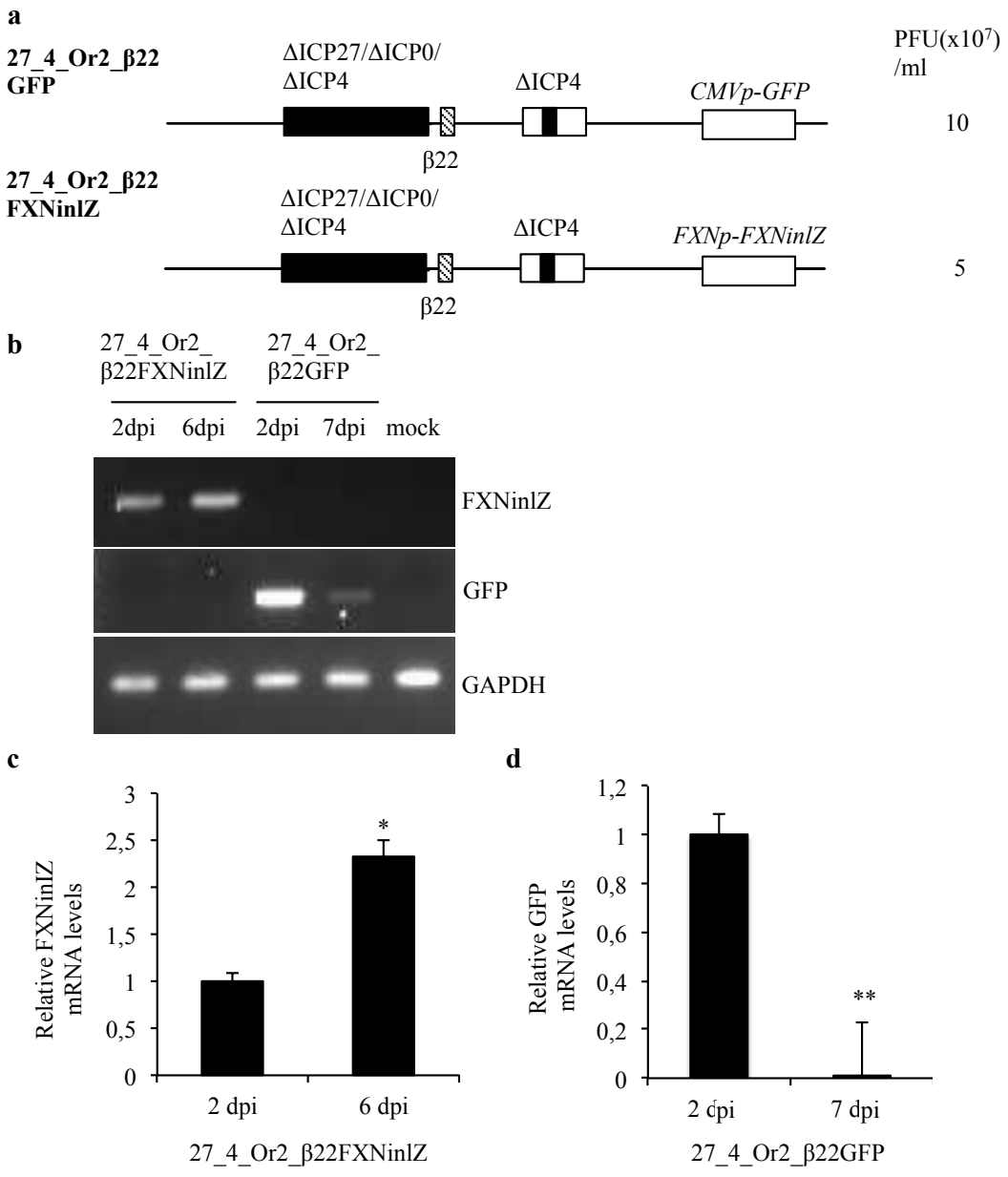

Figure 10. **Transgene expression by FXN genomic sequences compared to that driven by the viral promoter during 1 week in cultured dorsal root ganglion neurons.**

a. Schematic showing the 27_4_Or2_β22GFP and 27_4_Or2_β22 FXNinlZ replication defective HSV-1 vectors. The control vector 27_4_Or2_β22 GFP contains a CMV promoter-

GFP expression cassette introduced between the U_L3 and U_L4 genes located in the unique long region of HSV-1 genome, whereas the 27_4_Or2_β22 FXNinlZ vector contains the FXNinlZ transgene under the control of the 5kb FXN promoter (FXNp) at the same insertion site. Large black boxes represent the HSV-1 sequence deletion from the *U_L54* gene up to the ori_S copy of the IR sequence and small black boxes represent the *ICP4* gene deletion. Hatched boxes represent the ICP22 promoter TAATGARAT sequence deletion (β22). Immediate early genes deleted are listed above each deletion (Δ). Titers of viral stocks (plaque-forming units, PFU) are shown on the right of each construct.
b. RT-PCR detection of the two transgenes FXNinlZ and GFP. Fetal rat DRG neurons were infected with 27_4_Or2_β22 FXNinlZ or 27_4_Or2_β22 GFP vector at a MOI of 1 and harvested 2, 6 or 7 days after infection for mRNA extraction. As negative control for both transgenes, mRNA extracted from non-infected cells was used. Primers specific for rat glyceraldehyde phosphate dehydrogenase (*GAPDH*) detection were used to indicate loading quantities.
c. Determination of transgene mRNA levels in fetal rat DRG neurons by qRT-PCR after infection at a MOI of 1 with 27_4_Or2_β22 FXNinlZ or 27_4_Or2_β22 GFP vector. Infected cells were harvested 2, 6 or 7 days after infection for mRNA extraction. Expression normalized to GAPDH is shown relative to each respective vector-infected sample on day 2. The designations * and ** indicate statistically significant differences with p values <0.02 and <0.005, respectively. Results shown are mean values ± standard deviation (SD) from three independent experiments.

We next examined human FXN protein expression in rat DRG neurons infected by the 27_4_Or2_β22 FXNinlZ vector at a MOI of 1 (**Figure 11**). Western blot analysis of cell lysates made after 2 and 6 dpi using human FXN-specific antibody (**Figure 11**, top panel) revealed the three bands corresponding to the precursor, intermediate and mature FXN forms. As previously seen, these recombinant forms migrate with lower mobility than that of the endogenous human FXN present in human embryonic kidney (HEK293) cells due to the C-terminal fusion of the 22 amino acid 2A peptide. Moreover, the full-length translation product (frataxin-2A-βGal) could be also detected. Consistent with the qRT-PCR data, frataxin and β-Galactosidase protein levels increased from 2 dpi to 6 dpi.

Taken together, these *in vitro* results indicate that the human *FXN* genomic sequences present in our FXNinlZ transgene are capable of sustaining FXN expression in the context of a nonreplicative genomic HSV-1 vector in DRG neurons.

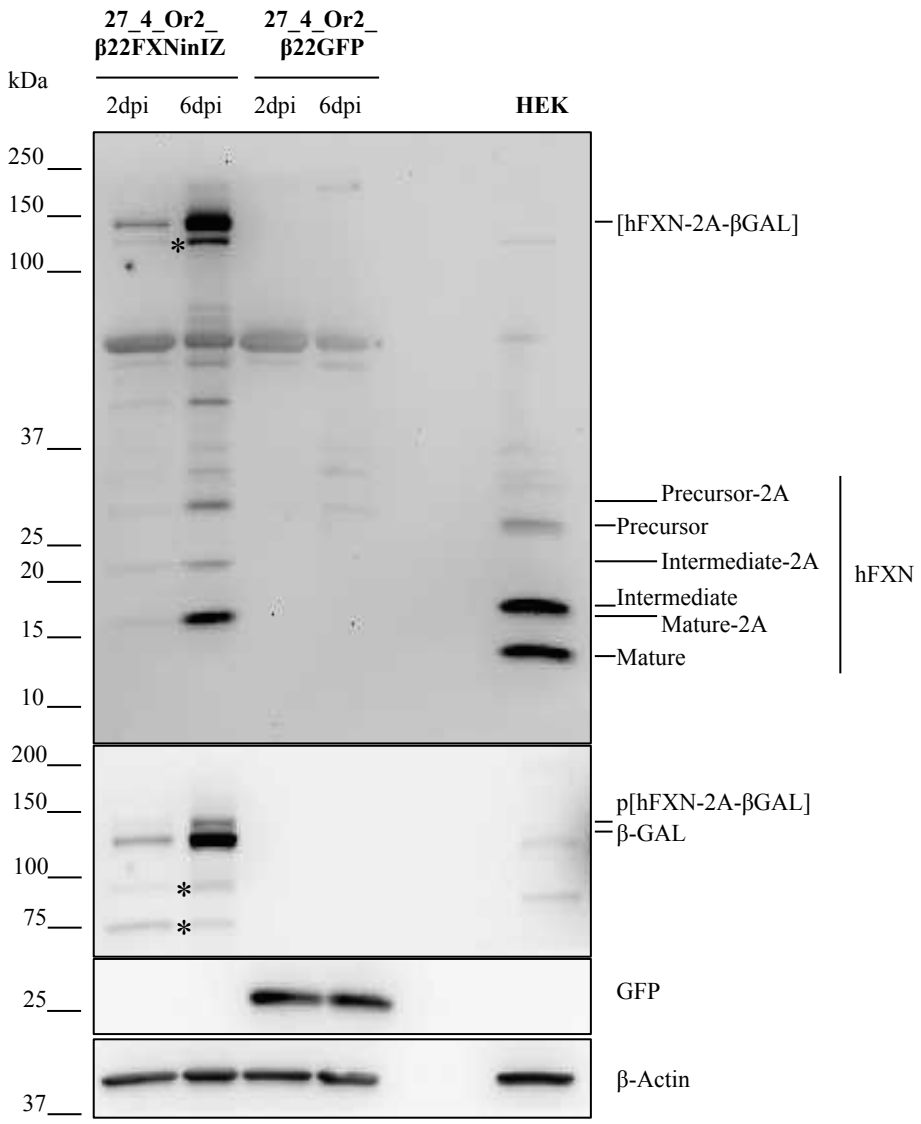

Figure 11. Human FXN protein expression after infection of cultured dorsal root ganglion neurons with the 27_4_Or2_β22 FXNinlZ vector.

Western blot of extracts derived from cultured fetal rat DRG neurons after infection with 27_4_Or2_β22 FXNinlZ or 27_4_Or2_β22 GFP for 2 or 6 days at a MOI of 1. Incubation of the blot with human FXN-specific antibody revealed expression of the three human FXN forms fused to the 2A peptide (precursor-2A, intermediate-2A and mature-2A) by the 27_4_Or2_β22 FXNinlZ vector. Due to the presence of the fused 2A peptide, these recombinant polypeptides exhibit a lower mobility compared to the three forms found in human embryonic kidney cells (HEK) protein extract, used as positive control for human FXN expression. Uncleaved full length FXNinlZ fusion protein (hFXN-2A-βGAL) expressed by the 27_4_Or2_β22 FXNinlZ vector can be also detected, as well as lower molecular weight fusion proteins containing breakdown fragments of β-Galactosidase (asterisks). Protein extracts were also probed with the indicated antibodies against the two reporter gene products β-Galactosidase (β-GAL) and GFP expressed respectively by 27_4_Or2_β22 FXNinlZ and by 27_4_Or2_β22 GFP. Protein loading quantity was detected by using antibodies specific for β-Actin. Numbers to the right indicate the molecular weight (kDa) of

protein marker standards.

6.6. Sustained *in vivo* expression of human *FXN* in rat dorsal root ganglia 1 month after peripheral inoculation with a nonreplicative genomic HSV-1 vector

To examine *in vivo* expression from our nonreplicative genomic HSV-1 vectors, adult rats were injected 1.5 x 10^6 plaque forming units (pfu) of the 27_4_Or2_β22 FXNinlZ vector or 3 x 10^6 pfu of the control 27_4_Or2_β22 GFP vector in the plantar surface of both hind paws. Total mRNA was prepared from the L4-6 DRG from rats sacrificed at seven or thirty days after inoculation, and analysed by RT-PCR using primers specific for the FXNinlZ transgene (**Figure 12a**). A PCR product with the expected electrophoretic mobility was detected in samples at both time points of rats injected with the FXNinlZ vector but not with the control GFP vector (**Figure 12a**). To confirm that the RT-PCR products obtained in **figure 4a** are indeed due to the expression of the human *FXN* transgene after retrograde transport from the rat hind paws to the DRG, the corresponding bands were extracted and analysed by DNA sequencing (**Figure 12b**).

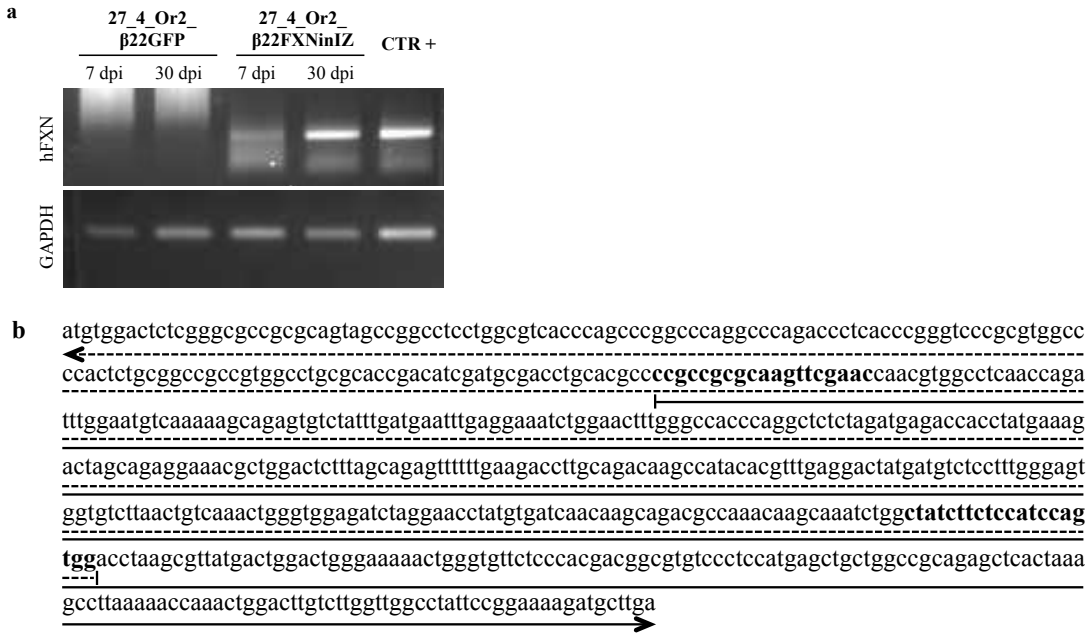

Figure 12. Human *FXN* expression in adult rat dorsal root ganglia 1 month after footpad inoculation with the 27_4_Or2_β22 FXNinlZ vector.

a. Rats were inoculated by subcutaneous injection with the 27_4_Or2_β22 FXNinlZ vector or the 27_4_Or2_β22 GFP control vector. Expression of human FXN mRNA (*hFXN*) in rat

DRG was analysed by RT-PCR 7 and 30 days post injection. As a positive control (CTR+) for the human *FXN* transgene, we used total mRNA from cultured DRG neurons after infection for 2 days with 27_4_Or2_β22 FXNinlZ. Primers specific for rat glyceraldehyde phosphate dehydrogenase (*GAPDH*) detection were used to indicate loading quantities.
b. Complementing DNA sequence corresponding to the protein coding region of the human *FXN* canonical transcript containing exons 1, 2, 3, 4 and 5a. Solid and dotted arrows indicate the two sequencing reads of the RT-PCR products from figure 12a. Boldface nucleotide sequences represent the binding site for the two primers used.

These preliminary results of sustained *FXN* expression *in vivo* after delivery of a *FXN* transgene regulated by its natural genomic sequences are an encouraging indication for the possibility of FRDA gene therapy using the 27_4_Or2_β22 FXNinlZ vector.

DISCUSSION

7. DISCUSSION

Gene therapy is as wide a field as that of pharmacology of small molecule compounds, and the vastly different effects of different vectors on dosage, biodistribution, toxicology and pharmacokinetics should be considered. As human gene therapy trials demonstrating beneficial effects begin to accumulate, it is clear that precise transgene regulation will be essential for this field to become a clinical reality. When gene transfer is carried out in dividing cells, low transduction efficiencies and loss of cells due to toxicity can often still yield a good clinical outcome due to expansion of a small number of rescued cells, but in postmitotic cells such as neurons, not only is high transduction efficiency important, but any cell loss due to the treatment is permanent and should therefore be minimized. Significantly, frataxin overexpression has been observed to be toxic in cultured fibroblasts [126], and in a Drosophila model, to provoke deleterious effects at biochemical, physiological and developmental levels [127], underlining the importance of controlling FXN levels in FRDA gene therapy approaches. Thus, efficacious treatment of FRDA patients using FXN-encoding viral vectors will require sustained and physiological expression from the therapeutic transgene, an unresolved challenge in gene therapy so far.

7.1. Nonessential elements of the HSV-1 IE4/5 promoter region play a critical role in the viability of multiply deleted nonreplicative HSV-1 genomic vectors

The most rapid technological advances in viral vectors for gene delivery, especially in the clinic [197], have been made by vectors derived from viruses such as adenoviruses, retroviruses, lentiviruses, and adeno-associated viruses, which is understandable since their small genomes have simplified their comprehension and manipulation. However, there is now increasingly a need of larger capacity vectors able to deliver multiple transgenes or to encode genomic regulatory regions. With this aim, in the present study we have generated high capacity nonreplicative genomic HSV-1 vectors deleted for up to 24 kb of viral genome sequences in which transgenes can be inserted by Cre/loxP-mediated recombination into the vector-encoding bacterial artificial chromosome (BAC) plasmid.

In this study, we show that the viral growth of an HSV-1 vector deleted for ICP4, ICP27, U_L55, U_L56 and the IR sequence, in an ICP4/ICP27 complementing cell line, depends on the presence of the two ori_S copies although addition of a third copy of ori_S does not confer further replication advantages. A similar high capacity vector deleted for ICP4, ICP27, ICP0, ICP22 and the IR sequence, was however reported by Craft and coworkers to be able to grow in the same ICP4/ICP27 complementing cell line in the presence of a single copy of ori_S, although they observed that vector yield was extremely limited.[198] It should be noted that this mutant was engineered from a parental HSV-1 strain KOS while the parental virus strain used in the present study was the HSV-1 strain F cloned in a BAC plasmid. Recent observations by Miyagawa and colleagues also suggest the requirement of only one copy of ori_S in a deleted backbone for ICP4, ICP27, ICP0, IR and the TAATGARAT elements of ICP22.[56] However this mutant and our mutants were engineered using different HSV-1 isomers and different complementing cell lines. In our mutants, deletion of the IR in 27_22_4_Or includes the ICP22 promoter sequence and the cell line used to propagate the vector did not complement the deleted copy of ICP0 removed with the IR. By contrast, deletion of the IR described by Miyagawa and colleagues included the ICP47 promoter sequence and the elimination of both ICP0 copies was complemented by vector amplification in cells derived from the U2OS cell line, which expresses an activity that can compensate for the lack of ICP0. Taking into account that ICP0 and ICP22 have a key role in viral genome transcription while ICP47 is involved in evasion of the host immune system, we hypothesize that the necessity for an ori_S and/or the ICP22 promoter reflects the advantages of maintaining a synergy between the viral DNA replication machinery and the activation of the viral genome transcription by the IE genes, in order to retain the growth capacity of multiply deleted genomic vectors.

In agreement with previous studies showing the growth advantages that ICP22 confers to multiply deleted vectors[49,51], we show that the reconstitution of the entire ICP22 IE4/5 promoter region at its natural location in the IR, not only reverts the replication failure caused by additional deletion of ICP4, ICP27, U_L55 and U_L56, but also significantly improves titers compared to the ectopic addition of a single ori_S sequence. Whether the growth defect of the 27_22_4_Or mutant can be rescued by reconstitution of the ICP22 promoter without the ori_S is difficult to determine since the ori_S sequence is embedded in the ICP22 promoter region. One study has shown

that deletion of the ori_S sequence from the IE4/5 promoter does not drastically affect expression of a linked luciferase reporter gene [199] but whether this can be extrapolated to the independence of ICP22 expression on ori_S remains to be tested.

Supporting previous observations of Samaniego and coworkers [52], we have also confirmed that deletion of the TAATGARAT elements of the ICP22 IE4/5 promoter to convert ICP22 expression from immediate-early to early kinetics, maintains ICP22 growth-supporting functions and that additional deletion of the TAATGARAT elements of the ICP47 IE4/5 promoter also does not interfere with the replication capacity of multiply deleted vectors.

Half of the HSV-1 genome, comprising more than 40 genes, has been described as non-essential for viral replication in cell culture. Deletions of these genome sequences have been individually studied and described as non-essential in the context of a wild-type HSV-1 backbone. Notwithstanding, combination of non-essential deletions may lead to synergistic lethal effects reflecting essential functions resulting from interactions among these gene products.

The large genome and slow replication of multiply deleted HSV-1 vectors present technical challenges for their manipulation and further modification. A key step in the development of HSV-1 vectors was the cloning of the entire viral genome as a BAC vector and its use for *in vitro* site-directed mutagenesis. However complementation of large genome sequence deletions through generation of complementing cell lines expressing these sequences have not been achieved so far. In order to generate high capacity non-replicative genomic vectors that maintain their amplification capacity there is a clear need of rapidly generation of stable and efficient complementing cell lines.

7.2. A reduced *FXN* genomic transgene maintains the elements necessary to undergo physiological neuronal regulation

Although the transgene capacity achieved in our vectors is almost 24 kb, which widely exceeds that of most viral vectors in current use, it is insufficient to accommodate the entire *FXN* genomic locus, previously demonstrated to direct longterm expression in the adult mouse cerebellum.[164] Therefore we have instead inserted in our vectors, a reduced *FXN* genomic transgene comprising the 5 kb promoter and a cDNA which includes the complete sequence of intron 1, which has previously been shown to give rise to nervous system transcript variants of *FXN*. We

have confirmed that our reduced transgene does indeed support sustained expression of both the canonical *FXN* I isoform as well as the nervous system-specific *FXN* II isoform after delivery into dorsal root ganglia. Moreover, detection of the precursor, intermediate and mature FXN forms indicate successful translation and mitochondrial processing of transgenic frataxin. Potential gene therapies to treat FRDA cardiomyopathy[160,161] use vectors containing the cDNA which encodes only the canonical *FXN* I isoform. However the possibility of a significant contribution of the other isoforms to the pathology of FRDA cannot be ignored. The availability of our reduced *FXN* transgene in a neurotropic viral vector will facilitate the further identification of functional elements in *FXN* locus important for the regulation of frataxin in the nervous system.

7.3. Native regulatory elements conserved in a reduced *FXN* genomic transgene sustain *FXN* expression in the context of non-replicative HSV-1 genomic vector in DRG neurons

As mentioned in this study, one of the important issues to be addressed in the use of viral vectors for gene delivery is the maintenance of transgene expression. Of special relevance, the role of transgene regulatory sequences and their interaction with both viral as well as cellular proteins are known to be important.

In the context of non-replicative genomic HSV-1 vectors, virus-derived promoters with immediate early kinetics have been used to drive strong and transient transgene expression. Thus, these promoters are potential tools for short-term transgene expression in a wide range of cell types and can serve to generate marker transgenes to monitor the distribution and spread of recombinant viruses. Conversely, latency-associated promoters have been used to achieve persistent transgene expression from HSV-1 genomic vectors in neurons.[37,200] Native cellular regulatory regions have been less studied for gene delivery with HSV-1 genomic vectors due to their large size, often extending thousands of base pairs, exceeding the limited capacity of these vectors to date.

In this study, a genomic vector carrying a reduced *FXN-lacZ* transgene was first tested by infecting different types of dividing cells (data not shown). After infection with the recombinant virus at different time points (up to 5-6 days, mainly limited by overgrowth of the cells after this time) and various multiplicities of infection (MOI 0.5, 1 and 5), none of the cell types tested showed *lacZ* enzymatic

activity or protein expression although vector infection could be confirmed by immunostaining for HSV-1 virion proteins or expression of the ICP0 protein. Therefore, the lack of detectable transgene expression did not simply reflect the lack of infected cells. Some *lacZ* RNA expression was observed by RT-PCR, indicating that only a very low level of transgene expression occurs in dividing cells infected by our vector. *LacZ* enzymatic activity was also undetectable when the HSV-1 FXN-lacZ vector genome was transfected into dividing cells but it was clearly evident in dividing cells transfected with DNA encoding the *FXN-lacZ* transgene alone, thus confirming the correct functionality of this transgene, and that its silencing in the context of the HSV-1 FXN-lacZ vector is due to interference by the HSV-1 genome in dividing cells. Significantly, we have observed that the presence of the viral genome does not silence transgene expression in dorsal root ganglion neurons. Indeed the genomic elements conserved in the reduced *FXN* transgene appear to protect frataxin expression against neuronal silencing of the viral vector genome; using the same viral vector, we confirmed that this neuronal silencing response reduces GFP expression driven by the CMV promoter down to undetectable levels, in concordance with previous observations of transgene expression using strong viral promoters in nonreplicative genomic HSV-1 vectors.[58,70]

Based on these preliminary studies revealing the interactions between the *FXN* transgene, the nonreplicative HSV-1 vector genome and host cell responses to vector infection, we propose the following hypothesis. Upon the entry of the recombinant vector genome into the host cell, two early events could be crucial for the *FXN* transgene expression: a gradual host immune response to the viral infection and the immediate introduction of virion proteins (eg VP16 and the virion host shutoff protein (VHS)) as well as the expression of the remaining IE vector genes. During this period the host immune response may reduce gene expression of all DNA within the cell. Since the virion proteins have been selected during evolution to function in spite of the host antiviral response, all the genes transactivated by these proteins would keep expressing, while other cellular and viral genes would be silenced, including the *FXN* transgene. In addition, the presence of viral proteins such as VHS, which reduce host translation to favour viral protein synthesis, could further impair *FXN* transgene expression. It should be noted that these processes could be stimulated in mitotic cells by factors associated with cell division thus further promoting the *FXN* transgene silencing. Conversely, in DRG neurons the IE and

virion proteins present upon infection would eventually degrade due to the lack of cell division and cellular transactivation of IE or other viral gene expression. Moreover, since the vector genome is transported to the DRG neurons along axons, virion proteins like VP16 and VHS may not reach the DRG neurons in the same amounts as in infected dividing cells.

In DRG neurons, apart from the general host antiviral response, there are specific anti-HSV-1 responses, such as the miRNA against ICP0 expression (miR-138)[203], which promotes establishment of the vector genome quiescent state and thus the recovery of normal cellular activity. The transgene, which contains cellular regulatory elements, would then be expressed similarly to the rest of the cellular genome. Regulatory elements of the *FXN* transgene, which normally direct cellular epigenetic modifications for active gene expression, could thus counteract the cellular silencing of the rest of the viral genome.

7.4. In vivo delivery and sustained expression of a reduced *FXN* genomic transgene by a non-replicative genomic HSV-1 vector in dorsal root ganglia

To date gene therapy of Friedreich's ataxia has been explored with only a few types of vectors.[201] It is important that development and evaluation of all of these continue to be supported since different aspects of the same disease may be better treated by different vector types and delivery strategies. For the cardiomyopathy associated with FRDA, AAV-derived vectors have shown promising efficacy in mouse models when administered by intravenous[160] or intraperitoneal injection.[161] In the latter case, application for the neurological aspects of FRDA were considered, since these vectors could be detected in the brain when very high doses were used. However, given the elevated number of host cells being genetically modified by vector genomes, these encouraging results now await careful studies of biodistribution and biotoxicity. In a more recent study, intravenous injection of *FXN* mRNA encapsulated in lipid nanoparticles was shown to increase liver frataxin levels in mice and some expression could be detected in DRG neurons if the nanoparticles were administered by intrathecal delivery.[202] These promising observations open the possibility of using easily manufactured nanoparticles although the requirement for repeated intrathecal injections due to their short persistence of therapeutic effect remains an obstacle to overcome before translation to the clinic.

In our approach to neurological gene therapy of FRDA we aim to target the DRG neurons using a non invasive gene delivery strategy already validated to be safe in human clinical trials.[53] Using the rat footpad inoculation model we have confirmed that our HSV-1 vector preserves the capacity of retrograde axonal transport and gene delivery into DRG neurons, one of the first sites of neurodegeneration in FRDA. In these tissues our reduced *FXN* transgene supported sustained human *FXN* expression similar to our previous observations with the entire *FXN* locus in the mouse cerebellum.[164] Taken together, the data in this present work urge a more extensive study of our reduced genomic FXN vector in an FRDA animal model to test efficacy and safety. The high capacity genomic HSV-1 vector generated can be further used to deliver other transgenes for alternative gene therapy strategies of the DRG.

CONCLUSIONS

8. CONCLUSIONS

The conclusions drawn from this work can be summarized as follows:

1. Within the herpes simplex virus type-1 (HSV-1) genome the non-essential sequences comprising ori_S and the *ICP22* gene play a critical role in the growth of multiply deleted nonreplicative HSV-1 genomic vectors.

2. A nonreplicative HSV-1 genomic vector deleted for 23 kb, which include the sequences between the *ICP27* gene and the TAATGARAT motifs of the ICP22 promoter and the remaining *ICP4* gene sequence, can be produced at high titers and preserves the capacity of retrograde axonal transport and gene delivery into dorsal root ganglion (DRG) neurons.

3. A reduced human *FXN* genomic transgene, comprising the 5 kb promoter and a complementary DNA which includes the complete sequence of intron 1, maintains the elements necessary to direct physiological alternative splicing and protein maturation in neurons.

4. Native regulatory elements conserved in a reduced human *FXN* genomic transgene sustain *FXN* expression in the context of a nonreplicative HSV-1 genomic vector in DRG neurons *in vitro and in vivo.*

CONCLUSIONES

Las conclusiones extraídas de este trabajo son las siguientes:

1. El origen de replicación (ori_S) y el gen *ICP22*, definidos como secuencias no esenciales del virus del herpes simple tipo 1 (VHS-1), desempeñan un papel crítico en el crecimiento de los vectores genómicos no replicativos de deleción múltiple derivados a partir del VHS-1.

2. El vector genómico no replicativo derivado del VHS-1 cuya deleción de 23 kb elimina las secuencias comprendidas entre el gen *ICP27* y los motivos TAATGARAT del promotor del gen *ICP22*, así como la secuencia de la segunda copia del gen *ICP4*, se produce a altos títulos virales conservando tanto la capacidad de transporte axonal retrogrado así como de entrega del transgen en neuronas de los ganglios de la raíz dorsal.

3. La versión reducida del locus genómico humano de *FXN* que consiste en el promotor de 5 kb, la secuencia del ADN complementario y la secuencia completa del intrón 1, contiene las secuencias necesarias tanto para el 'splicing' alternativo como para la maduración de FXN en neuronas.

4. El transgen de FXN generado, clonado en el vector genómico no replicativo derivado de VHS-1, contiene las secuencias y elementos reguladores necesarios para la expresión sostenida de *FXN* en neuronas de los ganglios de la raíz dorsal.

BIBLIOGRAPHY

9. BIBLIOGRAPHY

1. Lowenstein, A (1919). Aetiologische untersuchungen uber den fieber- haften, herpes. *Munch Med Wochenschr* **66:** 769-770.

2. Liesegang, TJ (2001). Herpes simplex virus epidemiology and ocular importance. *Cornea* **20**(1): 1-13.

3. Becker, Y, Dym, H and Sarov, I (1968). Herpes simplex virus DNA. *Virology* **36**(2): 184-192.

4. Roizman, B and Whitley, RJ (2013). An inquiry into the molecular basis of HSV latency and reactivation. *Annu Rev Microbiol* **67**: 355-374.

5. Sawtell, NM and Thompson, RL (1992). Rapid in vivo reactivation of herpes simplex virus in latently infected murine ganglionic neurons after transient hyperthermia. *J Virol* **66**(4): 2150-2156.

6. Wagner, EK, Rice, M and Sutherland, BM (1975). Photoreactivation of herpes simplex virus in human fibroblasts. *Nature* **254**(5501): 627-628.

7. Whitley, RJ, Kimberlin, DW and Roizman, B (1998). Herpes simplex viruses. *Clin Infect Dis* **26**(3): 541-53; quiz 554-5.

8. Sheldrick, P and Berthelot, N (1975). Inverted repetitions in the chromosome of herpes simplex virus. *Cold Spring Harb Symp Quant Biol* **39 Pt 2** 667-678.

9. Mocarski, ES and Roizman, B (1982). Structure and role of the herpes simplex virus DNA termini in inversion, circularization and generation of virion DNA. *Cell* **31**(1): 89-97.

10. Strang, BL and Stow, ND (2005). Circularization of the herpes simplex virus type 1 genome upon lytic infection. *J Virol* **79**(19): 12487-12494.

11. Nishiyama, Y (1996). Herpesvirus genes: molecular basis of viral replication and pathogenicity. *Nagoya J Med Sci* **59**(3-4): 107-119.

12. Ward, PL and Roizman, B (1994). Herpes simplex genes: the blueprint of a successful human pathogen. *Trends Genet* **10**(8): 267-274.

13. Honess, RW and Roizman, B (1974). Regulation of herpesvirus macromolecular synthesis. I. Cascade regulation of the synthesis of three groups of viral proteins. *J Virol* **14**(1): 8-19.

14. Gaffney, DF, McLauchlan, J, Whitton, JL and Clements, JB (1985). A modular system for the assay of transcription regulatory signals: the sequence TAATGARAT is required for herpes simplex virus immediate early gene activation. *Nucleic Acids Res* **13**(21): 7847-7863.

15. Mackem, S and Roizman, B (1982). Differentiation between alpha promoter and regulator regions of herpes simplex virus 1: the functional domains and sequence of a movable alpha regulator. *Proc Natl Acad Sci U S A* **79**(16): 4917-4921.

16. Gerster, T and Roeder, RG (1988). A herpesvirus trans-activating protein interacts with transcription factor OTF-1 and other cellular proteins. *Proc Natl Acad Sci U S A* **85**(17): 6347-6351.

17. O'Hare, P, Goding, CR and Haigh, A (1988). Direct combinatorial interaction between a herpes simplex virus regulatory protein and a cellular octamer-binding factor mediates specific induction of virus immediate-early gene expression. *EMBO J* **7**(13): 4231-4238.

18. Coen, DM, Weinheimer, SP and McKnight, SL (1986). A genetic approach to promoter recognition during trans induction of viral gene expression. *Science* **234**(4772): 53-59.

19. Steffy, KR and Weir, JP (1991). Mutational analysis of two herpes simplex virus type 1 late promoters. *J Virol* **65**(12): 6454-6460.

20. Woerner, AM and Weir, JP (1998). Characterization of the initiator and downstream promoter elements of herpes simplex virus 1 late genes. *Virology* **249**(2): 219-230.

21. Watson, RJ and Clements, JB (1980). A herpes simplex virus type 1 function continuously required for early and late virus RNA synthesis. *Nature* **285**(5763): 329-330.

22. Everett, RD (1984). Trans activation of transcription by herpes virus products: requirement for two HSV-1 immediate-early polypeptides for maximum activity. *EMBO J* **3**(13): 3135-3141.

23. DeLuca, NA, McCarthy, AM and Schaffer, PA (1985). Isolation and characterization of deletion mutants of herpes simplex virus type 1 in the gene encoding immediate-early regulatory protein ICP4. *J Virol* **56**(2): 558-570.

24. Smith, CA, Bates, P, Rivera-Gonzalez, R, Gu, B and DeLuca, NA (1993). ICP4, the major transcriptional regulatory protein of herpes simplex virus type 1, forms a tripartite complex with TATA-binding protein and TFIIB. *J Virol* **67**(8): 4676-4687.

25. Carrozza, MJ and DeLuca, NA (1996). Interaction of the viral activator protein ICP4 with TFIID through TAF250. *Mol Cell Biol* **16**(6): 3085-3093.

26. Hardy, WR and Sandri-Goldin, RM (1994). Herpes simplex virus inhibits host cell splicing, and regulatory protein ICP27 is required for this effect. *J Virol* **68**(12): 7790-7799.

27. Rice, SA, Su, LS and Knipe, DM (1989). Herpes simplex virus alpha protein ICP27 possesses separable positive and negative regulatory activities. *J Virol* **63**(8): 3399-3407.

28. McMahan, L and Schaffer, PA (1990). The repressing and enhancing functions of the herpes simplex virus regulatory protein ICP27 map to C-terminal regions and are required to modulate viral gene expression very early in infection. *J Virol* **64**(7): 3471-3485.

29. Everett, RD (2000). ICP0, a regulator of herpes simplex virus during lytic and latent infection. *Bioessays* **22**(8): 761-770.

30. Hagglund, R and Roizman, B (2004). Role of ICP0 in the strategy of conquest of the host cell by herpes simplex virus 1. *J Virol* **78**(5): 2169-2178.

31. Everett, RD and Chelbi-Alix, MK (2007). PML and PML nuclear bodies: implications in antiviral defence. *Biochimie* **89**(6-7): 819-830.

32. Rice, SA, Long, MC, Lam, V, Schaffer, PA and Spencer, CA (1995). Herpes simplex virus immediate-early protein ICP22 is required for viral modification of host RNA polymerase II and establishment of the normal viral transcription program. *J Virol* **69**(9): 5550-5559.

33. Hill, A, Jugovic, P, York, I, Russ, G, Bennink, J, Yewdell, J*, et al.* (1995). Herpes simplex virus turns off the TAP to evade host immunity. *Nature* **375**(6530): 411-415.

34. Marconi, P, Manservigi, R and Epstein, AL (2010). HSV-1-derived helper-independent defective vectors, replicating vectors and amplicon vectors, for the treatment of brain diseases. *Curr Opin Drug Discov Devel* **13**(2): 169-183.

35. Manservigi, R, Argnani, R and Marconi, P (2010). HSV Recombinant Vectors for Gene Therapy. *Open Virol J* **4** 123-156.

36. Marconi, P, Fraefel, C and Epstein, AL (2015). Herpes simplex virus type 1 (HSV-1)-derived recombinant vectors for gene transfer and gene therapy. *Methods Mol Biol* **1254** 269-293.

37. Glorioso, JC (2014). Herpes simplex viral vectors: late bloomers with big potential. *Hum Gene Ther* **25**(2): 83-91.

38. Jerusalinsky, D, Baez, MV and Epstein, AL (2012). Herpes simplex virus type 1-based amplicon vectors for fundamental research in neurosciences and gene therapy of neurological diseases. *J Physiol Paris* **106**(1-2): 2-11.

39. Burton, EA, Bai, Q, Goins, WF and Glorioso, JC (2002). Replication-defective genomic herpes simplex vectors: design and production. *Curr Opin Biotechnol* **13**(5): 424-428.

40. Burton, EA, Fink, DJ and Glorioso, JC (2002). Gene delivery using herpes simplex virus vectors. *DNA Cell Biol* **21**(12): 915-936.

41. Spaete, RR and Frenkel, N (1982). The herpes simplex virus amplicon: a new eucaryotic defective-virus cloning-amplifying vector. *Cell* **30**(1): 295-304.

42. Jerusalinsky, D and Epstein, AL (2006). Amplicon vectors as outstanding tools to study and modify cognitive functions. *Curr Gene Ther* **6**(3): 351-360.

43. Smiley, JR and Duncan, J (1997). Truncation of the C-terminal acidic transcriptional activation domain of herpes simplex virus VP16 produces a phenotype similar to that of the in1814 linker insertion mutation. *J Virol* **71**(8): 6191-6193.

44. Steiner, I, Spivack, JG, Deshmane, SL, Ace, CI, Preston, CM and Fraser, NW (1990). A herpes simplex virus type 1 mutant containing a nontransinducing Vmw65 protein establishes latent infection in vivo in the absence of viral replication and reactivates efficiently from explanted trigeminal ganglia. *J Virol* **64**(4): 1630-1638.

45. McFarlane, M, Daksis, JI and Preston, CM (1992). Hexamethylene bisacetamide stimulates herpes simplex virus immediate early gene expression in the absence of trans-induction by Vmw65. *J Gen Virol* **73 (Pt 2)**(Pt 2): 285-292.

46. Thomas, SK, Lilley, CE, Latchman, DS and Coffin, RS (1999). Equine herpesvirus 1 gene 12 can substitute for vmw65 in the growth of herpes simplex virus (HSV) type 1, allowing the generation of optimized cell lines for the propagation of HSV vectors with multiple immediate-early gene defects. *J Virol* **73**(9): 7399-7409.

47. Johnson, PA, Wang, MJ and Friedmann, T (1994). Improved cell survival by the reduction of immediate-early gene expression in replication-defective mutants of herpes simplex virus type 1 but not by mutation of the virion host shutoff function. *J Virol* **68**(10): 6347-6362.

48. Samaniego, LA, Webb, AL and DeLuca, NA (1995). Functional interactions between herpes simplex virus immediate-early proteins during infection: gene expression as a consequence of ICP27 and different domains of ICP4. *J Virol* **69**(9): 5705-5715.

49. Wu, N, Watkins, SC, Schaffer, PA and DeLuca, NA (1996). Prolonged gene expression and cell survival after infection by a herpes simplex virus mutant defective in the immediate-early genes encoding ICP4, ICP27, and ICP22. *J Virol* **70**(9): 6358-6369.

50. Samaniego, LA, Wu, N and DeLuca, NA (1997). The herpes simplex virus immediate-early protein ICP0 affects transcription from the viral genome and infected-cell survival in the absence of ICP4 and ICP27. *J Virol* **71**(6): 4614-4625.

51. Krisky, DM, Wolfe, D, Goins, WF, Marconi, PC, Ramakrishnan, R, Mata, M*, et al.* (1998). Deletion of multiple immediate-early genes from herpes simplex virus reduces cytotoxicity and permits long-term gene expression in neurons. *Gene Ther* **5**(12): 1593-1603.

52. Samaniego, LA, Neiderhiser, L and DeLuca, NA (1998). Persistence and expression of the herpes simplex virus genome in the absence of immediate-early proteins. *J Virol* **72**(4): 3307-3320.

53. Fink, DJ, Wechuck, J, Mata, M, Glorioso, JC, Goss, J, Krisky, D*, et al.* (2011). Gene therapy for pain: results of a phase I clinical trial. *Ann Neurol* **70**(2): 207-212.

54. DeLuca, NA and Schaffer, PA (1987). Activities of herpes simplex virus type 1 (HSV-1) ICP4 genes specifying nonsense peptides. *Nucleic Acids Res* **15**(11): 4491-4511.

55. Yao, F and Schaffer, PA (1995). An activity specified by the osteosarcoma line U2OS can substitute functionally for ICP0, a major regulatory protein of herpes simplex virus type 1. *J Virol* **69**(10): 6249-6258.

56. Miyagawa, Y, Marino, P, Verlengia, G, Uchida, H, Goins, WF, Yokota, S*, et al.* (2015). Herpes simplex viral-vector design for efficient transduction of nonneuronal cells without cytotoxicity. *Proc Natl Acad Sci U S A* **112**(13): E1632-41.

57. Chiocca, EA, Choi, BB, Cai, WZ, DeLuca, NA, Schaffer, PA, DiFiglia, M*, et al.* (1990). Transfer and expression of the lacZ gene in rat brain neurons mediated by herpes simplex virus mutants. *New Biol* **2**(8): 739-746.

58. Puskovic, V, Wolfe, D, Goss, J, Huang, S, Mata, M, Glorioso, JC*, et al.* (2004). Prolonged biologically active transgene expression driven by HSV LAP2 in brain in vivo. *Mol Ther* **10**(1): 67-75.

59. Yokoyama, H, Sasaki, K, Franks, ME, Goins, WF, Goss, JR, de Groat, WC*, et al.* (2009). Gene therapy for bladder overactivity and nociception with herpes simplex virus vectors expressing preproenkephalin. *Hum Gene Ther* **20**(1): 63-71.

60. Stevens, JG, Wagner, EK, Devi-Rao, GB, Cook, ML and Feldman, LT (1987). RNA complementary to a herpesvirus alpha gene mRNA is prominent in latently infected neurons. *Science* **235**(4792): 1056-1059.

61. Ramakrishnan, R, Levine, M and Fink, DJ (1994). PCR-based analysis of herpes simplex virus type 1 latency in the rat trigeminal ganglion established with a ribonucleotide reductase-deficient mutant. *J Virol* **68**(11): 7083-7091.

62. Devi-Rao, GB, Goodart, SA, Hecht, LM, Rochford, R, Rice, MK and Wagner, EK (1991). Relationship between polyadenylated and nonpolyadenylated herpes simplex virus type 1 latency-associated transcripts. *J Virol* **65**(5): 2179-2190.

63. Farrell, MJ, Dobson, AT and Feldman, LT (1991). Herpes simplex virus latency-associated transcript is a stable intron. *Proc Natl Acad Sci U S A* **88**(3): 790-794.

64. Zwaagstra, J, Ghiasi, H, Nesburn, AB and Wechsler, SL (1989). In vitro promoter activity associated with the latency-associated transcript gene of herpes simplex virus type 1. *J Gen Virol* **70 (Pt 8)**(Pt 8): 2163-2169.

65. Goins, WF, Sternberg, LR, Croen, KD, Krause, PR, Hendricks, RL, Fink, DJ*, et al.* (1994). A novel latency-active promoter is contained within the herpes simplex virus type 1 UL flanking repeats. *J Virol* **68**(4): 2239-2252.

66. Marshall, KR, Lachmann, RH, Efstathiou, S, Rinaldi, A and Preston, CM (2000). Long-term transgene expression in mice infected with a herpes simplex virus type 1 mutant severely impaired for immediate-early gene expression. *J Virol* **74**(2): 956-964.

67. Palmer, JA, Branston, RH, Lilley, CE, Robinson, MJ, Groutsi, F, Smith, J*, et al.* (2000). Development and optimization of herpes simplex virus vectors for multiple long-term gene delivery to the peripheral nervous system. *J Virol* **74**(12): 5604-5618.

68. Goins, WF, Yoshimura, N, Phelan, MW, Yokoyama, T, Fraser, MO, Ozawa, H*, et al.* (2001). Herpes simplex virus mediated nerve growth factor expression in bladder and afferent neurons: potential treatment for diabetic bladder dysfunction. *J Urol* **165**(5): 1748-1754.

69. Sasaki, K, Chancellor, MB, Goins, WF, Phelan, MW, Glorioso, JC, de Groat, WC*, et al.* (2004). Gene therapy using replication-defective herpes simplex virus vectors expressing nerve growth factor in a rat model of diabetic cystopathy. *Diabetes* **53**(10): 2723-2730.

70. Scarpini, CG, May, J, Lachmann, RH, Preston, CM, Dunnett, SB, Torres, EM*, et al.* (2001). Latency associated promoter transgene expression in the central nervous system after stereotaxic delivery of replication-defective HSV-1-based vectors. *Gene Ther* **8**(14): 1057-1071.

71. Smith, SN, Paige, C, Velazquez, KT, Smith, TP, Raja, SN, Wilson, SP*, et al.* (2015). Injury-specific promoters enhance herpes simplex virus-mediated gene therapy for treating neuropathic pain in rodents. *J Pain* **16**(3): 283-290.

72. Schmeisser, F, Donohue, M and Weir, JP (2002). Tetracycline-regulated gene expression in replication-incompetent herpes simplex virus vectors. *Hum Gene Ther* **13**(18): 2113-2124.

73. Jiang, Y, Wei, N, Zhu, J, Zhai, D, Wu, L, Chen, M*, et al.* (2012). A new approach with less damage: intranasal delivery of tetracycline-inducible replication-defective herpes simplex virus type-1 vector to brain. *Neuroscience* **201** 96-104.

74. Wu, Z, Wang, S, Gruber, S, Mata, M and Fink, DJ (2013). Full-length membrane-bound tumor necrosis factor-alpha acts through tumor necrosis factor receptor 2 to modify phenotype of sensory neurons. *Pain* **154**(9): 1778-1782.

75. Blau, HM and Rossi, FM (1999). Tet B or not tet B: advances in tetracycline-inducible gene expression. *Proc Natl Acad Sci U S A* **96**(3): 797-799.

76. Zhu, Z, Ma, B, Homer, RJ, Zheng, T and Elias, JA (2001). Use of the tetracycline-controlled transcriptional silencer (tTS) to eliminate transgene leak in inducible overexpression transgenic mice. *J Biol Chem* **276**(27): 25222-25229.

77. Furth, PA, St Onge, L, Boger, H, Gruss, P, Gossen, M, Kistner, A*, et al.* (1994). Temporal control of gene expression in transgenic mice by a tetracycline-responsive promoter. *Proc Natl Acad Sci U S A* **91**(20): 9302-9306.

78. Friedreich, N (1863a). Ueber degenerative Atrophie der spinalen Hinterstrange. *Virchows Arch Pathol Anat* **26**: 391-419.

79. Friedreich, N (1863b). Ueber degenerative Atrophie der spinalen Hinterstrange. *Virchows Arch Pathol Anat* **26**:433-459.

80. Friedreich, N (1863c). Ueber degenerative Atrophie der spinalen Hinterstrange. *Virchows Arch Pathol Anat* **26**: 1-26.

81. Friedreich, N (1876). Uber ataxie mit besonderer berucksichtigung der hereditaren formen. *Virchows Arch Pathol Anat* **68**:145-245.

82. Friedreich, N (1877). Uber ataxie mit besonderer berucksichtigung der hereditaren formen. *Virchows Arch Pathol Anat* **70**:140-152.

83. Harding, AE and Hewer, RL (1983). The heart disease of Friedreich's ataxia: a clinical and electrocardiographic study of 115 patients, with an analysis of serial electrocardiographic changes in 30 cases. *Q J Med* **52**(208): 489-502.

84. Campuzano, V, Montermini, L, Molto, MD, Pianese, L, Cossee, M, Cavalcanti, F*, et al.* (1996). Friedreich's ataxia: autosomal recessive disease caused by an intronic GAA triplet repeat expansion. *Science* **271**(5254): 1423-1427.

85. Cossee, M, Schmitt, M, Campuzano, V, Reutenauer, L, Moutou, C, Mandel, JL*, et al.* (1997). Evolution of the Friedreich's ataxia trinucleotide repeat expansion: founder effect and premutations. *Proc Natl Acad Sci U S A* **94**(14): 7452-7457.

86. Harding, AE (1981). Friedreich's ataxia: a clinical and genetic study of 90 families with an analysis of early diagnostic criteria and intrafamilial clustering of clinical features. *Brain* **104**(3): 589-620.

87. Pandolfo, M (2009). Friedreich ataxia: the clinical picture. *J Neurol* **256 Suppl 1** 3-8.

88. Delatycki, MB, Williamson, R and Forrest, SM (2000). Friedreich ataxia: an overview. *J Med Genet* **37**(1): 1-8.

89. Tsou, AY, Paulsen, EK, Lagedrost, SJ, Perlman, SL, Mathews, KD, Wilmot, GR*, et al.* (2011). Mortality in Friedreich ataxia. *J Neurol Sci* **307**(1-2): 46-49.

90. Durr, A, Cossee, M, Agid, Y, Campuzano, V, Mignard, C, Penet, C*, et al.* (1996). Clinical and genetic abnormalities in patients with Friedreich's ataxia. *N Engl J Med* **335**(16): 1169-1175.

91. Koeppen, AH and Mazurkiewicz, JE (2013). Friedreich ataxia: neuropathology revised. *J Neuropathol Exp Neurol* **72**(2): 78-90.

92. Hughes, JT, Brownell, B and Hewer, RL (1968). The peripheral sensory pathway in friedreich's ataxia. An examination by light and electron microscopy of the posterior nerve roots, posterior root ganglia, and peripheral sensory nerves in cases of friedreich's ataxia. *Brain* **91**(4): 803-818.

93. Koeppen, AH, Morral, JA, Davis, AN, Qian, J, Petrocine, SV, Knutson, MD*, et al.* (2009). The dorsal root ganglion in Friedreich's ataxia. *Acta Neuropathol* **118**(6): 763-776.

94. Koeppen, AH, Ramirez, RL, Becker, AB and Mazurkiewicz, JE (2016). Dorsal root ganglia in Friedreich ataxia: satellite cell proliferation and inflammation. *Acta Neuropathol Commun* **4**(1): 46-016-0288-5.

95. Dyck, PJ and Lambert, EH (1968). Lower motor and primary sensory neuron diseases with peroneal muscular atrophy. I. Neurologic, genetic, and electrophysiologic findings in hereditary polyneuropathies. *Arch Neurol* **18**(6): 603-618.

96. Dyck, PJ, Lais, AC and Offord, KP (1974). The nature of myelinated nerve fiber degeneration in dominantly inherited hypertrophic neuropathy. *Mayo Clin Proc* **49**(1): 34-39.

97. Barbeau, A (1980). Friedreich's ataxia 1980. An overview of the physiopathology. *Can J Neurol Sci* **7**(4): 455-468.

98. Said, G, Marion, MH, Selva, J and Jamet, C (1986). Hypotrophic and dying-back nerve fibers in Friedreich's ataxia. *Neurology* **36**(10): 1292-1299.

99. Morral, JA, Davis, AN, Qian, J, Gelman, BB and Koeppen, AH (2010). Pathology and pathogenesis of sensory neuropathy in Friedreich's ataxia. *Acta Neuropathol* **120**(1): 97-108.

100. Jitpimolmard, S, Small, J, King, RH, Geddes, J, Misra, P, McLaughlin, J*, et al.* (1993). The sensory neuropathy of Friedreich's ataxia: an autopsy study of a case with prolonged survival. *Acta Neuropathol* **86**(1): 29-35.

101. Koeppen, AH, Michael, SC, Knutson, MD, Haile, DJ, Qian, J, Levi, S*, et al.* (2007). The dentate nucleus in Friedreich's ataxia: the role of iron-responsive proteins. *Acta Neuropathol* **114**(2): 163-173.

102. Koeppen, AH, Davis, AN and Morral, JA (2011). The cerebellar component of Friedreich's ataxia. *Acta Neuropathol* **122**(3): 323-330.

103. Hewer, R (1969). The heart in Friedreich's ataxia. *Br Heart J* **31**(1): 5-14.

104. Michael, S, Petrocine, SV, Qian, J, Lamarche, JB, Knutson, MD, Garrick, MD*, et al.* (2006). Iron and iron-responsive proteins in the cardiomyopathy of Friedreich's ataxia. *Cerebellum* **5**(4): 257-267.

105. Unverferth, DV, Schmidt, WR,2nd, Baker, PB and Wooley, CF (1987). Morphologic and functional characteristics of the heart in Friedreich's ataxia. *Am J Med* **82**(1): 5-10.

106. Raman, SV, Phatak, K, Hoyle, JC, Pennell, ML, McCarthy, B, Tran, T*, et al.* (2011). Impaired myocardial perfusion reserve and fibrosis in Friedreich ataxia: a mitochondrial cardiomyopathy with metabolic syndrome. *Eur Heart J* **32**(5): 561-567.

107. Lamarche, JB, Cote, M and Lemieux, B (1980). The cardiomyopathy of Friedreich's ataxia morphological observations in 3 cases. *Can J Neurol Sci* **7**(4): 389-396.

108. Abruzzo, PM, Marini, M, Bolotta, A, Malisardi, G, Manfredini, S, Ghezzo, A*, et al.* (2013). Frataxin mRNA isoforms in FRDA patients and normal subjects: effect of tocotrienol supplementation. *Biomed Res Int* **2013** 276808.

109. Li, K, Singh, A, Crooks, DR, Dai, X, Cong, Z, Pan, L*, et al.* (2010). Expression of human frataxin is regulated by transcription factors SRF and TFAP2. *PLoS One* **5**(8): e12286.

110. Greene, E, Entezam, A, Kumari, D and Usdin, K (2005). Ancient repeated DNA elements and the regulation of the human frataxin promoter. *Genomics* **85**(2): 221-230.

111. Puspasari, N, Rowley, SM, Gordon, L, Lockhart, PJ, Ioannou, PA, Delatycki, MB*, et al.* (2011). Long range regulation of human FXN gene expression. *PLoS One* **6**(7): e22001.

112. Greene, E, Mahishi, L, Entezam, A, Kumari, D and Usdin, K (2007). Repeat-induced epigenetic changes in intron 1 of the frataxin gene and its consequences in Friedreich ataxia. *Nucleic Acids Res* **35**(10): 3383-3390.

113. Oktay, Y, Dioum, E, Matsuzaki, S, Ding, K, Yan, LJ, Haller, RG*, et al.* (2007). Hypoxia-inducible factor 2alpha regulates expression of the mitochondrial aconitase chaperone protein frataxin. *J Biol Chem* **282**(16): 11750-11756.

114. Pianese, L, Tammaro, A, Turano, M, De Biase, I, Monticelli, A and Cocozza, S (2002). Identification of a novel transcript of X25, the human gene involved in Friedreich ataxia. *Neurosci Lett* **320**(3): 137-140.

115. Pianese, L, Turano, M, Lo Casale, MS, De Biase, I, Giacchetti, M, Monticelli, A*, et al.* (2004). Real time PCR quantification of frataxin mRNA in the peripheral blood leucocytes of Friedreich ataxia patients and carriers. *J Neurol Neurosurg Psychiatry* **75**(7): 1061-1063.

116. Xia, H, Cao, Y, Dai, X, Marelja, Z, Zhou, D, Mo, R*, et al.* (2012). Novel frataxin isoforms may contribute to the pathological mechanism of Friedreich ataxia. *PLoS One* **7**(10): e47847.

117. Boehm, T, Scheiber-Mojdehkar, B, Kluge, B, Goldenberg, H, Laccone, F and Sturm, B (2011). Variations of frataxin protein levels in normal individuals. *Neurol Sci* **32**(2): 327-330.

118. Sacca, F, Puorro, G, Antenora, A, Marsili, A, Denaro, A, Piro, R*, et al.* (2011). A combined nucleic acid and protein analysis in Friedreich ataxia: implications for diagnosis, pathogenesis and clinical trial design. *PLoS One* **6**(3): e17627.

119. Koutnikova, H, Campuzano, V, Foury, F, Dolle, P, Cazzalini, O and Koenig, M (1997). Studies of human, mouse and yeast homologues indicate a mitochondrial function for frataxin. *Nat Genet* **16**(4): 345-351.

120. Campuzano, V, Montermini, L, Lutz, Y, Cova, L, Hindelang, C, Jiralerspong, S*, et al.* (1997). Frataxin is reduced in Friedreich ataxia patients and is associated with mitochondrial membranes. *Hum Mol Genet* **6**(11): 1771-1780.

121. Rotig, A, de Lonlay, P, Chretien, D, Foury, F, Koenig, M, Sidi, D*, et al.* (1997). Aconitase and mitochondrial iron-sulphur protein deficiency in Friedreich ataxia. *Nat Genet* **17**(2): 215-217.

122. Al-Mahdawi, S, Pinto, RM, Varshney, D, Lawrence, L, Lowrie, MB, Hughes, S*, et al.* (2006). GAA repeat expansion mutation mouse models of Friedreich ataxia exhibit oxidative stress leading to progressive neuronal and cardiac pathology. *Genomics* **88**(5): 580-590.

123. Santos, R, Lefevre, S, Sliwa, D, Seguin, A, Camadro, JM and Lesuisse, E (2010). Friedreich ataxia: molecular mechanisms, redox considerations, and therapeutic opportunities. *Antioxid Redox Signal* **13**(5): 651-690.

124. De Biase, I, Rasmussen, A, Monticelli, A, Al-Mahdawi, S, Pook, M, Cocozza, S*, et al.* (2007). Somatic instability of the expanded GAA triplet-repeat sequence in Friedreich ataxia progresses throughout life. *Genomics* **90**(1): 1-5.

125. Cossee, M, Puccio, H, Gansmuller, A, Koutnikova, H, Dierich, A, LeMeur, M*, et al.* (2000). Inactivation of the Friedreich ataxia mouse gene leads to early embryonic lethality without iron accumulation. *Hum Mol Genet* **9**(8): 1219-1226.

126. Fleming, J, Spinoulas, A, Zheng, M, Cunningham, SC, Ginn, SL, McQuilty, RC*, et al.* (2005). Partial correction of sensitivity to oxidant stress in Friedreich ataxia patient fibroblasts by frataxin-encoding adeno-associated virus and lentivirus vectors. *Hum Gene Ther* **16**(8): 947-956.

127. Navarro, JA, Llorens, JV, Soriano, S, Botella, JA, Schneuwly, S, Martinez-Sebastian, MJ*, et al.* (2011). Overexpression of human and fly frataxins in Drosophila provokes deleterious effects at biochemical, physiological and developmental levels. *PLoS One* **6**(7): e21017.

128. Filla, A, De Michele, G, Cavalcanti, F, Pianese, L, Monticelli, A, Campanella, G*, et al.* (1996). The relationship between trinucleotide (GAA) repeat length and clinical features in Friedreich ataxia. *Am J Hum Genet* **59**(3): 554-560.

129. Bidichandani, SI, Ashizawa, T and Patel, PI (1998). The GAA triplet-repeat expansion in Friedreich ataxia interferes with transcription and may be associated with an unusual DNA structure. *Am J Hum Genet* **62**(1): 111-121.

130. Grabczyk, E and Usdin, K (2000). The GAA*TTC triplet repeat expanded in Friedreich's ataxia impedes transcription elongation by T7 RNA polymerase in a length and supercoil dependent manner. *Nucleic Acids Res* **28**(14): 2815-2822.

131. Wells, RD (2008). DNA triplexes and Friedreich ataxia. *FASEB J* **22**(6): 1625-1634.

132. Castaldo, I, Pinelli, M, Monticelli, A, Acquaviva, F, Giacchetti, M, Filla, A*, et al.* (2008). DNA methylation in intron 1 of the frataxin gene is related to GAA repeat length and age of onset in Friedreich ataxia patients. *J Med Genet* **45**(12): 808-812.

133. Evans-Galea, MV, Carrodus, N, Rowley, SM, Corben, LA, Tai, G, Saffery, R*, et al.* (2012). FXN methylation predicts expression and clinical outcome in Friedreich ataxia. *Ann Neurol* **71**(4): 487-497.

134. Al-Mahdawi, S, Pinto, RM, Ismail, O, Varshney, D, Lymperi, S, Sandi, C*, et al.* (2008). The Friedreich ataxia GAA repeat expansion mutation induces comparable epigenetic changes in human and transgenic mouse brain and heart tissues. *Hum Mol Genet* **17**(5): 735-746.

135. Herman, D, Jenssen, K, Burnett, R, Soragni, E, Perlman, SL and Gottesfeld, JM (2006). Histone deacetylase inhibitors reverse gene silencing in Friedreich's ataxia. *Nat Chem Biol* **2**(10): 551-558.

136. Soragni, E, Xu, C, Cooper, A, Plasterer, HL, Rusche, JR and Gottesfeld, JM (2011). Evaluation of histone deacetylase inhibitors as therapeutics for neurodegenerative diseases. *Methods Mol Biol* **793** 495-508.

137. Canizares, J, Blanca, JM, Navarro, JA, Monros, E, Palau, F and Molto, MD (2000). dfh is a Drosophila homolog of the Friedreich's ataxia disease gene. *Gene* **256**(1-2): 35-42.

138. Busi, MV, Zabaleta, EJ, Araya, A and Gomez-Casati, DF (2004). Functional and molecular characterization of the frataxin homolog from Arabidopsis thaliana. *FEBS Lett* **576**(1-2): 141-144.

139. Babcock, M, de Silva, D, Oaks, R, Davis-Kaplan, S, Jiralerspong, S, Montermini, L*, et al.* (1997). Regulation of mitochondrial iron accumulation by Yfh1p, a putative homolog of frataxin. *Science* **276**(5319): 1709-1712.

140. Vazquez-Manrique, RP, Gonzalez-Cabo, P, Ros, S, Aziz, H, Baylis, HA and Palau, F (2006). Reduction of Caenorhabditis elegans frataxin increases sensitivity to oxidative stress, reduces lifespan, and causes lethality in a mitochondrial complex II mutant. *FASEB J* **20**(1): 172-174.

141. Knight, SA, Sepuri, NB, Pain, D and Dancis, A (1998). Mt-Hsp70 homolog, Ssc2p, required for maturation of yeast frataxin and mitochondrial iron homeostasis. *J Biol Chem* **273**(29): 18389-18393.

142. Koutnikova, H, Campuzano, V and Koenig, M (1998). Maturation of wild-type and mutated frataxin by the mitochondrial processing peptidase. *Hum Mol Genet* **7**(9): 1485-1489.

143. Schmucker, S, Argentini, M, Carelle-Calmels, N, Martelli, A and Puccio, H (2008). The in vivo mitochondrial two-step maturation of human frataxin. *Hum Mol Genet* **17**(22): 3521-3531.

144. Cavadini, P, Adamec, J, Taroni, F, Gakh, O and Isaya, G (2000). Two-step processing of human frataxin by mitochondrial processing peptidase. Precursor and intermediate forms are cleaved at different rates. *J Biol Chem* **275**(52): 41469-41475.

145. Condo, I, Ventura, N, Malisan, F, Rufini, A, Tomassini, B and Testi, R (2007). In vivo maturation of human frataxin. *Hum Mol Genet* **16**(13): 1534-1540.

146. Bulteau, AL, O'Neill, HA, Kennedy, MC, Ikeda-Saito, M, Isaya, G and Szweda, LI (2004). Frataxin acts as an iron chaperone protein to modulate mitochondrial aconitase activity. *Science* **305**(5681): 242-245.

147. He, Y, Alam, SL, Proteasa, SV, Zhang, Y, Lesuisse, E, Dancis, A*, et al.* (2004). Yeast frataxin solution structure, iron binding, and ferrochelatase interaction. *Biochemistry* **43**(51): 16254-16262.

148. Gonzalez-Cabo, P, Vazquez-Manrique, RP, Garcia-Gimeno, MA, Sanz, P and Palau, F (2005). Frataxin interacts functionally with mitochondrial electron transport chain proteins. *Hum Mol Genet* **14**(15): 2091-2098.

149. Stemmler, TL, Lesuisse, E, Pain, D and Dancis, A (2010). Frataxin and mitochondrial FeS cluster biogenesis. *J Biol Chem* **285**(35): 26737-26743.

150. Lill, R, Hoffmann, B, Molik, S, Pierik, AJ, Rietzschel, N, Stehling, O*, et al.* (2012). The role of mitochondria in cellular iron-sulfur protein biogenesis and iron metabolism. *Biochim Biophys Acta* **1823**(9): 1491-1508.

151. Ramirez, RL, Qian, J, Santambrogio, P, Levi, S and Koeppen, AH (2012). Relation of cytosolic iron excess to cardiomyopathy of Friedreich's ataxia. *Am J Cardiol* **110**(12): 1820-1827.

152. Waldvogel, D, van Gelderen, P and Hallett, M (1999). Increased iron in the dentate nucleus of patients with Friedrich's ataxia. *Ann Neurol* **46**(1): 123-125.

153. Shan, Y and Cortopassi, G (2012). HSC20 interacts with frataxin and is involved in iron-sulfur cluster biogenesis and iron homeostasis. *Hum Mol Genet* **21**(7): 1457-1469.

154. Bayot, A, Santos, R, Camadro, JM and Rustin, P (2011). Friedreich's ataxia: the vicious circle hypothesis revisited. *BMC Med* **9** 112-7015-9-112.

155. Perlman, SL (2012). A review of Friedreich ataxia clinical trial results. *J Child Neurol* **27**(9): 1217-1222.

156. Aranca, TV, Jones, TM, Shaw, JD, Staffetti, JS, Ashizawa, T, Kuo, SH*, et al.* (2016). Emerging therapies in Friedreich's ataxia. *Neurodegener Dis Manag* **6**(1): 49-65.

157. Chapdelaine, P, Coulombe, Z, Chikh, A, Gerard, C and Tremblay, JP (2013). A Potential New Therapeutic Approach for Friedreich Ataxia: Induction of Frataxin Expression With TALE Proteins. *Mol Ther Nucleic Acids* **2** e119.

158. Li, Y, Lu, Y, Polak, U, Lin, K, Shen, J, Farmer, J*, et al.* (2015). Expanded GAA repeats impede transcription elongation through the FXN gene and induce transcriptional silencing that is restricted to the FXN locus. *Hum Mol Genet* **24**(24): 6932-6943.

159. Li, L, Matsui, M and Corey, DR (2016). Activating frataxin expression by repeat-targeted nucleic acids. *Nat Commun* **7** 10606.

160. Perdomini, M, Belbellaa, B, Monassier, L, Reutenauer, L, Messaddeq, N, Cartier, N*, et al.* (2014). Prevention and reversal of severe mitochondrial cardiomyopathy by gene therapy in a mouse model of Friedreich's ataxia. *Nat Med* **20**(5): 542-547.

161. Gerard, C, Xiao, X, Filali, M, Coulombe, Z, Arsenault, M, Couet, J*, et al.* (2014). An AAV9 coding for frataxin clearly improved the symptoms and prolonged the life of Friedreich ataxia mouse models. *Mol Ther Methods Clin Dev* **1** 14044.

162. Lim, F, Palomo, GM, Mauritz, C, Gimenez-Cassina, A, Illana, B, Wandosell, F*, et al.* (2007). Functional recovery in a Friedreich's ataxia mouse model by frataxin gene transfer using an HSV-1 amplicon vector. *Mol Ther* **15**(6): 1072-1078.

163. Gomez-Sebastian, S, Gimenez-Cassina, A, Diaz-Nido, J, Lim, F and Wade-Martins, R (2007). Infectious delivery and expression of a 135 kb human FRDA genomic DNA locus complements Friedreich's ataxia deficiency in human cells. *Mol Ther* **15**(2): 248-254.

164. Gimenez-Cassina, A, Wade-Martins, R, Gomez-Sebastian, S, Corona, JC, Lim, F and Diaz-Nido, J (2011). Infectious delivery and long-term persistence of transgene expression in the brain by a 135-kb iBAC-FXN genomic DNA expression vector. *Gene Ther* **18**(10): 1015-1019.

165. Perez-Luz, S, Gimenez-Cassina, A, Fernandez-Frias, I, Wade-Martins, R and Diaz-Nido, J (2015). Delivery of the 135 kb human frataxin genomic DNA locus gives rise to different frataxin isoforms. *Genomics* **106**(2): 76-82.

166. Katsu-Jimenez, Y, Loria, F, Corona, JC and Diaz-Nido, J (2016). Gene Transfer of Brain-derived Neurotrophic Factor (BDNF) Prevents Neurodegeneration Triggered by FXN Deficiency. *Mol Ther* **24**(5): 877-889.

167. Chapdelaine, P, Gerard, C, Sanchez, N, Cherif, K, Rousseau, J, Ouellet, DL*, et al.* (2016). Development of an AAV9 coding for a 3XFLAG-TALEfrat#8-VP64 able to increase in vivo the human frataxin in YG8R mice. *Gene Ther* **23**(7): 606-614.

168. Durfee, T, Nelson, R, Baldwin, S, Plunkett, G,3rd, Burland, V, Mau, B*, et al.* (2008). The complete genome sequence of Escherichia coli DH10B: insights into the biology of a laboratory workhorse. *J Bacteriol* **190**(7): 2597-2606.

169. Grant, SG, Jessee, J, Bloom, FR and Hanahan, D (1990). Differential plasmid rescue from transgenic mouse DNAs into Escherichia coli methylation-restriction mutants. *Proc Natl Acad Sci U S A* **87**(12): 4645-4649.

170. Taylor, RG, Walker, DC and McInnes, RR (1993). E. coli host strains significantly affect the quality of small scale plasmid DNA preparations used for sequencing. *Nucleic Acids Res* **21**(7): 1677-1678.

171. Earley, EM JK (1988). The lineage of Vero, Vero 76 and its clone C1008 in the United States, Vero cells: origin, properties and biomedical applications. *TokyoChiba Univ***:** 26-29.

172. Smith, IL, Sekulovich, RE, Hardwicke, MA and Sandri-Goldin, RM (1991). Mutations in the activation region of herpes simplex virus regulatory protein ICP27 can be trans dominant. *J Virol* **65**(7): 3656-3666.

173. Klebe, RJ, and Ruddle, FH (1969). Neuroblastoma: cell culture analysis of a differentiating stem cell system. *J Cell Biol* **43**: 69A.

174. Graham, FL, Smiley, J, Russell, WC and Nairn, R (1977). Characteristics of a human cell line transformed by DNA from human adenovirus type 5. *J Gen Virol* **36**(1): 59-74.

175. Biedler, JL, Roffler-Tarlov, S, Schachner, M and Freedman, LS (1978). Multiple neurotransmitter synthesis by human neuroblastoma cell lines and clones. *Cancer Res* **38**(11 Pt 1): 3751-3757.

176. Alting-Mees, MA and Short, JM (1989). pBluescript II: gene mapping vectors. *Nucleic Acids Res* **17**(22): 9494.

177. Saeki, Y, Fraefel, C, Ichikawa, T, Breakefield, XO and Chiocca, EA (2001). Improved helper virus-free packaging system for HSV amplicon vectors using an ICP27-deleted, oversized HSV-1 DNA in a bacterial artificial chromosome. *Mol Ther* **3**(4): 591-601.

178. Wang, S, Zhao, Y, Leiby, M and Zhu, J (2009). A new positive/negative selection scheme for precise BAC recombineering. *Mol Biotechnol* **42**(1): 110-116.

179. Schultze, N, Burki, Y, Lang, Y, Certa, U and Bluethmann, H (1996). Efficient control of gene expression by single step integration of the tetracycline system in transgenic mice. *Nat Biotechnol* **14**(4): 499-503.

180. Ejercito, PM, Kieff, ED and Roizman, B (1968). Characterization of herpes simplex virus strains differing in their effects on social behaviour of infected cells. *J Gen Virol* **2**(3): 357-364.

181. Tanaka, M, Kagawa, H, Yamanashi, Y, Sata, T and Kawaguchi, Y (2003). Construction of an excisable bacterial artificial chromosome containing a full-length infectious clone of herpes simplex virus type 1: viruses reconstituted from the clone exhibit wild-type properties in vitro and in vivo. *J Virol* **77**(2): 1382-1391.

182. Livak, KJ and Schmittgen, TD (2001). Analysis of relative gene expression data using real-time quantitative PCR and the 2(-Delta Delta C(T)) Method. *Methods* **25**(4): 402-408.

183. BERTANI, G (1951). Studies on lysogenesis. I. The mode of phage liberation by lysogenic Escherichia coli. *J Bacteriol* **62**(3): 293-300.

184. Hanahan, D (1983). Studies on transformation of Escherichia coli with plasmids. *J Mol Biol* **166**(4): 557-580.

185. Muyrers, JP, Zhang, Y and Stewart, AF (2001). Techniques: Recombinogenic engineering--new options for cloning and manipulating DNA. *Trends Biochem Sci* **26**(5): 325-331.

186. Zhang, Y, Buchholz, F, Muyrers, JP and Stewart, AF (1998). A new logic for DNA engineering using recombination in Escherichia coli. *Nat Genet* **20**(2): 123-128.

187. Kim, JH, Lee, SR, Li, LH, Park, HJ, Park, JH, Lee, KY*, et al.* (2011). High cleavage efficiency of a 2A peptide derived from porcine teschovirus-1 in human cell lines, zebrafish and mice. *PLoS One* **6**(4): e18556.

188. Brown, SM, Harland, J and Subak-Sharpe, JH (1984). Isolation of restriction endonuclease site deletion mutants of herpes simplex virus. *J Gen Virol* **65 (Pt 6)**(Pt 6): 1053-1068.

189. Poffenberger, KL, Tabares, E and Roizman, B (1983). Characterization of a viable, noninverting herpes simplex virus 1 genome derived by insertion and deletion of sequences at the junction of components L and S. *Proc Natl Acad Sci U S A* **80**(9): 2690-2694.

190. Jenkins, FJ, Donoghue, AM and Martin, JR (1996). Deletion of the Herpes simplex 1 internal repeat sequences affects pathogenicity in the mouse. *Front Biosci* **1** a59-68.

191. Nash, TC and Spivack, JG (1994). The UL55 and UL56 genes of herpes simplex virus type 1 are not required for viral replication, intraperitoneal virulence, or establishment of latency in mice. *Virology* **204**(2): 794-798.

192. Igarashi, K, Fawl, R, Roller, RJ and Roizman, B (1993). Construction and properties of a recombinant herpes simplex virus 1 lacking both S-component origins of DNA synthesis. *J Virol* **67**(4): 2123-2132.

193. Sears, AE, Halliburton, IW, Meignier, B, Silver, S and Roizman, B (1985). Herpes simplex virus 1 mutant deleted in the alpha 22 gene: growth and gene expression in permissive and restrictive cells and establishment of latency in mice. *J Virol* **55**(2): 338-346.

194. Post, LE and Roizman, B (1981). A generalized technique for deletion of specific genes in large genomes: alpha gene 22 of herpes simplex virus 1 is not essential for growth. *Cell* **25**(1): 227-232.

195. Ryan, MD, King, AM and Thomas, GP (1991). Cleavage of foot-and-mouth disease virus polyprotein is mediated by residues located within a 19 amino acid sequence. *J Gen Virol* **72 (Pt 11)**(Pt 11): 2727-2732.

196. Ryan, MD and Drew, J (1994). Foot-and-mouth disease virus 2A oligopeptide mediated cleavage of an artificial polyprotein. *EMBO J* **13**(4): 928-933.

197. Ginn, SL, Alexander, IE, Edelstein, ML, Abedi, MR and Wixon, J (2013). Gene therapy clinical trials worldwide to 2012 - an update. *J Gene Med* **15**(2): 65-77.

198. Craft, AM, Krisky, DM, Wechuck, JB, Lobenhofer, EK, Jiang, Y, Wolfe, DP*, et al.* (2008). Herpes simplex virus-mediated expression of Pax3 and MyoD in embryoid bodies results in lineage-Related alterations in gene expression profiles. *Stem Cells* **26**(12): 3119-3129.

199. Summers, BC and Leib, DA (2002). Herpes simplex virus type 1 origins of DNA replication play no role in the regulation of flanking promoters. *J Virol* **76**(14): 7020-7029.

200. Glorioso, JC, DeLuca, NA and Fink, DJ (1995). Development and application of herpes simplex virus vectors for human gene therapy. *Annu Rev Microbiol* **49:** 675-710.

201. Evans-Galea, MV, Pebay, A, Dottori, M, Corben, LA, Ong, SH, Lockhart, PJ*, et al.* (2014). Cell and gene therapy for Friedreich ataxia: progress to date. *Hum Gene Ther* **25**(8): 684-693.

202. Nabhan, JF, Wood, KM, Rao, VP, Morin, J, Bhamidipaty, S, LaBranche, TP*, et al.* (2016). Intrathecal delivery of frataxin mRNA encapsulated in lipid nanoparticles to dorsal root ganglia as a potential therapeutic for Friedreich's ataxia. *Sci Rep* **6**: 20019.

203. Pan, D, Flores, O, Umbach, JL, Pesola, JM, Bentley, P, Rosato, PC *et al.* (2014). A neuron-specific host microRNA targets herpes simplex virus-1 ICP0 expression and promotes latency. *Cell Host Microbe* **15**(4):446-456

APPENDIX I: SUPPLEMENTARY MATERIAL

10. APPENDIX I: SUPPLEMENTARY MATERIAL

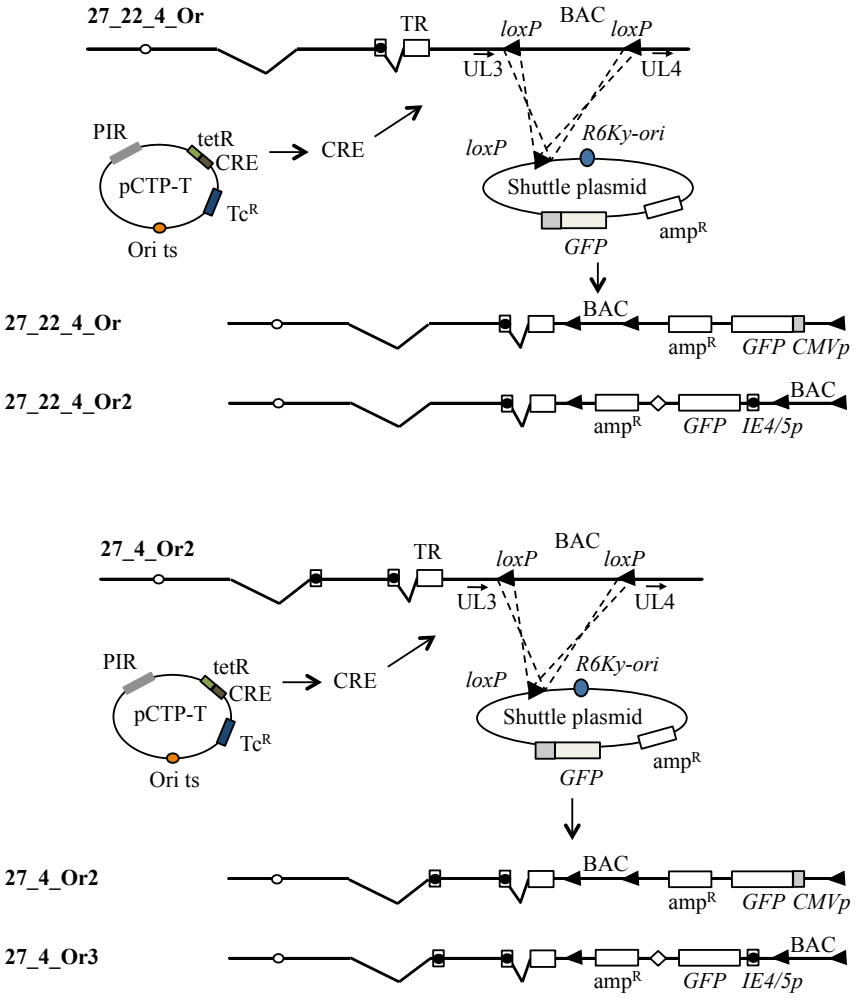

Figure S1. Schematic of the construction of 27_22_4_Or GFP, 27_4_Or2 GFP, 27_22_4_Or2 and 27_4_Or3

Schematic representation of Cre recombinase-mediated single insertion of the fluorescent protein reporter gene (*GFP*) or the double insertion of the *GFP* and the HSV-1 origin of replication (ori_S) sequence, at one of the *loxP* sites flanking the BAC vector bacterial sequences (BAC), which are located in the U_L3-U_L4 intergenic region of the 27_22_4_Or and 27_4_Or2 BAC DNAs. Dashed lines represent the two possible recombination events at either of the *loxP* sites of the HSV-1 BACs. Two shuttle plasmids were used: the pLCG plasmid, used for the single insertion of the the cytomegalovirus immediate early promoter (CMVp)-*GFP* transgene cassette to generate the vectors 27_22_4_Or GFP and 27_4_Or2 GFP, and the pHG plasmid, used for the simultaneous insertion of ori_S and the immediate early ICP22/47 promoter (IE4/5p)-*GFP* transgene cassette to generate the vectors

27_22_4_Or2 and 27_4_Or3. Both shuttle plasmids contain a *loxP* site (filled arrowhead); the beta-lactamase gene (amp^R, open box); the R6Kγ–*ori* (blue circle) which enables replication only when the π protein is supplied *in trans*; and the *GFP* reporter gene driven by the CMV promoter (*CMVp*) in the pLCG plasmid or driven by the IE4/5 promoter (IE4/5p, which includes the ori$_S$ sequence; filled circle enclosed by a box) in the pHG plasmid. The pHG plasmid contains in addition the HSV-1 packaging signal (open diamond). The temperature-sensitive (ts) helper plasmid pCTP-T contains a pSC101-derived thermosensitive replication origin (orange circle); the Tc^R gene conferring tetracycline resistance (dark blue box) for tetracycline-inducible Cre expression (light and dark green boxes); and PIR (grey box), the *pir* gene which expresses the π protein to support the replication of the co-introduced plasmids containing the R6Kγ-*ori*.

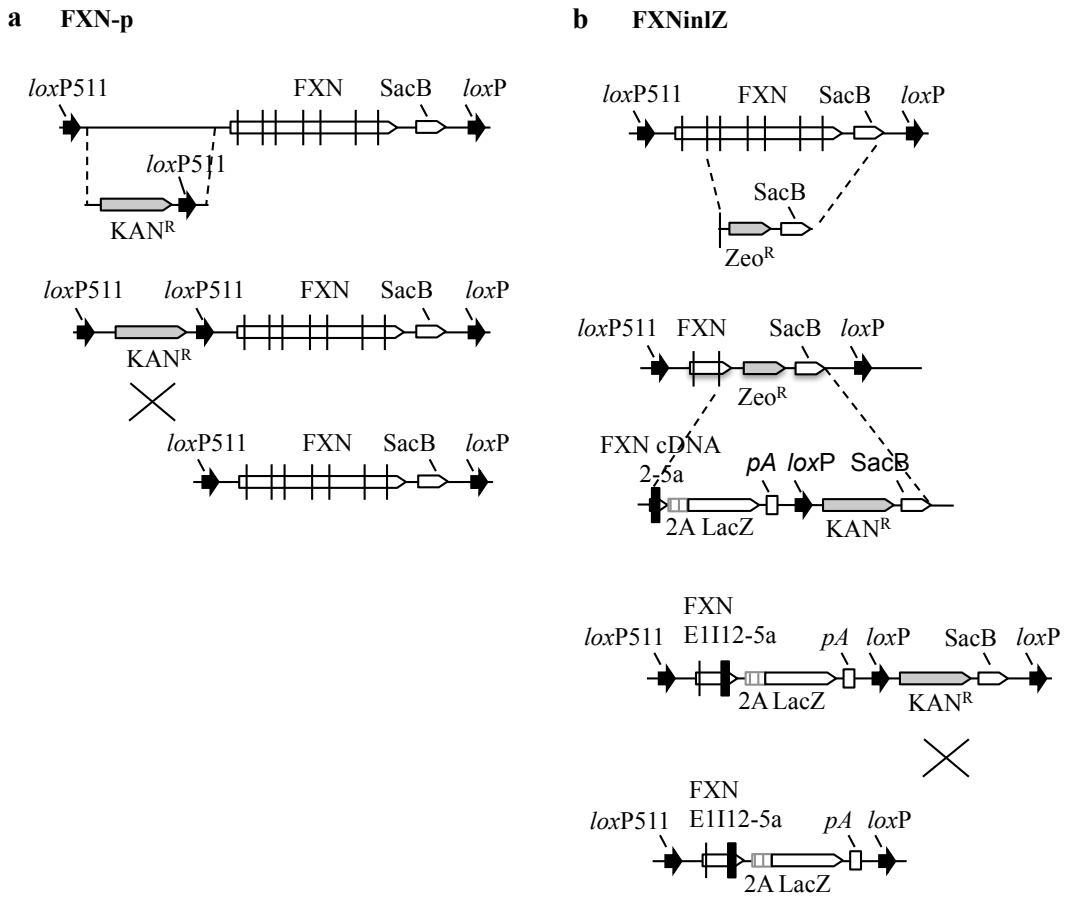

Figure S2. Schematic (not to the scale) of the construction of FXN-p and FXNinlZ.

a. Schematic representation of FXN-p construction. Starting from the FXN-WT BAC plasmid we inserted a cassette encoding a kanamycin resistance gene (Kan^R; grey arrowed box) and a flanking *loxP511* site (black arrow) in the 5' region upstream of the ATG start codon of the human *FXN* gene by Red/ET homologous recombination (dashed lines). The

Kan^{R} gene was then removed by Cre-mediated recombination (solid lines) between the introduced *loxP511* site and another located at the boundary between the BAC vector and the 5' end of the *FXN*. The seven exons of the *FXN* are marked as black vertical lines.

b. Schematic representation of FXNinlZ construction. Starting from the FXN-p BAC plasmid we inserted by Red/ET homologous recombination (dashed lines) a cassette encoding a zeocin resistance gene (Zeo^{R}; grey arrowed box) and the *sacB* gene (small open arrowed box) to delete all of the genomic insert sequences 3' to *FXN* exon 2 up to the *sacB* gene located within the BAC vector. In a second round of Red/ET homologous recombination, we next replaced the *Zeo*^{R} gene with the F2ALRK cassette which encodes the *FXN* cDNA from exon 2 to 5a (*FXN* cDNA 2-5a; black vertical box), the Porcine teschovirus-1 2A sequence (2A; grey hatched box), the *Escherichia coli lacZ* gene (open arrowed box), the polyadenylation signal (pA; open box), a *loxP* site (black arrow), a kanamycin resistance gene (*Kan*^{R})-encoding cassette (grey arrowed box) and the *sacB* gene (small open arrowed box). The *Kan*^{R} gene was then removed by Cre-mediated recombination (solid lines) between the introduced *loxP* site and another located in the BAC vector, 3' to the *sacB* gene. The resulting *FXN* reduced version includes the 5 kb promoter and the *FXN* cDNA with the inclusion of intron 1 (FXN E1I12-5a; open arrowed box with black vertical lines representing exon 1 and cDNA 2-5a).

APPENDIX II: PUBLICATIONS

11. APPENDIX II: PUBLICATIONS

Publications related to the thesis:

Lim, F, Khalique, H, Ventosa, M, and Baldo, A (2013). Biosafety of Gene Therapy Vectors Derived From Herpes Simplex Virus Type 1. *Current Gene Therapy* **13**: 478-491.

Ventosa, M, Wu, Z, and Lim, F. Sustained FXN expression in dorsal root ganglia from a nonreplicative genomic HSV-1. Submitted to *Molecular Therapy*, September 2016.

Publications non-related to the thesis:

García-Escudero, V, Rosales, M, Muñoz, JL, Scola, E, Medina, J, Khalique, H, Garaulet, G, Rodriguez, A, and Lim, F (2015). Patient-derived olfactory mucosa for study of the non-neuronal contribution to amyotrophic lateral sclerosis pathology. *J Cell Mol Med* **19**: 1284-1295.